BILINGUAL PUBLISHING CO.
Pioneer of Global Academics Since 1984

Journal of Computer Science Research

Volume 4 | Issue 1 | January 2022 | ISSN 2630-5151（Online）

BILINGUAL PUBLISHING CO.
Pioneer of Global Academics Since 1984

Volume 4 Issue 1 • January 2022 • ISSN 2630-5151 (Online)

Journal of Computer Science Research

BILINGUAL PUBLISHING CO.
Pioneer of Global Academics Since 1984

BILINGUAL PUBLISHING CO.
Pioneer of Global Academics Since 1984

Volume 4 | Issue 1 | January 2022 | Page1-53
Journal of Computer Science Research

Contents

Editorial

Articles

Correction

BILINGUAL PUBLISHING CO.
Pioneer of Global Academics Since 1984

Journal of Computer Science Research
https://ojs.bilpublishing.com/index.php/jcsr

ARTICLE

Embedding 3-D Gaze Points on a 3-D Visual Field: A Case of Transparency

Fatima Isiaka[1*] Zainab Adamu[2] Muhammad A. Adamu[3]

1. Department of Computer Science, Nasarawa State University, Keffi, Nigeria
2. Department of Computer Science, Ahmadu Bello University, Zaria, Nigeria
3. Department of Electrical Engineering, Federal University of Technology, Minna, Nigeria

ARTICLE INFO

Article history
Received: 1 November 2021
Accepted: 14 December 2021
Published Online: 12 January 2022

Keywords:
User Behaviour
3D gaze point
Eye movement
User behaviour
3D visual interface
3D game console
User experience

ABSTRACT

The paper seeks to demonstrates the likelihood of embedding a 3D gaze point on a 3D visual field, the visual field is inform of a game console where the user has to play from one level to the other by overcoming obstacles that will lead them to the next level. Complex game interface is sometimes difficult for the player to progress to next level of the game and the developers also find it difficult to regulate the game for an average player. The model serves as an analytical tool for game adaptations and also players can track their response to the game. Custom eye tracking and 3D object tracking algorithms were developed to enhance the analysis of the procedure. This is a part of the contributions to user interface design in the aspect of visual transparency. The development and testing of human computer interaction uses and application is more easily investigated than ever, part of the contribution to this is the embedding of 3-D gaze point on a 3-D visual field. This could be used in a number of applications, for instance in medical applications that includes long and short sightedness diagnosis and treatment. Experiments and Test were conducted on five different episodes of user attributes, result show that fixation points and pupil changes are the two most likely user attributes that contributes most significantly in the performance of the custom eye tracking algorithm the study. As the advancement in development of eye movement algorithm continues user attributes that showed the least likely appearance will prove to be redundant.

1. Introduction

Gaze points are attributes in an eye movement behaviour studies. It involves a voluntary or involuntary coordinates of points made by the movement of the eyes, which helps to acquire fixation and tracking of visual stimuli. The eyes are mostly the visual organ or part of the body that moves using a system of six muscles [1-4]. The retina part of the eye senses light and convert light

*Corresponding Author:
Fatima Isiaka,
Department of Computer Science, Nasarawa State University, Keffi, Nigeria;
Email: Fatima.isiaka@outlook.com

DOI: https://doi.org/10.30564/jcsr.v4i1.4037

into electro-chemical signals which travel along the optic nerve to the brain tissue and interpreted as vision in a practical visual cortex. Humans are one of the primates that uses natural phenomenon of voluntary eye movement to track objects of interest; this phenomenon includes the smooth pursuit (sideways movement), saccades and vergence shifts (Figure 1). These voluntary eye movement generated as gaze points appear to be initiated by captured by infrared light of an eye tracker which records the eye movementa tiny cortical region in the brain anterior lobe, this action and behaviour of the eye can be behaviour. The reflexes of the eyes can shift toward a moving light and is intact even though the voluntary control is annihilated. The eye movement not only reacts to light intensity and movement, but can also portray an emotional response to stimuli.

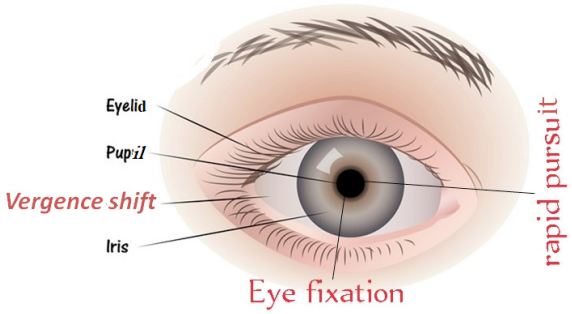

Figure 1. Picture showing the different attributes of the eye and direction of eye movements: Courtesy, Google images

In physiological response, gaze points of eye movement can be classified according to different systems:

1) The involvement of one eye as duction, both eyes as version, movement in similar and in opposite direction as vergence.

2) Also can be classified as fixational, gaze stabilising, shifting, whose movement is referred to as vestibulo-ocular reflex and optokinetic reflex, the mechanism is referred to as saccades and pursuit movements [6,7].

This paper is only limited to discussing representation of the gaze point of eye movement on a 3D context as a form of heat map and visualised in a 3D environment based on the vergence or convergence movement that involves both eyes, to make sure the image (3D object) being looked at falls on the corresponding spot on both retina of the eyes. This helps in the depth perception of the 3D object [5-8]. The area of the saccade, pursuit movement or smooth pursuit will be dealt with in later research. Saccades in relation to this paper is the space between two or more 3D gaze points, which could be overlapping in some cases and an enlarged gaze point depending on the amount of time a person spent looking at a particular area of the 3D visual field.

In actual sense, the eyes are never completely at rest: they make frequent fixations of eye movement even though they are in a particular point. We can relate these movements to the photoreceptors and the ganglion cells of the brain. A constant visual stimulus could lead to an unresponsive ganglion cell while a changing or dynamic stimulus makes the photoreceptors become responsive as illustrated by the dynamic 3D game interface used in this paper. Most of the eye control motor is generated based on saccades (rapid eye movement) which is used while scanning a visual scene. According to [9-12], the eyes do not move smoothly across a *XY* Cartesian plane or a printed page during for example a reading session, instead they make short and rapid movements which are the saccades. And during each saccade the eyes move very fast and an involuntary movement (not consciously controlled). Each of the movement is represented by a few minutes of arc about four to five seconds at regular intervals. This is represented by the space between gaze points in a visual field mostly indicated by straight lines across fixations points. One of its uses is to scan a greater part of the area of interest with a high-resolution fovea of the eyes.

The rational for using a 3D visualisation field in this paper is based on the fact that not always did the picture content in the catalogue correspond to the expectations of the intended clients and with the eventually expected results. Some users or customers turn out to be unhappy with what they saw through advertisement after all the design work is been finished or after purchase of an item online. With the advent of panoramic pictures in recent times, as well as the progression of different bulky programs and formats of image transmission, a lot of companies have moved towards the virtual catalogues. In this environment, they can get potential users or customers to be acquainted with the 3D game visualisation of the inner part of the environment in an immense format. A 3D visualisation of the game interior can give a finite definition to user behaviour with a 3D gaze point on a visual game interface and also an excellent opportunity to interact with the objects in every detail such as the entire panorama and also from a different angle [13-16]. The designers can also afford to see the weaknesses and strength of each level based on session overview.

Integrating a 3D eye movement algorithm in a 3D environment will allow consideration of not only the architectural shape of the visual objects, but also how the project will look like in its final stage of completion during decision making. A 3D gaze point on the 3D interphase visualisation of the game will have a common

vision of the future construction at the initial stage. The photo realistic rendering applied is an expensive and improved version of the current project [17-19].

Objectives

The objectives behind this paper are to:

1) Model a virtual scene that involves eye movement in a 3D environment

2) Create a 3D eye movement scene on objects in a 3D game interface

3) Develop a custom algorithm to identify basic user eye movement behaviour in a virtual environment.

This will open new opportunities in any field of human computer interface design, manufacturing, computer graphics and many others.

2. Literature Review

The 3D visual interface is the "Wonder World" a simple came designed using "Struckd", one of the first game console used in this area of research. The game is about a princess sent underworld to defeat some unnamed creatures and gain access to a porthole that leads to a dungeon to get a diamond crown to present to royals and bearers of the royal crown. She has to cross four levels to get to the crown. Each level leaves a more challenging and advanced battle than the other. Each level of the game interface enables the user (player) to cross to a higher level after overcoming the obstacles in the previous level. The embedded gaze point will allow for monitoring of the different stages of user behaviour through their eye movement. The user activity is recorded and used for predictions of user gaze points on the 3D visual field [20-22]. The aim and purpose is to create data-driven designs and eliminate guesswork of user engagement and interaction using the location of the gaze point [20-22]. This will allow user experience designers, web managers, developers to visualise usage patterns, optimize and also gather objective data that involves 3D-data visualisation [23-25]. Also the algorithm designed for the eye movement recognition will involve powerful features such as pupillary measurement and heat maps on both two dimensional and 3D visual field, this will automatically sort out areas of interest (AOI). The algorithm involves three (3) modules, this is inform of an engine that automatically detects the pupillary position of the eyes (Algorithm 1) using the camera lens of a PC, this is then used to identify the 3-D objects (Algorithm 2) in a virtual field. The gaze points Algorithm (Algorithm 3) is used to trace and locate 3-D objects at the AOI using the PC's camera lens to calibrate the eye's position.

The 3D object detection (Algorithm 2) detects images or scene in a virtual field given a reference image of the object. The algorithm presents a straight forward step used in detecting specific objects based on finding the point corresponding to reference and target image. This can also detect objects despite changes in the scale in plane rotation of movement [23-25]. It is basically robust to small amount of virtual plain rotation. The steps are suitable for most objects in the scene that exhibit non repeating texture patterns, which give rise to unique feature matches. This feature is suited for any object in the scene that moves both in a vertical or horizontal plane in the video game console [23-25].

As object detection is very important in many computer vision and HCI studies so is the discovery of ways to improve activity recognition, automotive safety and application of 3D visionary as applied in this is paper. Before tracing a particular 3D object, one needs to first detect it, hence the cascaded iris detection algorithm. This detects the location of the object in a video frame. It is configured to detect not only 3D objects but also two dimensional objects as it moves or changes direction. The behaviour of the subject's pupil is also recorded such as, 'Intense', 'Ease', Confused', 'Slack', 'Stressed' and 'Relaxed' mood, this represent the characteristical behaviour of the eyes during concentration (Table 1), it would enable designers to identify areas that need basic optimisation.

For the embedding phase the Java platform was used to integrate the eye tracking algorithms as a standalone on the 3D game console designed with "Stuckd". Both engines were sychronised to run on the same platform using the PC camera lens for calibration. Because of the easy steps with algorithm calibration runs faster with a minimum speed of 0.5 MHz per seconds. User can interact with the game while their eye movement behaviour is captured alongside the video game console.

3. Method

The pilot study started with simulation of gaze data containing one thousand five hundred instances as a training set. This was used as input to the custom eye movement detection algorithm for the video game console. In later study, fifty participants were recruited to take part in the game interface. They were given a consent form to sign confirming their involvement in the game and safety precautions were taken concerning their emotional status, such as their familiarity with the game and web interactions (Figure 2). The data are then simulated to a thousand and used as the test set. The performance on the dataset is demonstrated to show the predictive ability of

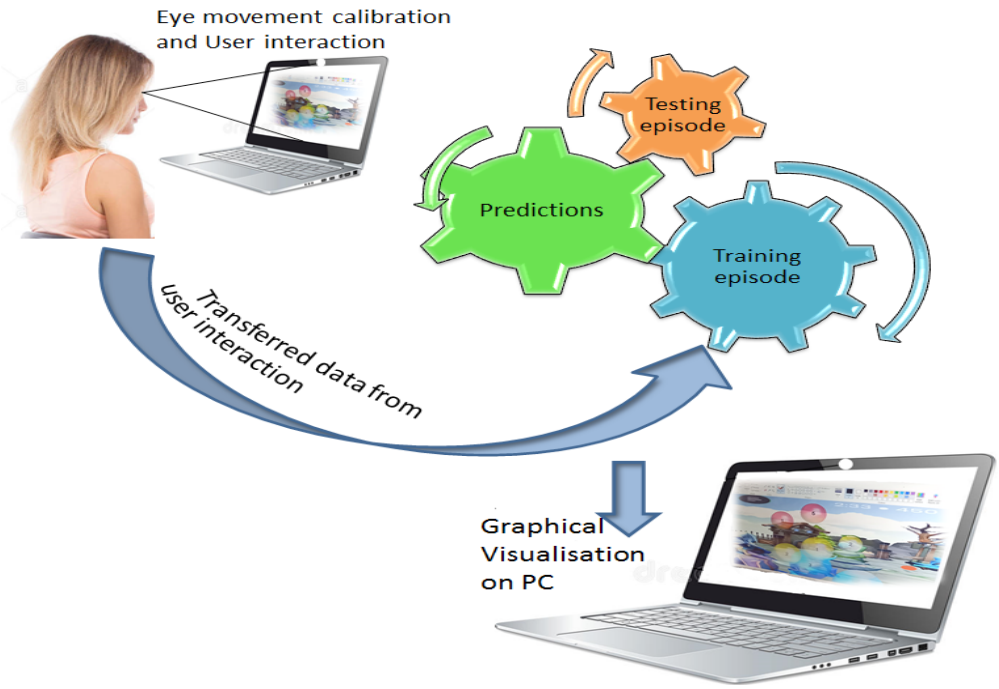

Figure 2. User interaction with game interface with data transferred and simulated for training, testing and predictions.

the custom eye movement detection algorithm (Algorithm 1, 2, 3). A graphical visualisation of the entire episode is visualised on a PC (Figure 2).

Algorithm 1. (Subject's iris detection)

1. *Ready subject's iris*
2. *Set pupil localisation*
3. *Trace iris position*
4. *If eye closed, wait else goto 2*
5. *If eye open and no iris detected to 2 else 3*
6. *End*

Algorithm 2. (3D object detection on a 3D video game console)

1. *Start*
2. *Initial the Algorithm 1 as a cascade detector object*
3. *Read in the video frame (V_F) and run the detector (Algorithm 1)*
4. *Read 3D objects from the scene*
5. *Detect feature points using Algorithm 1*
6. *Extract feature point descriptors by surrounding the object with 3D gaze cascade*
7. *Find the putative point matches*
8. *Locate the object in the scene using step 4*
9. *Detect another 3D object*
10. *Is video frame < total V_F goto 2 else goto 10*
11. *End*

Table 1. User Characteristical Behaviour of Eye movement detection on 3D game console: Overlapping colors tend to blend to give a unique hue.

User Behaviour	Parameter Value	Calibration point	Color
Intense	5	0.6	Light Red
Ease	2	0.4	White
Confused	3	0.8	Light Blue
Slack	1	0.7	Blue
Relaxed	4	0.2	Yellow
Stressed	6	0.3	Red

Algorithm 3. (Custom eye tracking on a 3D video game console)

1. *Begin*
2. *Set calibration for both eyes*
   i. *Locate iris position using Algorithm 1*
   ii. *Set point of location as middle of visual field*
   iii. *Set scan-path to four corners of visual field*
   iv. *Save gaze calibration data*
3. *Detect 3-D object at the virtual centre field*
4. *Locate eye positions*
5. *If eye position detection fails, goto 3 else goto 6*
6. *Save eye detection data $T_{c(k)}$*
7. *Detect other 3-D objects*
8. *Track eye position using iris detection algorithm*
9. *Verify eye positions using Iris detector (Algorithm 1)*
10. *If eye verification is complete, goto 11, else goto 8*

11. *Reset counter to update eye position*
12. *If counter < $T_{c(l)}$ goto 7 else goto 3*
13. *Set counter+1*
14. *If gaze off screen goto 4 to reset gaze position else goto 7*
15. *Search for 3-D objects complete? goto 16 else go 7*
16. *End.*

Task

The 3D Wonder World game consists of four levels and users were simply asked to play the game by first calibrating their eyes with the PC camera lens (Figure 1). The participants were asked to play the first two levels for twenty seconds and their activity was captured. The eye movements were recorded and sent to a subfolder for analysis.

4. Results

An initial detected object is first seen at the middle of the visual field based on the calibration of the point gaze from Algorithm 1. Figure 3 shows a predicted gaze point at the middle of the video game console as calibrated in the initial stage. There was no particular mechanism to define the appearance of this scene only that the red, blue, yellow and white color mixture indicates a vague reaction from the user. The proceeding section discusses some of the most significant results and performance of the algorithm on the dataset obtained from the experimental study.

Figure 3. Predicted Gaze point in the middle of the visual field of the 3D game console.

4.1 Level 1

This level (Figure 4) captured a scene of gaze point on the arrow held by the game character with the mood of the user indicating "ease" "relaxed" and "slack" which is represented by 1, 2, and 4. The gaze point also shows a stress mood overlapped by other expressions conveyed by the user while looking towards the porthole to the dungeon. Expression of emotion on visual field is very useful in so many ways, for instance our physical reaction to stress towards a visual scene can be reduced by minimising the level of obstacles encountered on a particular frame; or can be used to increase the level of intensity on a game console if the purpose is to hinder the player from crossing to the next level with ease. In most cases the aim is to encourage players to the first two levels by reducing the number of obstacles and increase the level of intensity in the proceeding levels. This induces or records the level of intelligence of the player and determines if the game console is suitable for an average or an advanced player.

Figure 4. Level one of the game interface showing gaze points representing different user behaviour towards the visual scene

4.2 Level 2

Level 2 (Figure 5) captures the scene where the player is looking towards the dungeon that holds the diamond crown with an "intense", "slack" and "ease" mood. The intense mood showed a bit of a stress hue (red color) and less stress hue at two locations. This would prompt a designer to optimise the process by picking one of the locations to apply either of the moods (picking slack mood with stress or slack mood without stress) to get to the target object. 3D object tracking across video frames can support object detection and frame segmentation. The detecting phenomena or activities are only recognised taking the entire stream of images into account; the video analysis used here presents unique challenging resource

management and model architecture that could be improved based on the performance of the object tracking or gaze data generated from the test phase.

To test the performance of the dataset generated from the study conducted with 3D gaze points on the game interface. A dynamic control model was used to predict the gaze and user behaviour data on both the simulated and actual data generated from the eye tracking study. The error plots from the model are discussed in the proceeding section.

Figure 5. Game interface showing captured scene of stress gaze point on the target object and location of arrow with intense (5), slack (1) and ease (2).

4.3 Performance on Dataset Models

The dataset generated were in two sets, the simulated and actual data, a dynamic control system based on discrete time variant models was used on the data models for both test (actual data) and training (simulated data). The rational for using the dynamic control system is the fact that it uses internal dynamics or memory of past state functions like integrators and tunable parameters (certain or uncertain values) of attributes to produce recurrent values. This is best suited for user behaviour data which are very complex and difficult to predict e.g. a residual or R^2 value of 0.62 score is highly probable for human behaviour data, especially those that involve complex eye movement readings. The control system can help decided whether anomalies in the dataset can be excluded or not. Due to environmental constraints, some outliers are termed feasible and important in datasets such as those involve with user behaviour studies.

The user attributes used in the datasets include the fixation points, fixation duration, pupil changes and saccades. These are basically the most significant variables that can help predict user eye movement behaviour on a 3D visual interface like the game console.

Error in the performance of the data models were visualised and discussed. Figure 6 shows the output in error performance of the training set on different scenes. The dataset for both the training and test set were divided into four different scenarios (two user attributes, three user attributes, four user attributes and all user attributes). The simulated dataset (training set) and original dataset (testing set) were executed on five different episodes, with the error in performance recorded.

The data settings changes every time the model is executed. To give a constant or an alleviated edge to the dataset output, the ranging style was set to default value. The least error appeared in the training set on the fifth episode (Figure 6a) with error in performance below 0.01, which is a recorded performance of 99%. This is on the training set with two important user attributes; the gaze point coordinates and pupil changes. This also demonstrates the importance and inevitability of the pupil dilation and fixation points in user eye movement readings.

The least error for the test dataset on five different scenarios appeared at the fifth episode (Figure 6b) with a minimum error of 0.1 above the expected rate of 0.01. This has a performance of 90% and above maximum expectations. This outcome is reflected on the dataset and has the same user attributes as the training set. The minimum error also appeared on test data with all user attributes (Figure 6d), showing a least performance of 0.2. As the advancement in development of eye movement algorithm continues user attributes that show the least likely appearance will prove redundant, based on the result of this paper and similar but different research outputs in some papers [26,27], these attributes contributes the least to behaviour predictions.

Figure 7 shows the error in test data on four different episode, these episode are situations where users' attributes are applied based on their level of importance such as saccade length and fixation coordinates in both the *XY* plane, fixation duration, pupil dilation, pupil constriction, off screen location and number of clicks per milliseconds. Figure 7d shows the error plot on test dataset with five attributes using five scenes. The least error (0.01) appeared on the fifth scene where all attributes are applied.

5. Conclusions

The paper demonstrates the possibility of embedding 3D gaze point on a 3D visual field, this visual field is inform of a game console where the user has to play from

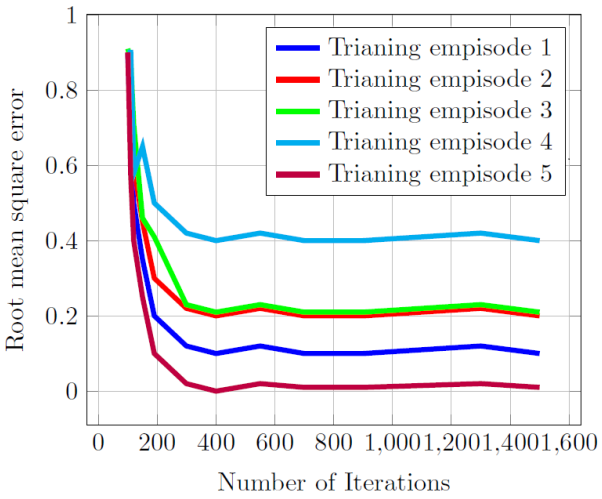

(a): Error plot for the training set on five episodes: the fifth episode shows the least error.

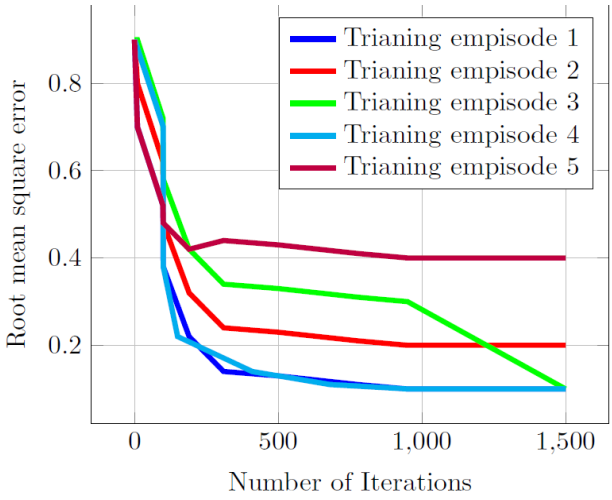

(b): Error plot on training set on five episodes for dataset with two user attributes: the first episode shows the least error.

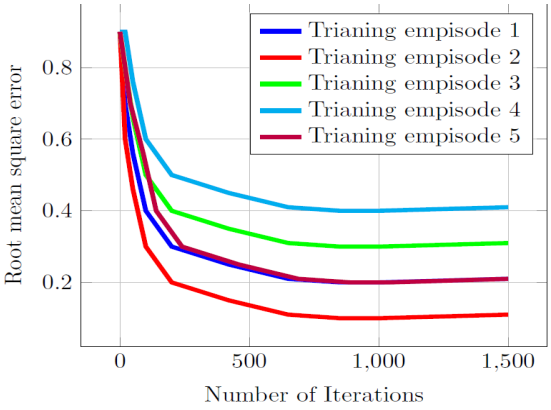

(c):Error plot for training set on five episodes for the dataset with three user attributes: the second episode showed the least error.

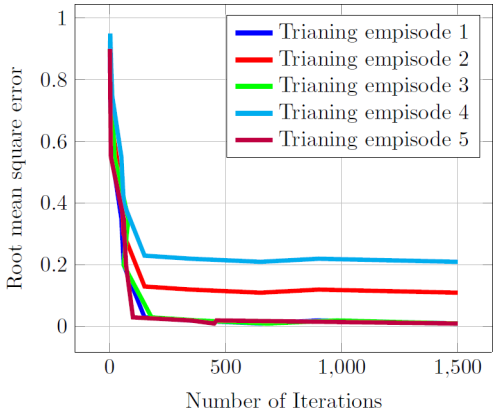

(d): Error plot show the fifth episode with the least error on test set data with four attributes

Figure 6. Error in Performance of the test dataset on five different episodes.

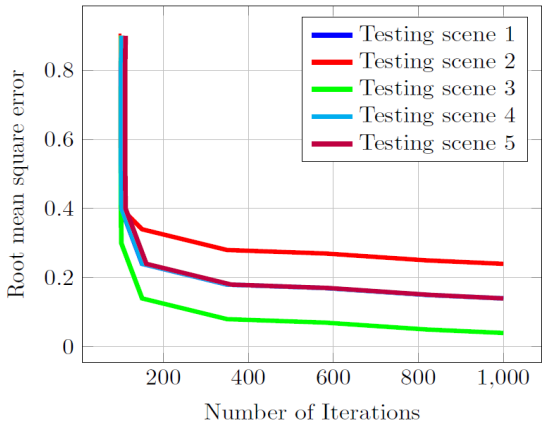

(a): Error plot on test dataset using five different scenario, the least error appeared in the fourth scene.

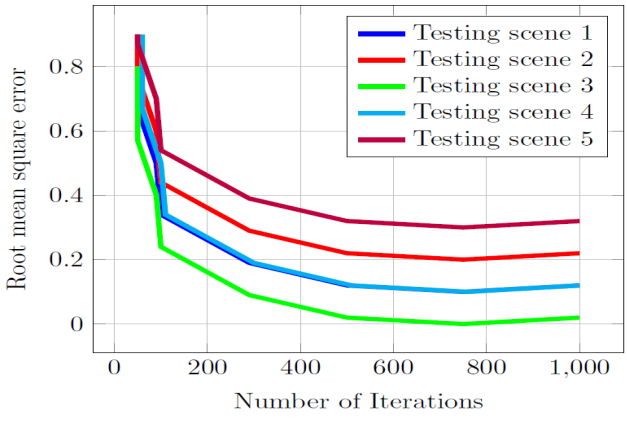

(b).: Error on dataset with two variables using five different scenario, the least error appeared on the third scene.

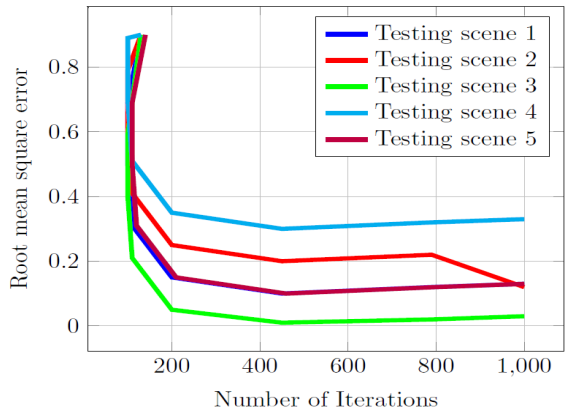

(c): Error plot on test dataset with three user attributes using four user attributes, the least error appeared on the third scene.

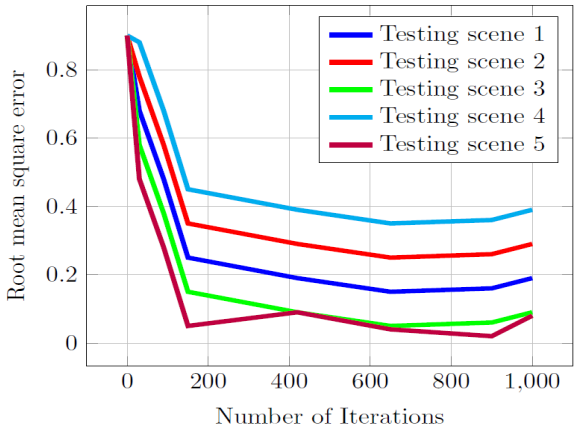

(d): Error plot on test dataset with five attributes using five scenes, the least error appeared on the fifth scene.

Figure 7. Error in Performance of dataset on four different episodes using five different scenes.

one level to the other by over overcoming obstacles that will take them to the next level. Custom eye tracking and 3D object tracking algorithms were developed to enhance the analysis of the procedures. This is part of the contributions to user interface design in the aspect of visual transparency.

The development and testing of human computer interaction uses and application is more easily investigated than ever, part of the contribution to this is the embedding of 3-D gaze point on a 3-D visual field. This could be used in a number of applications, for instance in medical applications that includes long and short sightedness, dyslevia and glaucoma diagnosis and treatment. The 3-D eye tracking gaze point model is user friendly and could be well suited for industrial use and across ergonomics laboratory for usability testing. Part of its limitations is the time synchronisation of events and custom eye and iris calibration at the initial stage of the algorithm. This problem can be tackled with constant testing and experimental setup that involves execution of standard classification algorithms. The system is just another example of eye tracking models that most organisations find more ways to incorporate for accuracy and user friendly capabilities with enhanced visual tendering and easy calibration. This will encourage more innovative and finite discoveries that offers research based eye tracking systems with both software and hardware capabilities.

References

[1] Wang, X.Y., Zhang, Y., Fu, X.J., Xiang, G.S., 2008. Design and kinematic analysis of a novel humanoid robot eye using pneumatic artificial muscles. Journal of Bionic Engineering. 5(3), 264-270.

[2] Leigh, R.J., Zee, D.S., 2015. The neurology of eye movements. Contemporary Neurology.

[3] Soechting, J.F., Flanders, M., 1992. Moving in three-dimensional space: frames of reference, vectors, and coordinate systems. Annual review of neuroscience. 15(1), 167-191.

[4] Donaldson, I.M.L., 2000. The functions of the proprioceptors of the eye muscles. Philosophical Transactions of the Royal Society of London. Series B: Biological Sciences. 355(1404), 1685-1754.

[5] Yoshimura, Y., Kizuka, T., Ono, S., 2021. Properties of fast vergence eye movements and horizontal saccades in athletes. Physiology & Behavior. 235, 113397.

[6] Gupta, P., Beylergil, S., Murray, J., Kilbane, C., Ghasia, F.F., Shaikh, A.G., 2021. Computational models to delineate 3D gaze-shift strategies in Parkinson's disease. Journal of Neural Engineering. 18(4), 0460a5.

[7] McCormack, G.L., Kulowski, K.A., 2021. Image Size and the Range of Clear and Single Binocular Vision in 3D Displays. Optometry and Vision Science. 98(8), 947-958.

[8] Chen, C.Y., Lin, H.C., Wu, P.J., Chuang, C.H., Lin, B.S., Lin, C.H., 2021. Reducing the discomfort in viewing 3D video with a prism device modified eye convergence. Heliyon. 7(4), e06877.

[9] Rajendran, S.K., Wei, Q., Zhang, F., 2021. Two degree-of-freedom robotic eye: design, modeling, and learning-based control in foveation and smooth pursuit. Bioinspiration & Biomimetics.

[10] Samadani, U., Ritlop, R., Reyes, M., Nehrbass, E., Li, M., Lamm, E., ... Huang, P., 2015. Eye tracking

detects disconjugate eye movements associated with structural traumatic brain injury and concussion. Journal of neurotrauma. 32(8), 548-556.

[11] Singh, T., Perry, C.M., Herter, T.M., 2016. A geometric method for computing ocular kinematics and classifying gaze events using monocular remote eye tracking in a robotic environment. Journal of neuroengineering and rehabilitation. 13(1), 1-17.

[12] Wöhle, L., Gebhard, M., 2021. Towards Robust Robot Control in Cartesian Space Using an Infrastructureless Head-and Eye-Gaze Interface. Sensors. 21(5), 1798.

[13] Yeamkuan, S., Chamnongthai, K., 2021. 3D Point-of-Intention Determination Using a Multimodal Fusion of Hand Pointing and Eye Gaze for a 3D Display. Sensors. 21(4), 1155.

[14] Li, Y., Shen, W., Gao, Z., Zhu, Y., Zhai, G., Guo, G., 2021. Looking Here or There? Gaze Following in 360-Degree Images. In Proceedings of the IEEE/CVF International Conference on Computer Vision. pp. 3742-3751.

[15] Zhang, K., Liu, H., Fan, Z., Chen, X., Leng, Y., de Silva, C.W., Fu, C., 2021. Foot placement prediction for assistive walking by fusing sequential 3D gaze and environmental context. IEEE Robotics and Automation Letters. 6(2), 2509-2516.

[16] Fang, Y., Tang, J., Shen, W., Shen, W., Gu, X., Song, L., Zhai, G., 2021. Dual Attention Guided Gaze Target Detection in the Wild. In Proceedings of the IEEE/CVF Conference on Computer Vision and Pattern Recognition. pp. 11390-11399.

[17] Liang, J., Perez-Rathke, A., 2021. Minimalistic 3D chromatin models: Sparse interactions in single cells drive the chromatin fold and form many-body units. Current Opinion in Structural Biology. 71, 200-214.

[18] Liang, J., Perez-Rathke, A., 2021. Minimalistic 3D chromatin models: Sparse interactions in single cells drive the chromatin fold and form many-body units. Current Opinion in Structural Biology. 71, 200-214.

[19] Wong, H., Marie-Nelly, H., Herbert, S., Carrivain, P., Blanc, H., Koszul, R., ... Zimmer, C., 2012. A predictive computational model of the dynamic 3D interphase yeast nucleus. Current biology. 22(20), 1881-1890.

[20] Mousa, M., Dong, Y., 2020. Towards sophisticated 3D interphase modelling of advanced bionanocomposites via atomic force microscopy. Journal of Nanomaterials.

[21] Ou, H.D., Phan, S., Deerinck, T.J., Thor, A., Ellisman, M.H., O'shea, C.C., 2017. ChromEMT: Visualizing 3D chromatin structure and compaction in interphase and mitotic cells. Science. 357(6349).

[22] Mortazavi, B., Bardon, J., Ahzi, S., 2013. Interphase effect on the elastic and thermal conductivity response of polymer nanocomposite materials: 3D finite element study. Computational Materials Science. 69, 100-106.

[23] Chen, C.P., Zhang, C.Y., 2014. Data-intensive applications, challenges, techniques and technologies: A survey on Big Data. Information sciences. 275, 314-347.

[24] Markl, M., Draney, M.T., Hope, M.D., Levin, J.M., Chan, F.P., Alley, M.T., ... Herfkens, R.J., 2004. Time-resolved 3-dimensional velocity mapping in the thoracic aorta: visualization of 3-directional blood flow patterns in healthy volunteers and patients. Journal of computer assisted tomography. 28(4), 459-468.

[25] Keim, D., Kohlhammer, J., Ellis, G., Mansmann, F., 2010. Mastering the information age: solving problems with visual analytics.

[26] Ndung'u, R.N., Kamau, G.N., Wambugu, G.M., 2021. Using Feature Selection Methods to Discover Common Users' Preferences for Online Recommender Systems.

[27] Horstmann, K.T., Rauthmann, J.F., Sherman, R.A., Ziegler, M., 2021. Unveiling an exclusive link: Predicting behavior with personality, situation perception, and affect in a preregistered experience sampling study. Journal of Personality and Social Psychology. 120(5), 1317.

BILINGUAL PUBLISHING CO.
Pioneer of Global Academics Since 1984

Journal of Computer Science Research
https://ojs.bilpublishing.com/index.php/jcsr

ARTICLE

Efficient Feature Selection and ML Algorithm for Accurate Diagnostics

Vincent Omollo Nyangaresi[1*] Nidhal Kamel Taha El-Omari[2] Judith Nyakanga Nyakina[3]

1. Faculty of Biological & Physical Sciences, Tom Mboya University College, Homabay, Kenya
2. The World Islamic Science and Education University, Amman, Jordan
3. School of Nursing, Uzima University, Kisumu, Kenya

ARTICLE INFO

Article history
Received: 19 October 2021
Accepted: 19 January 2022
Published Online: 25 January 2022

Keywords:
Accuracy
Classifier
Ensemble
F-measure
Machine learning
Precision
Recall

ABSTRACT

Machine learning algorithms have been deployed in numerous optimization, prediction and classification problems. This has endeared them for application in fields such as computer networks and medical diagnosis. Although these machine learning algorithms achieve convincing results in these fields, they face numerous challenges when deployed on imbalanced dataset. Consequently, these algorithms are often biased towards majority class, hence unable to generalize the learning process. In addition, they are unable to effectively deal with high-dimensional datasets. Moreover, the utilization of conventional feature selection techniques from a dataset based on attribute significance render them ineffective for majority of the diagnosis applications. In this paper, feature selection is executed using the more effective Neighbour Components Analysis (NCA). During the classification process, an ensemble classifier comprising of K-Nearest Neighbours (KNN), Naive Bayes (NB), Decision Tree (DT) and Support Vector Machine (SVM) is built, trained and tested. Finally, cross validation is carried out to evaluate the developed ensemble model. The results shows that the proposed classifier has the best performance in terms of precision, recall, F-measure and classification accuracy.

1. Introduction

Machine learning (ML) and data mining (DM) algorithms present powerful statistical and probabilistic techniques that permit intelligent systems to learn from previous experiences [1]. This learning is critical for detection and identification of patterns in the underlying dataset. As such, they present vital mechanisms for discovering hidden relationships in sophisticated datasets [2]. Basically, ML and DM algorithms endeavour to offer reliability and trustworthiness in predictive models so as to boost precision and accuracy [2]. As such, these algorithms have found applications in optimization and prediction problems in communication networks and

*Corresponding Author:
Vincent Omollo Nyangaresi,
Faculty of Biological & Physical Sciences, Tom Mboya University College, Homabay, Kenya;
Email: vnyangaresi@tmuc.ac.ke

DOI: https://doi.org/10.30564/jcsr.v4i1.3852

medical fields, among others. For instance, fuzzy logic (FL) and adaptive neural networks (ANNs) have been deployed in [3] for optimization while authors in [4] have utilized Multi-Layer Feed Forward Network (MFNN) and FL for prediction. On the other hand, MFNN has been deployed in [5] for target cell prediction, while FL has been utilized in [6] for efficiency enhancement.

An adaptive neuro-fuzzy inference system (ANFIS) has been deployed in [7] for destination network prediction. Similarly, FL has been deployed in [8] for target network prediction, while neuro-fuzzy technique is presented in [9] for delay optimization. FL based estimation technique is presented in [10], while authors in [11] have developed a neural network system for predicting the number of users in a network. To boost quality of service (QoS) in 5G networks, authors in [12] present ANN-FL scheme. Similarly, ANN algorithm is deployed in [13] for QoS and Quality of Experience (QoE) enhancement. ANFIS scheme is presented in [14] for handover optimization, while multilayer neural network (MLNN) technique is introduced in [15] for QoS and QoE enhancement. Similarly, ML based technique for optimizing QoS is presented in [16]. On the other hand, a multilayer perception neural network (MPNN) is presented in [17] for delay reduction. Similarly, a neuro-fuzzy based technique is developed in [18] for QoS optimization.

In the medical field, the application of ML algorithms for prediction and classification is on the increase [1]. This is specifically the case for cancer prediction, owing to the multi-facet nature of this disease. Here, ML techniques are critical for the extraction of useful information from heterogeneous, complex and large clinical data [19]. As explained in [20], ML techniques are also significant for psychopathology risk algorithms that are critical for preventive intervention. For instance, supervised ML techniques are vital for internalizing disorder (ID) early detection. Although many ML schemes have been developed for medical diagnosis, there is need to optimize and improve these algorithms [21]. One such improvement is ensemble learning in which a classifier comprises of a set of individual classifiers that are coupled with techniques such as majority voting [22]. Here, the ensemble classifier amalgamates the predictions of individual classifiers, and hence exhibit better performance compared with individual classifiers [23-25]. This can be attributed to the utilization of various decision making systems that deploy numerous strategies. Consequently, an ensemble classifier benefits from performance of diverse classifiers as well as the diversity of errors [26].

In this paper, an ensemble ML algorithm is developed for enhanced diagnostics in the medical field. To evaluate the developed ensemble algorithm, it is applied in breast cancer (BC) data. The choice of BC is informed by the fact that cancer is one of the leading causes of deaths worldwide. According to [1], BC is one of the most common types of cancer, whose recurrence prognosis is critical for patient survival rate enhancement. Consequently, there is need for the early stage prediction of BC. Authors in [27] point out that ML algorithms improvement in terms of effectiveness has received much attention. However, many cancer cases are still being diagnosed late [28]. As such, the predictive models for cancer diagnosis need to exhibit extremely low error rates for effective early diagnosis and treatment. In this environment, a need arises for the medical dataset to be carefully managed, owing to its complex nature [29]. Any form of predication errors will have serious consequences, and hence the need for accuracy enhancement in ML algorithms. The major contributions of this paper include the following:

- Neighbour Components Analysis (NCA) is deployed for feature selection so as to identify and eliminate irrelevant or redundant features.
- Five predictive models are formulated, trained and tested on the Wisconsin Diagnostic Breast Cancer (WDBC) dataset.
- A number of performance metrics are developed and deployed to evaluate the developed predictive models.
- The results show that the ensemble classifier comprising of KNN, SVM, DT and NB exhibits the best performance compared to individual classifiers.

The rest of this paper is organized as follows: Section 2 details related work in machine learning algorithms and diagnosis, while Section 3 outlines the adopted system model. On the other hand, Section 4 presents the results and discussion of these results, while Section 5 concludes the paper and gives future directions.

2. Related Work

The deployment of machine learning algorithms for diagnostics has received much attention among medical practitioners. As such, numerous schemes have been presented in literature. For instance, neural network based ensemble classifier has been presented in [30] for heart failure detection, yielding high classification accuracy. On the other hand, authors in [1] have applied Random Forest (RF), Linear regression (LR), Multi-layer Perceptron (MLP) and Decision Trees (DT) for breast cancer prediction, with MLP yielding the best performance. Similarly, ANN, DT, support vector machines (SVMs), Naive Bayes(NB), and K-Nearest neighbor (KNN) have

been deployed for medical diagnosis [31]. Among these, ANN is noted to be the best in capturing correlations among attributes. A nested ensemble learning algorithm is developed in [32] for breast cancer diagnosis, while an ensemble classifier for kidney stone prediction is introduced in [33]. Similarly, a tree ensemble model is developed in [34] for colorectal cancer survival prediction.

An ensemble learning scheme is presented in [35] for hepatitis disease diagnosis, with results showing that this classifier performed better than individual ANN, ANFIS, KNN and SVM classifiers. An ensemble deep learning algorithm is developed in [36] for heart disease prediction, while an ensemble classifier comprising of Logistic Regression (LR), RF, Adaboost and KNN is introduced in [37] for diabetic retinopathy dataset classification. The results showed that ensemble ML model performed better than individual ML algorithms. On the other hand, an ensemble learner consisting of multiple deep convolutional neural networks (CNNs) is developed in [38] for pulmonary nodules classification. Similarly, ensemble learning technique is presented in [39] for diabetes diagnosis, while semantic segmentation and ensemble learning have been introduced in [40] for cardiovascular pathology assessment.

Genetic algorithm (GA) and RF have been utilized in [41] for BC detection, while a deep ensemble learning scheme is developed in [24] for Alzheimer's disease (AD) prediction. Similarly, ensemble ML technique is introduced in [20] for internalizing disorders (ID) prediction, while an ensemble of neural network models is presented in [29] for Rheumatoid arthritis (RA) diagnosis. On the other hand, ensemble classifier is developed in [42] for heart disease prediction, while ensemble neural network models are utilized in [43] for medical captioning. An ensemble of deep learning and evolutionary computation is developed in [44] for coronary artery disease prediction, while an ensemble of Bagged Tree (BT), RF and AdaBoost is developed in [45] for heart disease prediction. In this classifier, Particle Swarm Optimization (PSO) is deployed for feature subset selection. The results showed that BT and PSO attained the highest accuracy. A hybrid of Fuzzy and KNN is deployed in [46] for heart disease prediction, while CNN model is amalgamated with recurrent neural network (RNN) in [47] for lung cancer prediction. An ensemble of CNN and RNN is developed in [48] for COVID-19 diagnosis, while a classifier combining CNNs and SVM is deployed in [49] for COVID-19 classification. On the other hand deep transfer learning scheme are coupled with three CNN models in [50] and [51] for COVID-19 diagnosis. Similarly, seven pre-trained CNN classifiers have been introduced in [52] for COVID-19 diagnosis from X-ray samples.

Apart from ensemble classifiers, other ML algorithms have also been deployed for diagnostics. For instance, an improved ML is presented in [53] for heart disease prediction, while SVM has been developed in [54] for heart valve diseases diagnosis. On the other hand, a deep RNN model is presented in [55] for prostate cancer diagnosis, while CNNs have been utilized in [56] and [57] for lung cancer prediction. A deep neural network is introduced in [58] for COVID-19 diagnosis. Similarly, a deep CNN is presented in [59] for COVID-19 diagnosis.

Although conventional ML techniques attain admirable classification accuracies in medical diagnoses, their performance diminishes when presented with imbalanced dataset. This is normally the case in detection of minority category [31]. In addition, numerous factors negatively impact the performance of current classification models when applied to real data [29]. Such issues include class imbalance of the training dataset, and hence these models are often biased towards majority class. Consequently, they are unable to generalize the learning process. Another challenge facing majority of the ML algorithms is the handling of high-dimensional datasets, owing to lack of a framework that employs diverse data sources [36]. In addition, the utilization of conventional feature selection techniques from a dataset based on their significance render them ineffective for disease diagnosis.

Although ensemble learning techniques perform exceptionally better than individual classifiers, optimum selection of diversity classifier members to form an ensemble, and the fusion of individual decisions of the base classifiers into a single decision present some challenges. On the other hand, the current deep learning feature extraction and classification models have limitations in both their feature extraction and weighting approaches. It is evident that major advances have been made in developing deep learning models, which are effective classifiers for detection of high-order data relationships to solve complex tasks. However, these models are curtailed by the fat-short property of transcript-based data, which negatively impact their cancer diagnosis effectiveness.

3. System Model

This section presents the description of the deployed dataset, data pre-processing steps, ensemble classifier model and experimentation.

3.1 DataSet Description

The Wisconsin Diagnostic Breast Cancer (WDBC)

dataset is utilized in this paper. It has 699 instances with 11 features as shown in Table 1.

Table 1. Summary of Attributes

Attribute number	Feature name	Domain
1	Sample code number	1-683
2	Clump Thickness	1-10
3	Uniformity of Cell Size	1-10
4	Uniformity of Cell Shape	1-10
5	Marginal Adhesion	1-10
6	Single Epithelial Cell Size	1-10
7	Bare Nuclei	1-10
8	Bland Chromatin	1-10
9	Normal Nucleoli	1-10
10	Mitoses	1-10
Y	Class	2 or 4

The class distribution comprises of 241 malignant (representing 34.48%) and 458 benign (representing 65.52%) subjects. On the other hand, the target label falls into two classes which include benign (2) or malignant (4).

3.2 Data Pre-processing

Prior to the classification process, data cleaning was executed to eliminate or lessen noise in the data. During this process, 16 instances for the *Bare Nuclei* feature were found to be missing and hence were eliminated from the dataset. In addition, the *Sample code number* and *Class* features are irrelevant during the classification process and hence are eliminated. Consequently, only 9 features and 683 instances remained, out of which 444 were benign while 239 were malignant. Table 2 gives the basic statistics (mean and standard deviation-std) of the remaining features.

Table 2. Attribute statistics

Feature name	Average	Std
Clump Thickness	4.44	2.82
Uniformity of Cell Size	3.15	3.07
Uniformity of Cell Shape	3.22	2.99
Marginal Adhesion	2.83	2.86
Single Epithelial Cell Size	3.23	2.22
Bare Nuclei	3.54	3.64
Bland Chromatin	3.45	2.45
Normal Nucleoli	2.87	3.05
Mitoses	1.60	1.73

To ensure that all features in the dataset have equal coefficients, the standard scalar was computed such that each feature has a mean of zero and variance of unity. This was followed by the Min-Max scalar computation that shifted the data in a way that all features have a domain of between zero and unity.

3.3 Ensemble Classifier Model

In this paper, an ensemble classifier is constructed, consisting of KNN, SVM, DT and NB. As shown in Figure 1, an ensemble model consists of K single classifiers and each single model has N inputs. As such, the entire model has $K*N$ input features and the output of this ensemble model is computed based on majority voting.

The classifiers of the proposed ensemble are individual KNN, DT, SVM and NB models. As such, four ensemble models can be established for classification, which include KNN ensemble (KNNE), DT ensemble (DTE), SVM ensemble (SVME) and NB ensemble (NBE). Consequently, the proposed ensemble model comprises of KNN, DT, SVM and NB classifiers. The DT model

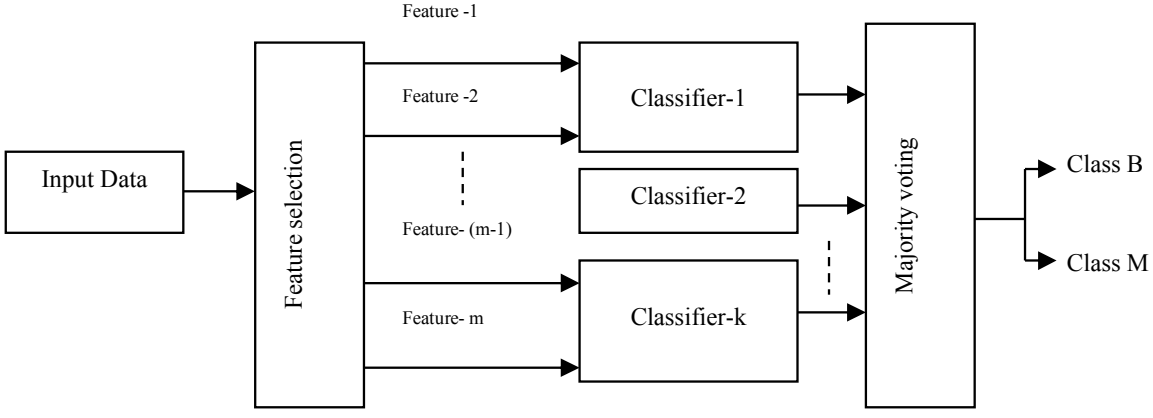

Figure 1. Generalized Ensemble Classifier

groups data samples based on numerous questions, where the root of the tree comprises of all data samples. Here, the tree is generated through a recursive process as shown in Algorithm 1.

Algorithm 1: Decision Tree Learning

BEGIN
Input: training set $T=\{(a_1, b_1), (a_2, b_2), (a_3, b_3), ..., (a_n, b_n)\}$,
feature set $F=\{f_1, f_2, f_3 ..., f_m\}$
function train (T, F)
create node K
IF $b_i = b_j (\quad b_i, b_i \in T)$ **OR** $a_i = a_j (\quad a_i, a_i \in T)$ **THEN**:
Label (K) = mode (b_j)
ENDIF
Select optimal partition attribute P
FOR every $Z \in P$:
derive a new branch $T_Z = \{a_i | a_i(P) = Z\}$
IF $T_Z = \emptyset$ **THEN:**
set branch T_Z as node K_Z
label (K_Z) = mode (b_i), $b_i \in T$
ELSE
function $(T_Z, F- P)$
ENDIF
ENDFOR
END

On the other hand, the NB algorithm is a probabilistic classification that derives its probability value by computing the frequency and value combinations from the dataset. The assumption made here is that all features are independent. Algorithm 2 gives the steps followed in this classification.

Algorithm 2: Naive Bayes Learning

BEGIN
Input: training set $T=\{(a_1, b_1), (a_2, b_2), (a_3, b_3), ..., (a_n, b_n)\}$,
feature set $F=\{f_1, f_2, f_3, ..., f_m\}$
FOR every $i \in m$ in class C:
read T
derive mean $\bar{Y}$ of F
compute standard deviation δ of F
ENDFOR
WHILE $i \leq m$ **DO:**
derive probability of f_i based on gauss density equation
ENDWHILE
FOR every $i \in m$ in class C:
Compute likelihood P_i for each C
ENDFOR
return maximum likelihood, P_{max}
END

On its part, the KNN is a non-parametric classification algorithm whose input comprises of k, which is positive integer representing the number of classes in the underlying dataset. Here, the classification of input data is based on the majority of its neighbours. Consequently, input data is assigned to a class that is higher in its k-nearest neighbours as shown in Algorithm 3. The Euclidean distance D is utilized to measure the distance between data points.

Algorithm 3: K-Nearest Neighbours Learning

BEGIN
Input: training set $T=\{(a_1, b_1), (a_2, b_2), (a_3, b_3), ..., (a_n, b_n)\}$,
feature set $F=\{f_1, f_2, f_3, ..., f_m\}$
positive integer, k
FOR every $i \in m$:
compute D (a_i, b_i)
ENDFOR
arrange computed Ds in ascending order
extract the first k Ds from this list
determine k-points corresponding to these k Ds
designate k_i as the number of points belonging to i^{th} class among k-points
IF $k_i > k_i \quad I \neq j$ **THEN:**
assign a to class i
ENDIF
END

On the other hand, SVM is a classification algorithm that employs subset of training data points in its decision function. These data points become support vectors and this algorithm has been demonstrated to be highly effective for high dimensional data. Algorithm 4 presents the steps necessary for the deployment of SVM.

Algorithm 4: Support Vector Machine Learning

BEGIN
Input: training set $T=\{(a_1, b_1), (a_2, b_2), (a_3, b_3), ..., (a_n, b_n)\}$,
feature set $F=\{f_1, f_2, f_3, ..., f_m\}$
initialize learning rate r
instantiate number of runs N
function train (T, F)
FOR r in N:
Error = 0;
FOR i in a:
IF $(b[i]*(a[i]*w)) < 1$ **THEN:**
update: $w=w + r * ((a[i]*(b[i]*(-2*(w * N^{-1})$
ELSE:
update: $w=w + r * (-2*(w * N^{-1})$
ENDIF
ENDFOR
ENDFOR
END

As already alluded, the ensemble model comprises of KNN, DT, SVM and NB whose algorithms have been presented above. The fifth ensemble model consists of some clusters of these classifiers as shown in Figure 2. In this ensemble model, the input features fed to individual classifiers are replicated and similar to each cluster.

In this paper, feature selection is executed using neighbour components analysis (NCA). The aim is to identify and eliminate irrelevant or redundant features so so as to remain with the most relevant ones. NCA was chosen due to its ability to maximize classification accuracy. It does this through dataset dimensionality reduction and hence achieves optimal objective function. Normally, the gradient-based optimizer is deployed for this purpose. Finally, the output of the ensemble model is obtained through majority voting strategy.

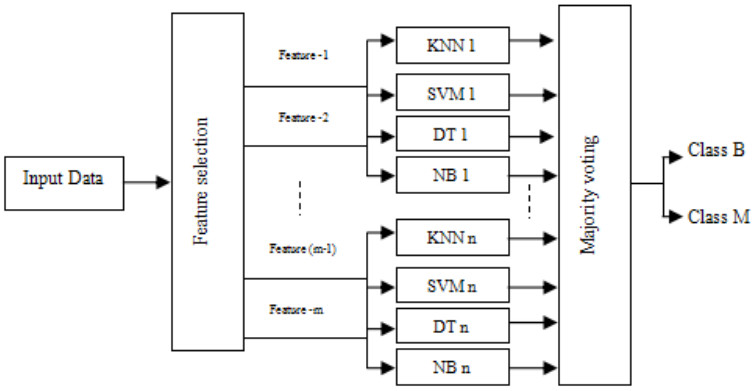

Figure 2. Proposed Ensemble Classifier

3.3 Experimentations

During training and testing process, the dataset was portioned into 80% training instances and 20% testing instances. The goal is to classify the tumor either as malignant or benign. Feature selection is then accomplished using NCA before individual models are trained, tested and deployed to classify the dataset. This was followed by the deployment of the proposed ensemble model to classify the same dataset as shown in Figure 3.

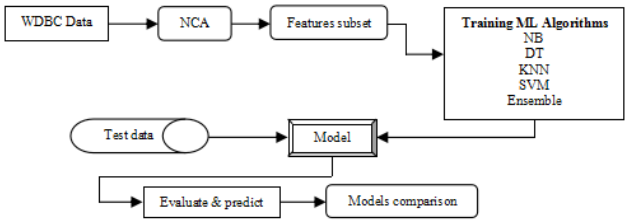

Figure 3. Flowchart of the Proposed Model

Thereafter, comparisons are executed to investigate the effectiveness of the proposed model. To accomplish this, accuracy, precision and recall are deployed as shown in Table 3.

Table 3. Performance Metrics

Metric	Formulation
Accuracy	$\frac{TP+TN}{TP+TN+FP+FN}$
Precision	$\frac{TP}{TP+FP}$
Recall	$\frac{TP}{TP+FN}$
F-measure	$\frac{2*Precision*Recall}{Precision+Recall}$

Here, TP is the true positive, TN is true negative, FP is false positive, and FN is false negative.

4. Results and Discussion

In this section, the training and testing results of the developed machine learning algorithms are presented. Table 4 shows the precision, recall and F-measure values obtained for the various classifiers. It is evident that the lowest value for precision was 94.21 which was recorded by NB classifier while the highest value for precision was 99.12 which belonged to the proposed ensemble classifier. Regarding recall, NB had the lowest value of 94.28 while the proposed ensemble classifier had the highest value of 99.45. On the other hand, 94.245 was the lowest F-measure value that was recorded by NB classifier while 99.285 was the highest F-measure value that was recorded by the proposed classifier.

Table 4. Performance Comparisons

Classifier	Precision	Recall	F-Measure
DT	95.07	95.23	95.150
SVM	98.15	98.26	98.205
NB	94.21	94.28	94.245
KNN	97.16	97.34	97.250
Ensemble	99.12	99.45	99.285

As shown in Figure 4, the proposed ensemble classifier had the highest values for precision, recall and F-measure. This was followed by SVM, KNN, DT and NB in that order. It is also clear that the values for recall remained the highest among other metrics in all the five classifiers.

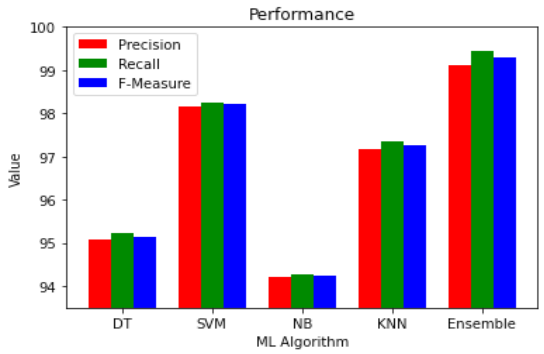

Figure 4. Performance Metrics Comparisons

Table 5 presents the values obtained for prediction accuracy during training and testing. It is clear from Table 5 that during training, the highest value of accuracy was 98.95% while the lowest value was 94.03. On the other hand, 99.27% accuracy was the highest during testing while 94.34% accuracy was the lowest during testing.

Table 5. Prediction Accuracy

Classifier	Prediction Accuracy (%)		
	Training	Testing	Overall
DT	93.65	94.91	94.280
SVM	97.98	98.56	98.270
NB	94.03	94.34	94.185
KNN	97.06	97.45	97.255
Ensemble	98.95	99.27	99.110

Based on Figure 5, NB classifier had the lowest overall classification accuracy of 94.185% while the proposed ensemble classifier had the highest overall classification accuracy of 99.11%. It is also evident that training had lower classification accuracy compared with testing phase.

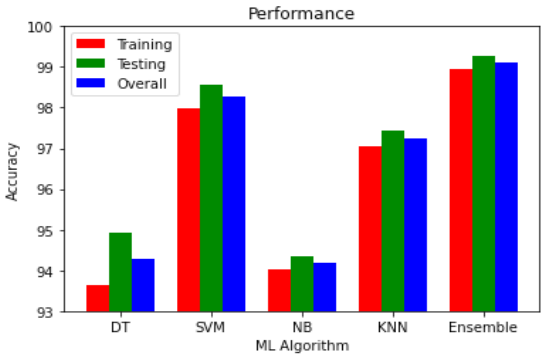

Figure 5. Prediction Accuracy Comparisons

This disparity can be attributed to the lower percentage of instances of 20% that are used during testing compared to 80% instances during training. To validate the proposed ensemble classification model, 10 folds cross validation was executed. To achieve this, the entire dataset is portioned in 10 equal sets. Next, 9 of these sets are deployed for training while the remaining 1 set is utilized for testing the model. This process is repeated ten times with each of the ten sub-samples being used at least once. The results obtained are depicted in Figure 6 below.

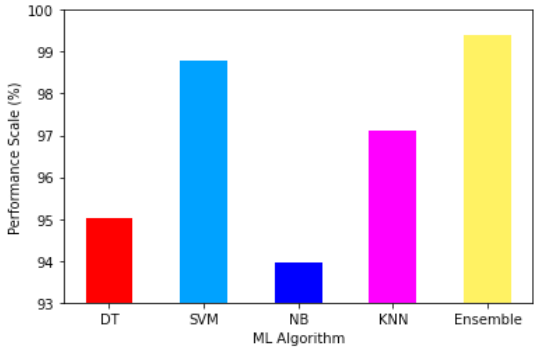

Figure 6. Cross Validation

It is evident from Figure 6 that NB classifier had the least performance of 93.96%, followed by DT, KNN, SVM and the proposed ensemble classifier with 95.02%, 97.11%, 98.79 and 99.39% respectively. Based on the results above, it is evident that the deployed NCA feature selection and majority voting in the proposed classifier boosted precision, recall, F-measure and classification accuracy. This explains the slightly better performance of the proposed ensemble classifier when compared with individual classifiers.

5. Conclusions

Many machine learning algorithms have been developed to aid in optimization, prediction and diagnostics. However, these machine learning algorithms have been noted to have numerous challenges that may impede their effectiveness. These challenges revolve around the feature selection methods, imbalanced datasets and inability of learning generalization, among other issues. For instance, ensemble models perform better than individual classifiers, but the ideal selection of diversity classifier members to construct an ensemble, and the fusion of individual decisions of the base classifiers into a single decision present some setbacks. On their part, deep learning models have issues with the deployed weighting schemes. Moreover, the fat-short property of transcript-based data reduces the prediction accuracies of some of the deep learning models. The developed ensemble classifier deploys a more effective feature selection technique to eliminate irrelevant features from the dataset. The results show that this ensemble classifier is more effective when compared to individual classifiers such as NB, KNN, DT and SVM. Future work lies in the testing

of the developed classifier in different datasets to validate its effectiveness.

References

[1] Gupta, M., Gupta, B., 2018. A comparative study of breast cancer diagnosis using supervised machine learning techniques. in 2018 second international conference on computing methodologies and communication (ICCMC), IEEE. 997-1002.

[2] Alkeshuosh, A.H., Moghadam, M.Z., Al Mansoori, I., Abdar, M., 2017. Using PSO Algorithm for Producing Best Rules in Diagnosis of Heart Disease. in 2017 International Conference on Computer and Applications (ICCA), IEEE. 306-311.

[3] Nyangaresi, V.O., Rodrigues, A.J., Abeka, S.O., 2020. Secure Handover Protocol for High Speed 5G Networks. Int. J. Advanced Networking and Applications. 11(06), 4429-4442.

[4] Rashad, T., Sudhir, A., 2019. Fuzzy-Neural based Cost Effective Handover Prediction Technique for 5G-IoT networks. International Journal of Innovative Technology and Exploring Engineering. 9(2S3), 191-197.

[5] Mahira, A.G., Subhedar, M.S., 2017. Handover decision in wireless heterogeneous networks based on feed forward artificial neural network. in Computational Intelligence in Data Mining, Springer, Singapore. 663-669.

[6] Nyangaresi, V.O., Abeka, S.O., Rodgrigues, A., 2018. Secure Timing Advance Based Context-Aware Handover Protocol for Vehicular Ad-Hoc Heterogeneous Networks. International Journal of Cyber-Security and Digital Forensics. 7(3), 256-275.

[7] Wafa, B., Adnane, L., Vicent, P., 2019. Applying ANFIS Model in Decision-making of Vertical Handover between Macrocell and Femto-cell Integrated Network. Journal of Telecommunication, Electronic and Computer Engineering. 11(1), 57-62.

[8] Azzali, F., Ghazali, O., Omar, M.H., 2017. Fuzzy Logic-based Intelligent Scheme for Enhancing QoS of Vertical Handover Decision in Vehicular Ad-hoc Networks. International Research and Innovation Summit (IRIS2017). 226, 1-12.

[9] Nyangaresi, V.O., Abeka, S.O., Rodrigues, A.J., 2020. Delay Sensitive Protocol for High Availability LTE Handovers. American Journal of Networks and Communications. 9(1), 1-10.

[10] Shanmugam, K., 2017. A novel candidate network selection based handover management with fuzzy logic in heterogeneous wireless networks. in 4th International Conference on Advanced Computing and Communication Systems (ICACCS), IEEE. 1-6.

[11] Aibinu, A., Onumanyi, J.A., Adedigba, P., Ipinyomi, M., Folorunso, T., Salami, M., 2017. Development of hybrid artificial intelligent based handover decision algorithm. Int. J. Eng. Sci. Technol. 20(2), 381-390.

[12] Nyangaresi, V.O., Rodrigues, A.J., Abeka, S.O., 2020. ANN-FL secure handover protocol for 5G and beyond networks. in International Conference on e-Infrastructure and e-Services for Developing Countries, Springer, Cham. 99-118.

[13] Zineb, A., Ayadi, M., Tabbane, S., 2017. QoE-based vertical handover decision management for cognitive networks using ANN. in Proceedings of the 2017 Sixth International Conference on Communications and Networking (ComNet), IEEE. 1-7.

[14] Eman, Z., Amr, A., Abdelkerim, T., Abdelhalim, Z., 2018. A novel vertical handover algorithm based on Adaptive Neuro-Fuzzy Inference System (ANFIS). International Journal of Engineering & Technology. 7(1), 74-78.

[15] Nyangaresi, V.O., Rodrigues, A.J., 2022. Efficient handover protocol for 5G and beyond networks. Computers & Security. 113, 102546.

[16] Pragati, K., Haridas, S.L., 2019. Reducing Ping-Pong Effect in Heterogeneous Wireless Networks Using Machine Learning. Intelligent Communication, Control and Devices. 697-705.

[17] Jamal, F.A., Firudin, K.M., 2017. Direction prediction assisted handover using the multilayer perception neural network to reduce the handover time delays in LTE networks. in 9th International Conference on Theory and Application of Soft Computing, Computing with Words and Perception, Procedia Computer Science. 120, 719-727.

[18] Nyangaresi, V.O., Rodrigues, A.J., Abeka, S.O., 2020. Neuro-Fuzzy Based Handover Authentication Protocol for Ultra Dense 5G Networks. in 2020 2nd Global Power, Energy and Communication Conference (GPECOM), IEEE. 339-344.

[19] Eshtay, M., Faris, H., Obeid, N., 2018. Improving extreme learning machine by competitive swarm optimization and its application for medical diagnosis problems. Expert Syst. Appl. 104, 134-152.

[20] Rosellini, A.J., Liu, S., Anderson, G.N., Sbi, S., Tung, E.S., Knyazhanskaya, E., 2020. Developing algorithms to predict adult onset internalizing disorders: An ensemble learning approach. Journal of psychiatric research. 121, 189-196.

[21] Sevakula, R.K., Verma, N.K., 2017. Assessing generalization ability of majority vote point classifiers. IEEE Transactions on Neural Networks and Learning

Systems. 28(12), 2985-97.

[22] Miao, K.H., Miao, J.H., Miao, G.J., 2016. Diagnosing coronary heart disease using ensemble machine learning. Int J Adv Comput Sci Appl (IJACSA). 7(10), 1-12.

[23] Li, H., Cui, Y., Liu, Y., Li, W., Shi, Y., Fang, C., Lu, Y., 2018. Ensemble learning for overall power conversion efficiency of the all-organic dye-sensitized solar cells. IEEE Access. 6, 34118-34126.

[24] An, N., Ding, H., Yang, J., Au, R., Ang, T.F., 2020. Deep ensemble learning for Alzheimer's disease classification. Journal of biomedical informatics. 105, 103411.

[25] Sun, J., Lang, J., Fujita, H., Li, H., 2018. Imbalanced enterprise credit evaluation with DTE-SBD: Decision tree ensemble based on SMOTE and bagging with differentiated sampling rates. Inf. Sci. 425,76-91.

[26] Zhang, X., Mahadevan, S., 2019. Ensemble machine learning models for aviation incident risk prediction. Decis. Support Syst. 116, 48-63.

[27] Mittal, D., Gaurav, D., Roy, S.S., 2015. An effective hybridized classifier for breast cancer diagnosis. in 2015 IEEE international conference on advanced intelligent mechatronics (AIM), IEEE,1026-1031.

[28] Jiang, J., Li, X., Zhao, C., Guan, Y., Yu, Q., 2017. Learning and inference in knowledge-based probabilistic model for medical diagnosis. Knowledge-Based Systems. 138, 58-68.

[29] Baccouche, A., Garcia-Zapirain, B., Castillo Olea, C., Elmaghraby, A., 2020. Ensemble Deep Learning Models for Heart Disease Classification: A Case Study from Mexico. Information. 11(4), 207.

[30] Wang, L., Zhou, W., Chang, Q., Chen, J., Zhou, X., 2019. Deep Ensemble Detection of Congestive Heart Failure using Short-term RR Intervals. IEEE Access. 7, 69559-69574.

[31] Liu, N., Li, X., Qi, E., Xu, M., Li, L., Gao, B., 2020. A novel Ensemble Learning Paradigm for Medical Diagnosis with Imbalanced Data. IEEE Access. 8, 171263-171280.

[32] Abdar, M., Zomorodi-Moghadam, M., Zhou, X., Gururajan, R., Tao, X., Barua, P.D., Gururajan, R., 2020. A new nested ensemble technique for automated diagnosis of breast cancer. Pattern Recognit. Lett. 132, 123-131.

[33] Kazemi, Y., Mirroshandel, S.A., 2018. A novel method for predicting kidney stone type using ensemble learning. Artif. Intell. Med. 84, 117-126.

[34] Wang, Y., Wang, D., Ye, X., Wang, Y., Yin, Y., Jin, Y., 2019. A tree ensemble based two-stage model for advanced-stage colorectal cancer survival prediction. Inf. Sci. 474, 106-124.

[35] Nilashi, M., Ahmadi, H., Shahmoradi, L., Ibrahim, O., Akbari, E., 2019. A predictive method for hepatitis disease diagnosis using ensembles of neuro-fuzzy technique. Journal of infection and public health. 12(1), 13-20.

[36] Ali, F., El-Sappagh, S., Islam, S.R., Kwak, D., Ali, A., Imran, M., Kwak, K.S., 2020. A smart healthcare monitoring system for heart disease prediction based on ensemble deep learning and feature fusion. Information Fusion. 63, 208-222.

[37] Reddy, G.T., Bhattacharya, S., Ramakrishnan, S.S., Chowdhary, C.L., Hakak, S., Kaluri, R., Reddy, M.P.K., 2020. An ensemble based machine learning model for diabetic retinopathy classification. in 2020 international conference on emerging trends in information technology and engineering (ic-ETITE), IEEE. 1-6.

[38] Zhang, B., Qi, S., Monkam, P., Li, C., Yang, F., Yao, Y.D., Qian, W., 2019. Ensemble learners of multiple deep CNNs for pulmonary nodules classification using CT images. IEEE Access. 7, 110358-110371.

[39] Han, L., Luo, S., Yu, J., Pan, L., Chen, S., 2015. Rule extraction from support vector machines using ensemble learning approach: an application for diagnosis of diabetes. IEEE Journal of Biomedical and Health Informatics. 19(2), 728-34.

[40] Lindsey, T., Lee, J.J., 2020. Automated Cardiovascular Pathology Assessment Using Semantic Segmentation and Ensemble Learning. Journal of digital imaging. 1-6.

[41] Aličković, E., Subasi, A., 2017. Breast cancer diagnosis using GA feature selection and Rotation Forest. Neural Computing and Applications. 28(4), 753-763.

[42] Esfahani, H.A., Ghazanfari, M., 2017. Cardiovascular disease detection using a new ensemble classifier. in Proceedings of the 2017 IEEE 4th International Conference on Knowledge-Based Engineering and Innovation (KBEI), Tehran, Iran. 1011-1014.

[43] Yu, Y., Lin, H., Meng, J., Wei, X., Zhao, Z., 2017. Assembling deep neural networks for medical compound figure detection. Information. 8, 48.

[44] Pławiak, P., Acharya, U.R., 2020. Novel deep genetic ensemble of classifiers for arrhythmia detection using ECG signals. Neural Computing and Applications. 32(15), 11137-11161.

[45] Yekkala, I., Dixit, S., Jabbar, M.A., 2017. Prediction of heart disease using ensemble learning and Particle Swarm Optimization. in 2017 International Conference On Smart Technologies For Smart Nation (SmartTechCon), IEEE. 691-698.

[46] Krishnaiah, V., Srinivas, M., Narsimha, G., Chandra, N.S., 2014. Diagnosis of heart disease patients using fuzzy classification technique. in International Conference on Computing and Communication Technologies, IEEE. 1-7.

[47] Moitra, D., Mandal, R.K., 2019. Automated AJCC staging of non-small cell lung cancer (NSCLC) using deep convolutional neural network (CNN) and recurrent neural network (RNN). Health information science and systems. 7(1), 1-12.

[48] Islam, M.M., Islam, M.Z., Asraf, A., Ding, W., 2021. Diagnosis of COVID-19 from X-rays using combined CNN-RNN architecture with transfer learning. MedRxiv. 2020-08.

[49] Sethy, P.K., Behera, S.K., Ratha, P.K., Biswas, P., 2020. Detection of Coronavirus Disease (COVID-19) based on Deep Features and Support Vector Machine. International Journal of Mathematical Engineering and Management Sciences. 643-651.

[50] Narin, A., Kaya, C., Pamuk, Z., 2021. Automatic detection of coronavirus disease (covid-19) using x-ray images and deep convolutional neural networks. Pattern Analysis and Applications. 1-14.

[51] Loey, M., Smarandache, F., M Khalifa, N.E., 2020. Within the lack of chest COVID-19 X-ray dataset: a novel detection model based on GAN and deep transfer learning. Symmetry. 12(4), 651.

[52] Hemdan, E.E.D., Shouman, M.A., Karar, M.E., 2020. COVIDX-Net: A Framework of Deep Learning Classifiers to Diagnose COVID-19 in X-Ray Images, arXiv. 2003, 11055.

[53] Mienye, I.D., Sun, Y., Wang, Z., 2020. An improved ensemble learning approach for the prediction of heart disease risk. Informatics in Medicine Unlocked. 20, 100402.

[54] Tjahjadi, H., Ramli, K., 2020. Noninvasive Blood Pressure Classification Based on Photoplethysmography Using K-Nearest Neighbors Algorithm: A Feasibility Study. Information. 11, 93.

[55] Azizi, S., Bayat, S., Yan, P., Tahmasebi, A., Kwak, J.T., Xu, S., Abolmaesumi, P., 2018. Deep recurrent neural networks for prostate cancer detection: analysis of temporal enhanced ultrasound. IEEE transactions on medical imaging. 37(12), 2695-2703.

[56] Rossetto, A.M., Zhou, W., 2017. Deep learning for categorization of lung cancer CT images. in 2017 IEEE/ACM international conference on connected health: applications, systems and engineering technologies (CHASE), IEEE, Philadelphia, PA. 272-273.

[57] Coudray, N., Ocampo, P.S., Sakellaropoulos, T., Narula, N., Snuderl, M., Fenyö, D., Moreira, A.L., Razavian, N., Tsirigos, A., 2018. Classification and mutation prediction from non-small cell lung cancer histopathology images using deep learning. Nature medicine. 24(10), 1559-1567.

[58] Punn, N.S., Agarwal, S., 2021. Automated diagnosis of COVID-19 with limited posteroanterior chest X-ray images using fine-tuned deep neural networks. Applied Intelligence. 51(5), 2689-2702.

[59] Khan, M.A., 2020. An IoT Framework for Heart Disease Prediction Based on MDCNN Classifier. IEEE Access. 8, 34717-34727.

BILINGUAL PUBLISHING CO.
Pioneer of Global Academics Since 1984

Journal of Computer Science Research
https://ojs.bilpublishing.com/index.php/jcsr

CORRECTION

Correction to: Determining Learning Style Preferences of Learners

Sushil Shrestha* **Manish Pokharel**

Digital Learning Research Lab, Department of Computer Science and Engineering, Kathmandu University, Nepal

Published Online: 25 January 2022

The online version of the original article can be found at https://doi.org/10.30564/jcsr.v3i1.2761

The correct Table 7 is as follows:

Table 7. Aggregation of cluster value weight of learning style [24]

		Active			
		Very weak (0)	**Weak (1)**	**Moderate (2)**	**Strong (3)**
Reflective	**Very weak (0)**	Balanced	Moderate Active	Strong Active	Strong Active
	Weak(-1)	Moderate Reflective	Balanced	Moderate Active	Strong Active
	Moderate(-2)	Strong Reflective	Moderate Reflective	Balanced	Moderate Active
	Strong(-3)	Strong Reflective	Strong Reflective	Moderate Reflective	Balanced
		Visual			
		Very weak (0)	**Weak (1)**	**Moderate (2)**	**Strong (3)**
Verbal	**Very weak (0)**	Balanced	Moderate Visual	Strong Visual	Strong Visual
	Weak(-1)	Moderate Verbal	Balanced	Moderate Visual	Strong Visual
	Moderate(-2)	Strong Verbal	Moderate Verbal	Balanced	Moderate Visual
	Strong(-3)	Strong Verbal	Strong Verbal	Moderate Verbal	Balanced

*Corresponding Author:
Sushil Shrestha,
Digital Learning Research Lab, Department of Computer Science and Engineering, Kathmandu University, Nepal;
Email: sushil@ku.edu.np

DOI: https://doi.org/10.30564/jcsr.v4i1.4400

References

[24] Hmedna, B., El Mezouary, A., Baz, O., 2020. A predictive model for the identification of learning styles in MOOC environments. Cluster Comput. 23, 1303-1328.
DOI: https://doi.org/10.1007/s10586-019-02992-4

BILINGUAL PUBLISHING CO.
Pioneer of Global Academics Since 1984

Journal of Computer Science Research
https://ojs.bilpublishing.com/index.php/jcsr

ARTICLE

A Case Study of Mobile Health Applications: The OWASP Risk of Insufficient Cryptography

Suzanna Schmeelk[1*] Lixin Tao[2]

1. St. John's University, United States
2. Pace University, United States

ARTICLE INFO

Article history
Received: 25 December 2021
Accepted: 9 February 2022
Published Online: 24 February 2022

Keywords:
OWASP mobile threats
Cryptography
Mobile application
mHealth
Healthcare
Android

ABSTRACT

Mobile devices are being deployed rapidly for both private and professional reasons. One area of that has been growing is in releasing healthcare applications into the mobile marketplaces for health management. These applications help individuals track their own biorhythms and contain sensitive information. This case study examines the source code of mobile applications released to GitHub for the Risk of Insufficient Cryptography in the Top Ten Mobile Open Web Application Security Project risks. We first develop and justify a mobile OWASP Cryptographic knowledge-graph for detecting security weaknesses specific to mobile applications which can be extended to other domains involving cryptography. We then analyze the source code of 203 open source healthcare mobile applications and report on their usage of cryptography in the applications. Our findings show that none of the open source healthcare applications correctly applied cryptography in all elements of their applications. As humans adopt healthcare applications for managing their health routines, it is essential that they consider the privacy and security risks they are accepting when sharing their data. Furthermore, many open source applications and developers have certain environmental parameters which do not mandate adherence to regulations. In addition to creating new free tools for security risk identifications during software development such as standalone or compiler-embedded, the article suggests awareness and training modules for developers prior to marketplace software release.

1. Introduction

Smart mobile devices such as phones and tablets are being integrated rapidly into human life. The device usages range in mobility in that some are carried around daily for communications and others rest standalone to coordinate and provide human interaction for smart devices. Mobile applications are therefore employed for a wide-range of activities. The software assurance and resulting security risks of these mobile applications continue to

*Corresponding Author:
Suzanna Schmeelk,
St. John's University, United States;
Email: schmeels@stjohns.edu

DOI: https://doi.org/10.30564/jcsr.v4i1.4271

increase every year far out pacing legal regulations and ethical data training for the storage, use, and transfer of such private and sensitive information.

This paper explores building a knowledge-graph specific to mobile-device applications for the mobile risk of insufficient cryptography which can result in the loss of both data confidentiality and integrity. We report on a software assurance case study of healthcare specific mobile applications hosted on GitHub with respect to the OWASP Mobile Risk of Insecure Cryptography. Specifically we examine Android Java application source code as Android is reported to have over 2.8 billion active users with a global market share of 75 percent [1]. In fact, Curry [1] reports that over one billion Android smartphones were shipped in 2020. The loss of healthcare data confidentiality and integrity is further exacerbated with the fact that mobile applications can be connected to device identifiers and subsequently tracked. These aspects add higher degrees of risk to humans storing data and communicating information with mobile device applications.

2. Literature Review

Literature related to the OWASP Top 10 mobile risk of insufficient cryptography spans at least three pillars: software assurance, weakness analysis with ontology development, and other mobile device cryptography studies.

2.1 Cryptography Software Assurance

Software assurance specifically cryptographic best practices for software development one domain of literature for developing higher degrees of software assurance. A. M. Braga and R. Dahab [2] propose a methodology for development of secure cryptographic software agnostic to any programming language. The methodology is designed to provide a structured way to approach cryptography into secure development methods. The research is useful to inform the software development process and lifecycle.

Haney, Garfinkel, and Theofanos [3] identified challenges organizations face when developing cryptographic products. They are conducting a web-based survey of 121 individuals representing organizations involved in the development of products that include cryptography. The research found that participants used cryptography for a wide range of purposes, with most relying on generally accepted, standards-based implementations as guides. Their surveys reported on participants developing their own cryptography implementations by drawing on non-standard based resources during their development and testing processes. These results show that perhaps due to the lack of adequate resources and standardized training, cryptographic development and software assurance remains challenging to implement correctly.

Damanik and Sunaringtyas [4] reviewed the Open Web Application Security Testing Guide to determine and defend vulnerabilities identified in a web application, Sistem Informasi Akademik dan Pengasuhan (SIAP). Their research was specific to one particular web application.

2.2 Cryptography Ontologies and Weaknesses

The development of known cryptographic weaknesses and ontologies is another literature domain. Bojanova, Black, Yesha [5] reported on Cryptography Classes in Bugs Framework (BF): Encryption Bugs (ENC), Verification Bugs (VRF), and Key Management Bugs (KMN) but building a novel BF ontology with cryptography concerns at the National Institute of Standards and Technology (NIST). The ontology is currently updated and is linked to related risks identified in the Common Weakness Enumeration (CWE) [6], for example the 'CWE-780 Use of RSA Algorithm without OAEP.' The NIST BF encryption ontology remains under development and is agnostic to mobile devices.

Similar to categorizing weaknesses as in the CWE, the Common Vulnerability Enumeration (CVE) is a MITRE program to identify, define, and catalog publicly disclosed cybersecurity vulnerabilities. Lazar, Chen, Wang, and Zeldovich [7] examined reports to the 269 cryptographic vulnerabilities reported in the MITRE CVE from January 2011 to May 2014. Their results show that 17% of the bugs were in cryptographic libraries, and 83% of the reports were individual application misuses of cryptographic libraries. Overall, properly implementing cryptographic libraries and APIs remains a challenge across many domains.

2.3 Mobile Application Cryptography Studies

Mobile application research studies for the improvement of cryptography have been researched in the past few years. As cryptographic best practices change nearly annually, study reanalysis is necessary to keep pace with the changing cryptographic landscape. Egele, Brumley, Fratantonio, and Kruegel [8] introduced a static analysis tool CryptoLint to automatically check programs on the Google Play marketplace. They found that 88% applications of employing cryptographic APIs did not implement cryptography correctly.

Shuai, Guowei, Tao, Tianchang and Chenjie [9] introduced Cryptography Misuse Analyzer (CMA). Gao, Kong, Li, Bissyandé, and Klein [10] introduced CogniCryptSAST. Singleton, R. Zhao, M. Song and H. Siy, [11] introduced

FIREBugs. These static analysis tools were built to identify weaknesses in cryptography development based on best practices of that timeframe.

Gajrani, Tripathi, Laxmi, Gaur, Conti, and Rajarajan [12] introduce sPECTRA as an automated framework for analyzing wide range of cryptographic vulnerabilities in Android finding that 90% of the applications analyzed had cryptographic weaknesses.

As cryptography industry requirements change rapidly with changes to language APIs and the identification of both novel attacks and found weaknesses, actual weakness identification through static analysis tool pattern matching also must be updated to reflect the changing industry landscape causing the need for program reanalysis based on current best practices, regulations, and industry needs.

3. OWASP Top Mobile Risk Ontologies

The Open Web Application Security Project (OWASP) is a nonprofit foundation that works to improve the security of software with global participation and collaboration. The organization creates a forum for industry, academic, and government leads to discuss current best computing practices. One of the projects maintained by OWASP is a list of the reported Top 10 Mobile Risks to mobile applications. The list notes security concerns for mobile applications' data, internal/external device communications, among other risks. The actual OWASP risks have remained since the last publication in 2016. The last risk iteration was a variation from the risks reported in 2014. Although the risks remain the same, the supporting OWASP best practice guidance appears to be dynamically updated periodically. We develop a knowledge graph based on the OWASP guidance. A useful attribute of knowledge graphs is that they can expand with time so that we can see what has changed in security concerns over time. Building such a domain graph aids both software assurance tools and techniques. Deprecated security concerns can easily be traced in the graph along with design changes benefiting all phases of the secure software development lifecycle (sSDLC).

3.1 2014 Threat 6: Broken Cryptography

The OWASP 2014 Mobile Threat 6 is Broken Cryptography. Broken cryptography can potentially lead to data compromise in both confidentiality and integrity. To control data confidentiality, cryptography is primarily implemented with key-centric encryption/decryption methodologies. To mitigate from data integrity risks, cryptography can be used to generate cryptographic message digests to numerically validate data. These techniques coexist with repudiation techniques, for example with digital signatures.

Other security concerns in the CIA-model revolve around data and service availability. Availability is typically controlled with other primary mitigation controls; however, if there exists a lack of direct mitigating controls, further cryptographic weaknesses further expose services breaking defense-in-depth.

Figure 1 shows our knowledge graph for the OWASP threat of Broken Cryptography, labeled *M6_Broken_Cryptography*. Since the knowledge graph for the OWASP threat of Broken Cryptography is extensive, we review each sub-tree from Figure 1 in different figures, specifically Figures 2-9. Figure 1 is shown to give a full overview of the breadth and inter-connections for the OWASP threat.

From the perspective of an application, there are four main relationships for insufficient cryptography. First, insufficient cryptography can potentially *resultFrom* device specific issues such as compromised hardware. In addition, insufficient cryptography can *resultFrom* cryptography application programming interface (API) weaknesses or misuses. Third, insufficient cryptography can *resultFrom* improper key generation and management. Forth, broken cryptography can *resultFrom* entirely not using cryptography when it is needed.

Cryptography algorithms with weak environment parameters, shown in Figure 2, can cause higher security risks. The mobile threat of broken cryptography due to the implementation of a weak parameters can *resultFrom* from four main issues. First, cryptographic parameters such as weak initialization vector (IV) and improper salts will increase the risk of the output cipher text to be easily decoded. Second, weak algorithms [13] (e.g. DES, 3DES, SHA1, MD5) are known to have exploits and have been deprecated by industry and the U.S. Federal government. Third, weak key generation (e.g. less than 128-bits, non-random, etc.) and management are also known susceptible to brute force attacks [14]. Fourth, other predictable environment components such as imported flawed libraries or flawed cryptographic providers are means for security concerns. These four predominate issues can cause weak cryptographic output increasing the risk of information exposure to the loss of integrity and confidentiality.

Improperly implemented cryptography algorithms, shown in Figure 3, can cause higher security risks. Two main groups of algorithms that fall into this category are improperly implemented message digests and ciphers. Figure 4 shows sample best practice code for encryption from the Carnegie Mellon University Software Engineering Institute rules and recommendations [13].

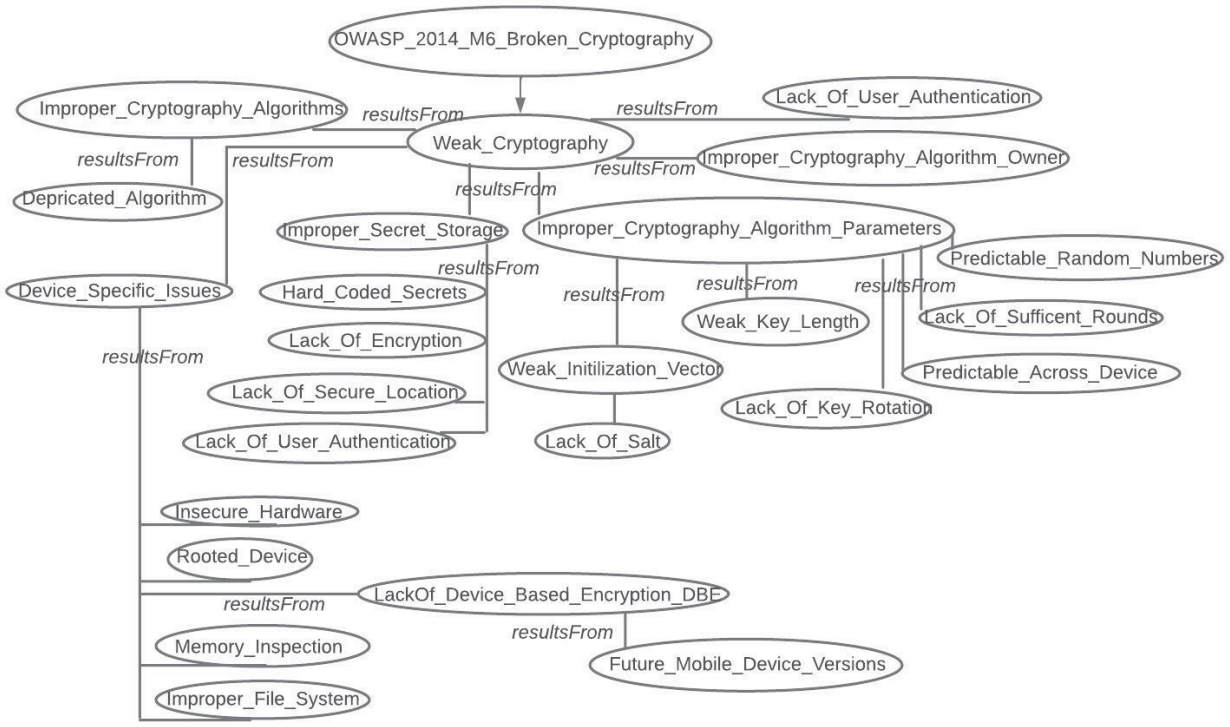

Figure 1. OWASP Mobile 2014 Threat: Broken Cryptography

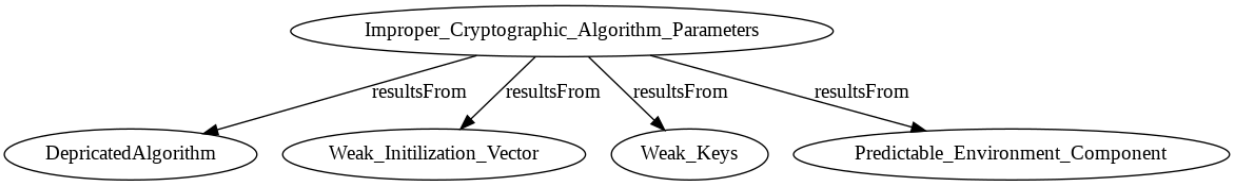

Figure 2. Improper_Cryptographic_Algorithm_Parameters

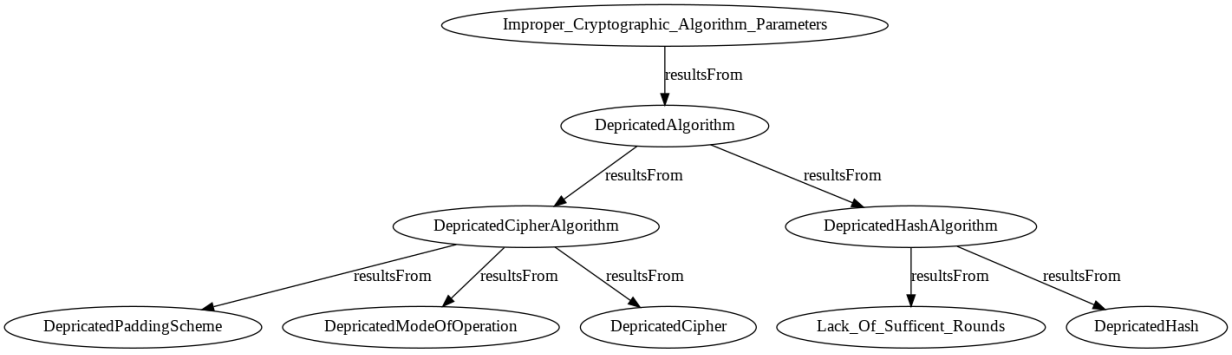

Figure 3. Deprecated Algorithm Parameters

Five common risks can be specific to devices, our knowledge-graph can be seen in Figure 5. Although we show the relationship with broken cryptography in our knowledge graph, software analysis of these underlying concerns breaking cryptography are directions for future research. First, a common device specific concern is related to hardware—either directly through compromised hardware, or indirectly through a side channel attack on the system power analysis. This issue is difficult to detect in a mobile application unless a watchdog application is involved but it faces similar issues. Insufficient hardware-specific power constraints can also cause in-

effective cryptography. Devices can linger on networks for many years [18]. Device platforms may not be able to keep up with modern cryptographic requirements for multiple reasons [19]. Second, a rooted or jail-broken device compromises application access controls. In such cases, applications should detect that they are running on a compromised system. Third, tools that harvest keys and passwords from memory are another device specific concern. Fourth, and improperly constructed file system for data storage can result in broken cryptography. Lastly, lack of device and/or file based encryption can also cause broken cryptography.

Figure 4. Condensed CMU SEI AES Implementation [13]

Insufficient cryptography can also arise from not properly encrypting certain sensitive data (i.e. physical domain). This lack of sufficient cryptography can occur on an endpoint communication channel during transmission. This lack of sufficient cryptography can occur on device without device based encryption (DBE) as DBE is a feature of only Android 5 [20]. Google has also issued a warning for pre-Android5 devices which have been upgraded, "Caution: Devices upgraded to Android 5.0 and then encrypted may be returned to an unencrypted state by factory data reset." [20] DBE will be deprecated in future versions of Android, perhaps due to performance constraints [86]. Google currently has posted, "Caution: Support for full-disk encryption is going away. If you're creating a new device, you should use file-based encryption." [21] This lack of sufficient cryptography can occur on a file without file based encryption (FBE) [22]. Google has already issued OS version specific issues in relation to FBE. For example, the Android Application API currently reads, "Caution: On devices running Android 7.0-8.1, file-based encryption can't be used together with adoptable storage [22]". On devices using FBE, new storage media (such as an external card) must be used as traditional storage. Devices running Android 9 and higher can use adoptable storage and FBE [22].

Cipher keys and passwords are known to have software assurance concerns for different reasons, as shown in Figure 6. First, keys may not be stored correctly (e.g. in Android KeyStore [14]) and therefore subject to compromise. An example of such a broken scenario is when a cryptographic key or password is stored in plaintext on a shared space next to the encrypted data.

Weak keys are known to cause other insufficient cryptographic problems. Second, the key derivation function may not be best practice, based on cryptographic random numbers, or have sufficient iterations. Third, the key length changes with industry best practices based on computational power. In such cases, legacy systems relying on shorter keys increase the risk around real time brute force attempts [15]. Finally, key rotations may not follow best practices.

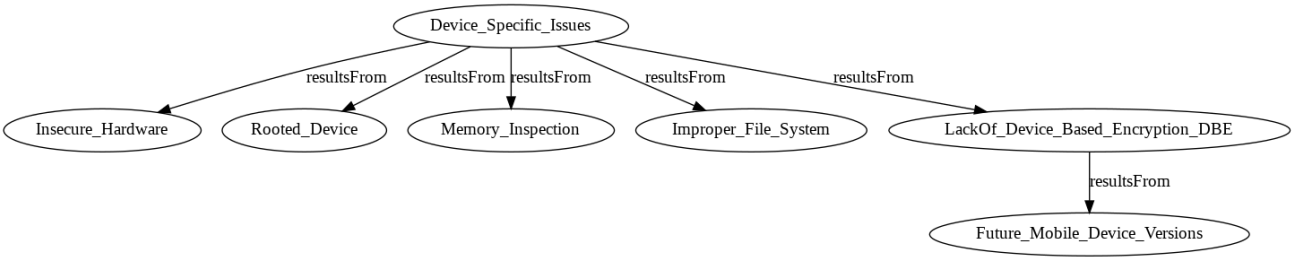

Figure 5. Device Specific Issue

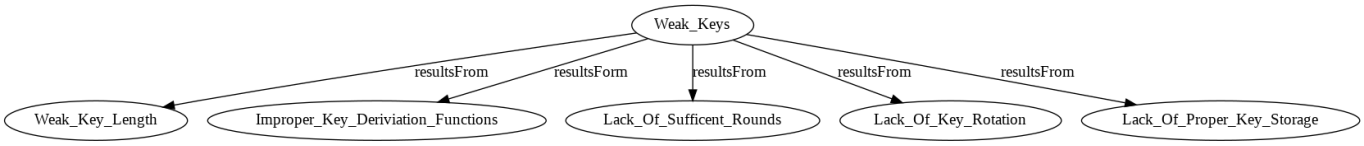

Figure 6. Knowledge graph for weak keys concerns

```
public static SecretKey generateKey() {
try {
 KeyGenerator kgen =
 KeyGenerator.getInstance("AES");
 kgen.init(256);
 return kgen.generateKey();
 } catch (NoSuchAlgorithmException e)
{ throw new
IllegalStateException(e.toString());} }
```

Figure 7. Condensed CMU SEI Key Generation [14]

CMU SEI [16] provides an example of a more secure implementation for storing passwords. Software can be analyzed by employing static analysis techniques (e.g. context sensitive analysis, string analysis, variable propagation, etc.) to detect the concerns on to password algorithms, iterations, salts, and other issues.

```
final class Password {
private SecureRandom random = …
private final int SALT_BYTE_LENGTH = 12;
private final int ITERATIONS = 100000;
private final String ALGORITHM =
"PBKDF2WithHmacSHA256";
/* Set password to new value, zeroing … */
void setPassword(char[] pass)  throws …
byte[] salt = new
byte[SALT_BYTE_LENGTH];
random.nextBytes(salt);
saveBytes(salt, "salt.bin");
byte[] hashVal = hashPassword(pass, salt); …
} ...
/* Encrypts password & salt and zeroes both */
private byte[] hashPass (char[] pass, byte[]
salt)
throws GeneralSecurityException {
KeySpec spec = new PBEKeySpec(pass, salt,
ITERATIONS); …
SecretKeyFactory f =
SecretKeyFactory.getInstance(ALGORITHM);
return f.generateSecret(spec).getEncoded();} ...
```

Figure 8. Condensed CMU Passwords Implementation [16]

3.2 2016 Threat 5: Insufficient Cryptography

The OWASP 2016 Mobile Threat Insufficient Cryptography (IC) is the fifth risk, labeled in Figure 9 as *OWASP_2016_M5_Insufficient_Cryptography*. The 2016 threat has the same implications as the 2014 [17]. The knowledge graph shows that the same general cryptographic concerns from 2014 directly translates into the risks of 2016, unlike many other risks from 2014 that were rearranged, removed, or merged together in the 2016 OWASP list. Differences between the years lie in identified weaknesses within the ciphers, digests, devices, and key management.

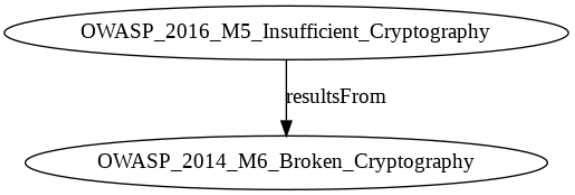

Figure 9. OWASP 2016 M5 Insufficient Cryptography

In summary, we have identified sub-areas where software assurance methodologies can be developed and improved to detect the OWASP Mobile Threat of Insufficient Cryptography. The standard Android encryption API calls include creating keys, encrypting, and decrypting, are all detectable using assurance methodologies such as program analysis.

4. Analysis Results

We examined the source code of 203 mobile applications written to store, track, and communicate healthcare related data. Healthcare data is typically sensitive information and is only regulated under certain conditions. For example, research shows that HIPAA and HITECH only apply to covered entities [23]. For data not covered under HIPAA, the FCC becomes involved when breaches affect > 500 individuals [24]. Smaller mobile applications, which may only serve a small population segment, may not fall under any regulations.

Specifically, we examined the source code of healthcare applications with publicly available source code to gain a sense of how they were implementing cryptography, if at all, in their programs.

The analyzed applications stored health data for many health-related concerns including mental health, pregnan-

cy, exercise management, hypertension, among other sensitive issues.

In total, we examined each application based on the knowledge-graphs reported in Section 3 to gain insights into these applications' source code confidentiality and integrity security for data-at-rest. We applied pattern-matching criteria to identify source code with concerns reported in our knowledge-graph.

Our main finding was that some of the 203 mobile applications made attempts at data-at-rest cryptography but were unsuccessful in perfectly implementing all data-at-rest knowledge graph elements reported in Section 3. These weaknesses in implementation cause a breakdown in confidentiality and integrity for people storing, using, and transmitting their health data with any of these applications.

4.1 Application Cryptography Utilization

Historically there have been two main packages in the Oracle Application Programming Interface (API) for Java cryptographic implementations. The message digests (hash) functions, secure random number generator for cryptography, certificates, key management implementations are contained in the java.security packages, known as the Java Cryptography Architecture (JCA). The key generation, agreement, and cipher algorithms are contained in the javax.crypto package, known as the Java Cryptography Extension (JCE). "Prior to JDK 1.4, the JCE was an unbundled product, and as such, the JCA and JCE were regularly referred to as separate, distinct components. As JCE is now bundled in the JDK, the distinction is becoming less apparent. Since the JCE uses the same architecture as the JCA, the JCE should be more properly thought of as a part of the JCA. [25]" When analyzing source code, one key indicator of properly implemented cryptography is by employing the standard Oracle API. Implementing one's own cryptographic algorithms can be successful but is highly prone to error.

Of the 203 mobile application source code analyzed, 25 imported the Oracle API cryptography libraries in their java source code, with three of these applications importing only cryptography policies, keys, or crypto related exceptions rather than importing libraries needed for cipher and/or hash algorithms. Analysis showed that a few source repositories may contain cryptography within embedded mobile application bytecode and is outside the scope of this research due to its low-likelihood that it adequately protects the confidentiality and integrity of the contained healthcare data.

4.2 Proper Confidentiality Implementations

Confidentiality mitigation implementation which results in low risk of data exposure have many elements that need to be satisfied as reported in Section 3. In this section we report on the 22 mobile applications which imported the proper cryptography libraries. Of these 22 applications, only 10 applications imported JCE extensions. We report on these 10 applications cryptography implementations in the following subsections.

4.2.1 Proper Cipher Algorithms

One important aspect to properly implementing cryptography is to employ the non-deprecated ciphers. Sheth [26] and CMU SEI [27] indicated that AES remains a compliant symmetric key algorithm for storing data-at-rest. Other properly implemented algorithms such as RSA are not entirely wrong given certain data-exchange use cases but may not be the best choice meeting same-device data-at-rest requirements. One application did interface with a blockchain therefore an RSA implementation could be needed. Of the 10 applications which imported JCE libraries, 6 applications employed the AES (5 apps) only, RSA (1 app) only, and 2 applications used both AES and RSA algorithms. One application employed DES algorithm which has been deprecated for years. The remainder either had their own encryption generation or did not import JCE libraries for encryption.

4.2.2 Proper Cipher Modes

In general, a cipher mode of operation lowers risks of generating predictable ciphertext. Sheth [26] reports on GCM and CBC mode as having lower risks from cryptanalyses attacks. The JCR currently supports other non-best practice mode operations, perhaps for legacy systems. Of the six applications that implemented non-deprecated ciphers, only four had known proper cipher modes implemented. Two applications relied on the defaults by employing either Cipher.getInstance ("AES") or "RSA" which do not default to best practices as guided by CMU SEI [27]. Four applications properly implemented the symmetric cipher mode. One of these four proper implementations also had an improper implementation of their key storage using the symmetric algorithm with transformation string "AES/ECB/PKCS5Padding" for key storage rather than storing a salted hash of the password as described by CMU SEI in Figure 7. Of the three applications with RSA implementations, one application employed the default "RSA" mode, one employed "ECB" mode, and one employed "NONE" mode subject to conflicting RSA

mode guidance.

4.2.3 Proper Cipher Padding.

Padding schemes can be employed to pad cleartext into acceptable cipher algorithm block sizes. Sheth [26] reports the best practice of employing PKCS5Padding or OAEP-With* padding schemas, although the JCR supports other non-best practice padding schemas. Of the applications with properly implemented modes, only one application properly implemented one of these padding schema.

4.2.4 Other Confidentiality Parameters

Other best practice parameters to consider during the encryption processes are employing cryptographically random numbers as initialization vectors (IVs) (i.e., nonces) [28,29]. Sheth [26] advised to make sure only a small number of plaintexts are encrypted with the same key and IV pair. The one application which properly implemented the symmetric cipher transformations string did not initialize the cipher with a cryptographically random IV therefore not implementing cryptography correctly.

4.3 Proper Integrity Implementations

We examined all 203 applications for proper data integrity implementations. Integrity risks can be mitigated through the use of cryptographic hash algorithms. In cases where data is changing on a regular basis and cannot be properly compared against a known duplicate, non-deprecated hash algorithms are essential to protect data integrity. In the case of these applications which do not contain data snapshot cryptographic hashes, non-deprecated algorithms are essential. In addition, when storing cryptographic password hashes, best practice mandates minimum generation iterations (e.g. NIST [30] standards identify a minimum of 10,000 iterations based on computing resources), certain creation algorithms, and adding randomness via salting.

4.3.1 Proper Message Digest Algorithms

Current best-practices mandate SHA2 (with SHA-512 or higher) or SHA3 family of cryptographic hash algorithms. We identified only 11 applications employing cryptographic hash algorithms, but all using MD5, SHA1, or other SHA algorithms below SHA-512 for integrity needs. Therefore, we were unable to identify any applications with proper cryptographic message digest algorithms.

4.3.2 Other Integrity Parameters

Other integrity parameters to consider are needed when storing cryptographic password hashes as reported by CMU SEI in Figure 7. In such cases, the salting and iterations are essential along with proper algorithms. We identified only one application attempting to store passwords correctly. The application applied a secure password generation algorithm of PBKDF2, but it was applied with only 100 iterations, which is below industry best practice standards such as NIST's recommendation of at least 10,000 iterations [30].

4.4. Other Cryptographic Issues

During application analysis we identified some other ancillary cryptographic issues within the mobile application source code. These findings may more appropriately belong in the OWASP secure storage knowledge-graph discussion, but since they include cryptographic techniques, we will reference the issues. We identified two applications which had upgraded their internal database from the standard SQLite database that comes with the device to instead implement a more secure version, the *net.sqlcipher* SQLiteDatabase [31]. This particular implementation claims to add cryptography to the database so that stored information is not stored in plaintext as it is in the standard SQLite database. The library analysis of the *sqlcipher* database cryptography usage and respective key management is outside the scope of this research. A knowledge graph is ideal for representing hybrid security concerns where mitigations overlap such as cryptographically secure storage implementations, where if any part of the secure implementation contains weaknesses, the overall concept will be of high risk.

5. Future Work

Best practice cryptographic implementations require community effort in maintain. Ancillary concerns such as cryptographic key generation and management and cryptography in commonly imported libraries are areas of future research. Similarly, cryptography encompasses certain aspects of data-in-motion however, there remains a vague distinction between the OWASP top ten threat of insufficient cryptography and other OWASP top ten threats, such as that of insecure communications. Knowledge-graphs can be useful to show longitudinal relationships between security concerns. These are other areas of future research. Lastly, the case study shows the importance of building

new tools and techniques to aid the secure software development lifecycle to identify weaknesses in cryptographic implementations and provide secure software training—whether developer or penetration testing. Currently, for example, penetration testing remains an art rather than science since the field lacks standardization. The creation of knowledge-graphs can be useful to provide standardization and to add risk ratings to inform sector-wide risk likelihoods. There remains a lot of further research to develop such standardized security ontologies.

6. Conclusions

This research examined the OWASP Top Ten mobile device security threats focusing on the OWASP Mobile Application Threat of insufficient cryptography. We first contributed the development of mobile device specific knowledge graph for insufficient cryptography. From the knowledge-graph we analyzed 203 mobile device applications source code uploaded to GitHub. The analyzed applications where healthcare applications that collect sensitive human information such mental health, exercise routines, pregnancy indicators, skin photographs, and other important body information needed for health. We were unable to identify any application that properly implemented confidentiality and integrity needs.

As our world becomes more interconnected, it is essential that we build more robust tools to identify privacy and security weaknesses. Many different software and software developers at large, such as developers of free healthcare applications, are neither required by regulations to implement security features nor have access, awareness, or training for such security features. The industry need has become dire for creating access to security training and tools to develop more secure applications especially when applications store extremely sensitive information about humans greatly affecting both their own lives and those of their family.

Conflict of Interest

The authors declare no conflict of interest.

References

[1] Curry, D., 2021. Android Statistics (2021) https://www.businessofapps.com/data/android-statistics

[2] Braga, A.M., Dahab, R., 2016. Towards a Methodology for the Development of Secure Cryptographic Software. 2016 International Conference on Software Security and Assurance (ICSSA). pp. 25-30. DOI: https://doi.org/10.1109/ICSSA.2016.12.

[3] Haney, J.M., Garfinkel, S.L., Theofanos, M.F., 2017. Organizational practices in cryptographic development and testing. 2017 IEEE Conference on Communications and Network Security (CNS). pp. 1-9. DOI: https://doi.org/10.1109/CNS.2017.8228643.

[4] Nanisura Damanik, V.N., Sunaringtyas, S.U., 2020. Secure Code Recommendation Based on Code Review Result Using OWASP Code Review Guide. 2020 International Workshop on Big Data and Information Security (IWBIS). pp. 153-158. DOI: https://doi.org/10.1109/IWBIS50925.2020.9255559.

[5] Bojanova, I., Black, P.E., Yesha, Y., September 25-28, 2017. Cryptography Classes in Bugs Framework (BF): Encryption Bugs (ENC), Verification Bugs (VRF), and Key Management Bugs (KMN). IEEE Software Technology Conference (STC 2017), NIST, Gaithersburg, USA.

[6] MITRE, 2021. CWE-780 Use of RSA Algorithm without OAEP. https://cwe.mitre.org/data/definitions/780.html

[7] Lazar, D., Chen, H.G., Wang, X., Zeldovich, N., 2014. Why does cryptographic software fail? a case study and open problems. In Proceedings of 5th Asia-Pacific Workshop on Systems (APSys '14). Association for Computing Machinery, New York, NY, USA. Article 7, 1-7. DOI: https://doi.org/10.1145/2637166.2637237

[8] Egele, M., Brumley, D., Fratantonio, Y., Kruegel, Ch., 2013. An empirical study of cryptographic misuse in android applications. In Proceedings of the 2013 ACM SIGSAC conference on Computer & communications security (CCS '13). Association for Computing Machinery, New York, NY, USA. pp. 73-84. DOI: https://doi.org/10.1145/2508859.2516693

[9] Shuai, S., Guowei, D., Tao, G., Tianchang, Y., Chenjie, S., 2014. Modelling Analysis and Auto-detection of Cryptographic Misuse in Android Applications. 2014 IEEE 12th International Conference on Dependable, Autonomic and Secure Computing. pp. 75-80. DOI: https://doi.org/10.1109/DASC.2014.22.

[10] Gao, J., Kong, P., Li, L., Bissyandé, T.F., Klein, J., 2019. Negative Results on Mining Crypto-API Usage Rules in Android Apps. 2019 IEEE/ACM 16th International Conference on Mining Software Repositories (MSR). pp. 388-398. DOI: https://doi.org/10.1109/MSR.2019.00065.

[11] Singleton, L., Zhao, R., Song, M., Siy, H., 2019. FireBugs: Finding and Repairing Bugs with Security Patterns. 2019 IEEE/ACM 6th International Conference on Mobile Software Engineering and Systems (MOBILESoft). pp. 30-34. DOI: https://doi.org/10.1109/MOBILESoft.2019.00014.

[12] Gajrani, J., Tripathi, M., Laxmi, V., Gaur, M.S., Conti, M., Rajarajan, M., 2017. sPECTRA: A precise framework for analyzing cryptographic vulnerabilities in Android apps. 2017 14th IEEE Annual Consumer Communications & Networking Conference (CCNC). pp. 854-860.
DOI: https://doi.org/ 10.1109/CCNC.2017.7983245.

[13] CMU SEI, 2021. MSC61-J. Do not use insecure or weak cryptographic algorithms https://wiki.sei.cmu.edu/confluence/display/java/MSC61-J.+Do+not+use+insecure+or+weak+cryptographic+algorithms

[14] Sabt, M., Traore, J., 2016. Breaking Into the KeyStore: A Practical Forgery Attack Against Android KeyStore. in 21st European Symposium on Research in Computer Security (ESORICS), Heraklion, Greece.

[15] Sincerbox, C., March/April 2014. Security Sessions: Exploring Weak Ciphers. [Online]. Available: https://electricenergyonline.com/energy/magazine/779/article/Security-Sessions-Exploring-Weak-Ciphers.htm

[16] CMU SEI, 2021. MSC62-J. Store passwords using a hash function https://wiki.sei.cmu.edu/confluence/display/java/MSC62-J.+Store+passwords+using+a+hash+function.

[17] OWASP, 2021. Mobile Top 10 2016-M5-Insufficient Cryptography. [Online]. Available: https://www.owasp.org/index.php/Mobile_Top_10_2016-M5-Insufficient_Cryptography.

[18] Cole, S., October 30 2018. New Study Suggests People Are Keeping Their Phones Longer Because There's Not Much Reason to Upgrade. [Online]. Available: https://www.wsj.com/articles/upgrade-no-thanks-americans-are-sticking-with-their-old-phones-1540818000.

[19] Henry, J., 3 August 2018. 3DES is Officially Being Retired. [Online]. Available: https://www.cryptomathic.com/news-events/blog/3des-is-officially-being-retired.

[20] Google, 26 January 2019. Full-Disk Encryption. [Online]. Available: https://source.android.com/security/encryption/full-disk.

[21] Google, 26 January 2019. Encryption. [Online]. Available: https://source.android.com/security/encryption.

[22] Google, 1 January 2019. File-Based Encryption. [Online]. Available: https://source.android.com/security/encryption/file-based.

[23] HHS, 2021. Covered Entities and Business Associates. https://www.hhs.gov/hipaa/for-professionAls/covered-entities/index.html

[24] FTC, 2021. Health Breach Notification Rule. https://www.ftc.gov/enforcement/rules/rulemaking-regulatory-reform-proceedings/health-breach-notification-rule

[25] Oracle, 2021. Java SE 14 Security Developer's Guide. https://docs.oracle.com/en/java/javase/14/security/java-cryptography-architecture-jca-reference-guide.html

[26] Mansi Sheth, 2017. Encryption and Decryption in Java Cryptography. https://www.veracode.com/blog/research/encryption-and-decryption-java-cryptography

[27] CMU SEI, 2021. DRD17-J. Do not use the Android cryptographic security provider encryption default for AES https://wiki.sei.cmu.edu/confluence/display/android/DRD17-J.+Do+not+use+the+Android+cryptographic+security+provider+encryption+default+for+AES

[28] CMU SEI, 2021. MSC63-J. Ensure that SecureRandom is properly seeded https://wiki.sei.cmu.edu/confluence/display/java/MSC63-J.+Ensure+that+SecureRandom+is+properly+seeded

[29] CMU SEI, 2021. MSC02-J. Generate strong random numbers. https://wiki.sei.cmu.edu/confluence/display/java/MSC02-J.+Generate+strong+random+numbers

[30] Grassi, P., Fenton, J., Newton, E., Perlner, R., Regensheid, A., Burr, W., Richer, J., 2017. National Institute of Standards and Technology (NIST) Special Publication 800-63B https://pages.nist.gov/800-63-3/sp800-63b.html

[31] Zetetic LLC, 2021. android-database-sqlcipher https://github.com/sqlcipher/android-database-sqlcipher

BILINGUAL PUBLISHING CO.
Pioneer of Global Academics Since 1984

Journal of Computer Science Research
https://ojs.bilpublishing.com/index.php/jcsr

ARTICLE

Periodic Solution for a Complex-Valued Network Model with Discrete Delay

Chunhua Feng*

Department of Mathematics and Computer Science, Alabama State University, Montgomery, AL, 36104, USA

ARTICLE INFO

Article history
Received: 21 January 2022
Accepted: 16 February 2022
Published Online: 28 February 2022

Keywords:
Complex-valued neural network model
Delay
Periodic solution

ABSTRACT

For a tridiagonal two-layer real six-neuron model, the Hopf bifurcation was investigated by studying the eigenvalue equations of the related linear system in the literature. In the present paper, we extend this two-layer real six-neuron network model into a complex-valued delayed network model. Based on the mathematical analysis method, some sufficient conditions to guarantee the existence of periodic oscillatory solutions are established under the assumption that the activation function can be separated into its real and imaginary parts. Our sufficient conditions obtained by the mathematical analysis method in this paper are simpler than those obtained by the Hopf bifurcation method. Computer simulation is provided to illustrate the correctness of the theoretical results.

1. Introduction

Recently, various complex-valued network models with or without time delays have been studied [1-4,6-20]. For example, Ji et al. have investigated the following complex-valued Wilson-Cowan neural network model:

$$\begin{aligned} w_1'(t) &= -w_1(t) + a_1 g\big(w_1(t)\big) + a_2 g\big(w_2(t-\tau)\big) + P \\ w_2'(t) &= -w_2(t) + a_3 g\big(w_1(t-\tau)\big) + a_4 g\big(w_2(t)\big) + Q \end{aligned} \tag{1}$$

By using proper translations and coordinate transformations, system (1) has been decomposed the functions $g(w_1)$, $g(w_2)$ and a_1, a_2, a_3, a_4 into their real and imaginary parts, thus an equivalent real-valued system has been constructed. Then, the sufficient conditions for the Hopf bifurcation and its directions were provided [1]. Hang et al. have investigated a two-node network system as follows [2]:

$$\begin{aligned} D^q z_1(t) &= -\mu_1 z_1(t) + af\big(z_1(t-\tau)\big) + bf\big(z_2(t-\tau)\big) \\ D^q z_2(t) &= -\mu_2 z_2(t) + cf\big(z_1(t-\tau)\big) + df\big(z_2(t-\tau)\big) \end{aligned} \tag{2}$$

About the dynamical behaviors, local asymptotical stability and the Hopf bifurcation were studied, the important conditions of emergence of bifurcation were also given. Li et al. [3]extended a real-valued network model into a complex-valued model as the following:

*Corresponding Author:
Chunhua Feng,
Department of Mathematics and Computer Science, Alabama State University, Montgomery, AL, 36104, USA;
Email: cfeng@alasu.edu

DOI: https://doi.org/10.30564/jcsr.v4i1.4374

$$\begin{aligned} z_1'(t) &= -z_1(t) + b_{11} f_{11}\left(z_1(t-\tau)\right) + b_{12} f_{12}\left(\int_{-\infty}^{t} F(t-s)\, z_2(s)\, ds\right) \\ z_2'(t) &= -z_2(t) + b_{21} f_{21}\left(z_1(t-\tau)\right) + b_{22} f_{22}\left(\int_{-\infty}^{t} F(t-s)\, z_2(s)\, ds\right) \end{aligned} \quad (3)$$

Regarding the discrete time delay as the bifurcating parameter, the problem of the Hopf bifurcation in the newly-proposed complex-valued neural network model was investigated under the assumption that the activation function can be separated into its real and imaginary parts. Based on the normal form theory and center manifold theorem, some sufficient conditions which determine the direction of the Hopf bifurcation and the stability of the bifurcating periodic solutions were established. Zhang et al. have considered a complex value delayed Hopfield neural networks model [4]:

$$\begin{aligned} z_1'(t) &= (a+ib)\, z_1(t) + (c+id) f\left(z_2(t)\right) + (m+in) f\left(w_1(t-\tau)\right) \\ z_2'(t) &= (a+ib)\, z_2(t) + (c+id) f\left(z_3(t)\right) + (m+in) f\left(w_2(t-\tau)\right) \\ z_3'(t) &= (a+ib)\, z_3(t) + (c+id) f\left(z_4(t)\right) + (m+in) f\left(w_3(t-\tau)\right) \\ z_4'(t) &= (a+ib)\, z_4(t) + (c+id) f\left(z_1(t)\right) + (m+in) f\left(w_4(t-\tau)\right) \\ w_1'(t) &= (a+ib)\, w_1(t) + (c+id) f\left(w_2(t)\right) + (m+in) f\left(z_1(t-\tau)\right) \\ w_2'(t) &= (a+ib)\, w_2(t) + (c+id) f\left(w_3(t)\right) + (m+in) f\left(z_2(t-\tau)\right) \\ w_3'(t) &= (a+ib)\, w_3(t) + (c+id) f\left(w_4(t)\right) + (m+in) f\left(z_3(t-\tau)\right) \\ w_4'(t) &= (a+ib)\, w_4(t) + (c+id) f\left(w_1(t)\right) + (m+in) f\left(z_4(t-\tau)\right) \end{aligned} \quad (4)$$

By using the basic bifurcation theory of delay differential equations, and the theory of Lie groups, the authors have discussed the bifurcating periodic solutions. The existence of multiple branches of the bifurcating periodic solution was also provided.

In this paper, we extend a real six-neuron network [5] to the following complex-valued model:

$$\begin{aligned} z_1'(t) &= -(a_1+ib_1) z_1(t) + (m_{14}+in_{14}) f_{14}\left(z_4(t-\tau)\right) + (m_{15}+in_{15}) f_{15}\left(z_5(t-\tau)\right) \\ z_2'(t) &= -(a_2+ib_2) z_2(t) + (m_{24}+in_{24}) f_{24}\left(z_4(t-\tau)\right) + (m_{25}+in_{25}) f_{25}\left(z_5(t-\tau)\right) \\ &\quad + (m_{26}+in_{26}) f_{26}\left(z_6(t-\tau)\right) \\ z_3'(t) &= -(a_3+ib_3) z_3(t) + (m_{35}+in_{35}) f_{35}\left(z_5(t-\tau)\right) + (m_{36}+in_{36}) f_{36}\left(z_6(t-\tau)\right) \\ z_4'(t) &= -(a_4+ib_4) z_4(t) + (m_{41}+in_{41}) f_{41}\left(z_1(t-\tau)\right) + (m_{42}+in_{42}) f_{42}\left(z_2(t-\tau)\right) \\ z_5'(t) &= -(a_5+ib_5) z_5(t) + (m_{51}+in_{51}) f_{51}\left(z_1(t-\tau)\right) + (m_{52}+in_{52}) f_{52}\left(z_2(t-\tau)\right) \\ &\quad + (m_{53}+in_{53}) f_{53}\left(z_3(t-\tau)\right) \\ z_6'(t) &= -(a_6+ib_6) z_6(t) + (m_{62}+in_{62}) f_{62}\left(z_2(t-\tau)\right) + (m_{63}+in_{63}) f_{63}\left(z_3(t-\tau)\right) \end{aligned} \quad (5)$$

where $z_j = x_j + iy_j$, a_j, b_j, m_{kj}, n_{kj} are real numbers, f_{kj} are activation functions, $k, j = 1, 2, \ldots, 6$. We will discuss the dynamic behavior of the solutions of system (5).

We point out that the bifurcating method is not easy to deal with system (5) if all a_j, b_j, m_{kj}, n_{kj} are different real numbers. In this paper, by means of the mathematical analysis method, we discuss the periodic oscillation for system (5). For convenience, let $f_{kj}\left(z_j(t-\tau)\right) = f_{kj}^{R}\left(x_j(t-\tau), y_j(t-\tau)\right) + if_{kj}^{I}\left(x_j(t-\tau), y_j(t-\tau)\right) = f_{kj}^{R} + f_{kj}^{I}$ ($z_j = x_j + iy_j$, $k, j = 1, 2, \ldots, 6$).

Then the complex-valued system (5) can be expressed by separating it into real and imaginary parts as the following:

$$\begin{aligned} x_1'(t) &= -a_1 x_1(t) + b_1 y_1(t) + m_{14} f_{14}^{R} - n_{14} f_{14}^{I} + m_{15} f_{15}^{R} - n_{15} f_{15}^{I} \\ y_1'(t) &= -b_1 x_1(t) - a_1 y_1(t) + n_{14} f_{14}^{R} + m_{14} f_{14}^{I} + n_{15} f_{15}^{R} + m_{15} f_{15}^{I} \\ x_2'(t) &= -a_2 x_2(t) + b_2 y_2(t) + m_{24} f_{24}^{R} - n_{24} f_{24}^{I} + m_{25} f_{25}^{R} - n_{25} f_{25}^{I} + m_{26} f_{26}^{R} - n_{26} f_{26}^{I} \\ y_2'(t) &= -b_2 x_2(t) - a_2 y_2(t) + n_{24} f_{24}^{R} + m_{24} f_{24}^{I} + n_{25} f_{25}^{R} + m_{25} f_{25}^{I} + n_{26} f_{26}^{R} + m_{26} f_{26}^{I} \\ x_3'(t) &= -a_3 x_3(t) + b_3 y_3(t) + m_{35} f_{35}^{R} - n_{35} f_{35}^{I} + m_{36} f_{36}^{R} - n_{36} f_{36}^{I} \\ y_3'(t) &= -b_3 x_3(t) - a_3 y_3(t) + n_{35} f_{35}^{R} + m_{35} f_{35}^{I} + n_{36} f_{36}^{R} + m_{36} f_{36}^{I} \\ x_4'(t) &= -a_4 x_4(t) + b_4 y_4(t) + m_{41} f_{41}^{R} - n_{41} f_{41}^{I} + m_{42} f_{42}^{R} - n_{42} f_{42}^{I} \\ y_4'(t) &= -b_4 x_4(t) - a_4 y_4(t) + n_{41} f_{41}^{R} + m_{41} f_{35}^{I} + n_{42} f_{42}^{R} + m_{42} f_{42}^{I} \\ x_5'(t) &= -a_5 x_5(t) + b_5 y_5(t) + m_{51} f_{51}^{R} - n_{51} f_{51}^{I} + m_{52} f_{52}^{R} - n_{52} f_{52}^{I} + m_{53} f_{53}^{R} - n_{53} f_{53}^{I} \\ y_5'(t) &= -b_5 x_5(t) - a_5 y_5(t) + n_{51} f_{51}^{R} + m_{51} f_{51}^{I} + n_{52} f_{52}^{R} + m_{52} f_{25}^{I} + n_{53} f_{53}^{R} + m_{53} f_{53}^{I} \\ x_6'(t) &= -a_6 x_6(t) + b_6 y_6(t) + m_{62} f_{62}^{R} - n_{62} f_{62}^{I} + m_{63} f_{63}^{R} - n_{63} f_{63}^{I} \\ y_6'(t) &= -b_6 x_6(t) - a_6 y_6(t) + n_{62} f_{62}^{R} + m_{62} f_{62}^{I} + n_{63} f_{63}^{R} + m_{63} f_{63}^{I} \end{aligned} \quad (6)$$

Therefore, in order to discuss the periodic solution of model (5), we only consider the periodic solution of system (6). Suppose that the derivative of $f_{kj}^{R}\left(x_j, y_j\right)$ $f_{kj}^{R}\left(x_j, y_j\right)$ with respect to x_j and y_j exist, continuous, and $f_{kj}^{R}(0,0) = 0$, $f_{kj}^{I}(0,0) = 0$. Then the linearized system of (6) is the following:

$$\begin{aligned} x_1'(t) &= -a_1 x_1(t) + b_1 y_1(t) + p_{14} x_4(t_\tau) + q_{14} y_4(t_\tau) + p_{15} x_5(t_\tau) + q_{15} y_5(t_\tau) \\ y_1'(t) &= -b_1 x_1(t) - a_1 y_1(t) + c_{14} x_4(t_\tau) + d_{14} y_4(t_\tau) + c_{15} x_5(t_\tau) + d_{15} y_5(t_\tau) \\ x_2'(t) &= -a_2 x_2(t) + b_2 y_2(t) + p_{24} x_4(t_\tau) + q_{24} y_4(t_\tau) + p_{25} x_5(t_\tau) + q_{25} y_5(t_\tau) \\ &\quad + p_{26} x_6(t_\tau) + q_{26} y_6(t_\tau) \\ y_2'(t) &= -b_2 x_2(t) - a_2 y_2(t) + c_{24} x_4(t_\tau) + d_{24} y_4(t_\tau) + c_{25} x_5(t_\tau) + d_{25} y_5(t_\tau) \\ &\quad + c_{26} x_6(t_\tau) + d_{26} y_6(t_\tau) \\ x_3'(t) &= -a_3 x_3(t) + b_3 y_3(t) + p_{35} x_5(t_\tau) + q_{35} y_5(t_\tau) + p_{36} x_6(t_\tau) + q_{36} y_6(t_\tau) \\ y_3'(t) &= -b_3 x_3(t) - a_3 y_3(t) + c_{35} x_5(t_\tau) + d_{35} y_5(t_\tau) + c_{36} x_6(t_\tau) + d_{36} y_6(t_\tau) \\ x_4'(t) &= -a_4 x_4(t) + b_4 y_4(t) + p_{41} x_1(t_\tau) + q_{41} y_1(t_\tau) + p_{42} x_2(t_\tau) + q_{42} y_2(t_\tau) \\ y_4'(t) &= -b_4 x_4(t) - a_4 y_4(t) + c_{41} x_1(t_\tau) + d_{41} y_1(t_\tau) + c_{42} x_2(t_\tau) + d_{42} y_2(t_\tau) \\ x_5'(t) &= -a_5 x_5(t) + b_5 y_5(t) + p_{51} x_1(t_\tau) + q_{51} y_1(t_\tau) + p_{52} x_2(t_\tau) + q_{52} y_2(t_\tau) \\ &\quad + p_{53} x_3(t_\tau) + q_{53} y_3(t_\tau) \\ y_5'(t) &= -b_5 x_5(t) - a_5 y_5(t) + c_{51} x_1(t_\tau) + d_{51} y_1(t_\tau) + c_{52} x_2(t_\tau) + d_{52} y_2(t_\tau) \\ &\quad + c_{53} x_3(t_\tau) + d_{53} y_3(t_\tau) \\ x_6'(t) &= -a_6 x_6(t) + b_6 y_6(t) + p_{62} x_2(t_\tau) + q_{62} y_2(t_\tau) + p_{63} x_3(t_\tau) + q_{63} y_3(t_\tau) \\ y_6'(t) &= -b_6 x_6(t) - a_6 y_6(t) + c_{62} x_2(t_\tau) + d_{62} y_2(t_\tau) + c_{63} x_3(t_\tau) + d_{63} y_3(t_\tau) \end{aligned} \quad (7)$$

where $x_j(t_\tau) = x_j(t-\tau)$, $y_j(t_\tau) = y_j(t-\tau)$, $p_{kj} = m_{kj} \dfrac{\partial f_{kj}^{R}(0,0)}{\partial x_j} - n_{kj} \dfrac{\partial f_{kj}^{I}(0,0)}{\partial x_j}$, $q_{kj} = m_{kj} \dfrac{\partial f_{kj}^{R}(0,0)}{\partial y_j} - n_{kj} \dfrac{\partial f_{kj}^{I}(0,0)}{\partial y_j}$, $c_{kj} = n_{kj} \dfrac{\partial f_{kj}^{I}(0,0)}{\partial x_j} + m_{kj} \dfrac{\partial f_{kj}^{R}(0,0)}{\partial x_j}$, $d_{kj} = n_{kj} \dfrac{\partial f_{kj}^{R}(0,0)}{\partial y_j} + m_{kj} \dfrac{\partial f_{kj}^{R}(0,0)}{\partial x_j}$.

The matrix form of system (7) is the following:

$$U'(t) = AU(t) + BU(t-\tau) \quad (8)$$

where $U(t) = [x_1(t), y_1(t), \ldots, x_6(t), y_6(t)]^T$, $U(t) = [x_1(t-\tau), y_1(t-\tau), \ldots, x_6(t-\tau), y_6(t-\tau)]^T$. Both A and B are 12 by 12 matrices as follows:

$$A=(a_{ij})_{12\times 12}=\begin{pmatrix} -a_1 & b_1 & & & & 0 & \cdots & 0 & 0 & 0 & & \\ -b_1 & -a_1 & & & & 0 & \cdots & 0 & 0 & 0 & & \\ 0 & 0 & -a_2 & \cdots & & 0 & & 0 & & 0 & & \\ \cdots & \cdots & \cdots & \cdots & & \cdots & & \cdots & & \cdots & & \\ 0 & 0 & 0 & \cdots & & -a_5 & & 0 & & 0 & & \\ 0 & 0 & 0 & \cdots & & 0 & & -a_6 & & b_6 & & \\ 0 & 0 & 0 & \cdots & & 0 & & -b_6 & & -a_6 & & \end{pmatrix}$$

$$B=(b_{ij})_{12\times 12}=\begin{pmatrix} 0 & 0 & & & 0 & \cdots & q_{15} & 0 & 0 & & \\ 0 & 0 & & & 0 & \cdots & d_{15} & 0 & 0 & & \\ 0 & 0 & 0 & \cdots & q_{25} & & p_{26} & & q_{26} & & \\ \cdots & \cdots & \cdots & \cdots & \cdots & & \cdots & & \cdots & & \\ c_{51} & d_{51} & c_{52} & \cdots & 0 & & 0 & & 0 & & \\ 0 & 0 & p_{62} & \cdots & 0 & & 0 & & 0 & & \\ 0 & 0 & c_{62} & \cdots & 0 & & 0 & & 0 & & \end{pmatrix}$$

2. Preliminaries

Lemma 1 Assume that $a_j>0,\ b_j>0, f_{kj}^R(0,\ 0)=0, f_{kj}^I(0,\ 0)=0, f_{kj}^R(x_j,y_j)>0,\ f_{kj}^I(x_j,y_j)>0$ when $x_j>0,\ y_j>0,$ while $f_{kj}^R(x_j,y_j)<0,\ f_{kj}^I(x_j,y_j)<0$ when $x_j<0,\ y_j<0\ (k, j=1, 2, \ldots, 6)$, $C=A+B$ is a nonsingular matrix, then system (6) has a unique equilibrium.

Proof An equilibrium $U^*=[x_1^*,\ y_1^*,\ \ldots,\ x_6^*,\ y_6^*]^T$ of system (8) is a constant solution of the following algebraic equation:

$$AU^*+BU^*=CU^*=0 \tag{9}$$

Since $C=A+B$ is a nonsingular matrix, then system (9) only has zero solution according to the linear algebra basic theorem. Noting that $f_{kj}^R(0,\ 0)=0, f_{kj}^I(0,\ 0)=0$ (k, j= 1,2,...,6). Therefore, zero is a solution of system (6). Obviously, zero is the unique equilibrium of system (6) since $f_{kj}^R(x_j,y_j)>0,\ f_{kj}^I(x_j,y_j)>0$ when $x_j>0,\ y_j>0,$ while $f_{kj}^R(x_j,y_j)<0,\ f_{kj}^I(x_j,y_j)<0$ when $x_j<0,\ y_j<0\ (k, j=1, 2, \ldots, 6)$.

Lemma 2 Assume that $f_{kj}^R(x_j,y_j),\ f_{kj}^I(x_j,y_j)$ (k, j=1,2, ...,6) are continuous bounded functions, $a_j>0,\ b_j>0$ $(k, j=1, 2, \ldots, 6)$. Then all solutions of system (6) are uniformly bounded.

Proof Since $f_{kj}^R(x_j,y_j),\ f_{kj}^I(x_j,y_j)$ (k, j=1,2,...,6) are continuous bounded functions, then from system (6) we have

$$\begin{aligned} x_j'(t) &\le -a_jx_j(t)+b_jy_j(t)+N_{1j} \\ y_j'(t) &\le -b_jx_j(t)-a_jy_j(t)+N_{2j} \end{aligned} \tag{10}$$

where N_{1j}, N_{2j} are some positive constants. It is easily to see that all solutions of system (10) are uniformly bounded since $a_j>0,\ b_j>0\ (k, j=1, 2, \ldots, 6)$, implying that all solutions of system (6) are uniformly bounded.

3. Main Results

It is known that the instability of the trivial solution of system (7) guarantees the instability of the trivial solution of system (6). Thus, we have the following theorems.

Theorem 1 Assume that Lemma 1 and Lemma 2 hold for selecting parameter values of $a_j,\ b_j, m_{kj},\ n_{kj}(k, j=1, 2, \ldots, 6)$. Let the eigenvalues of matrices A, B be α_j and β_j $(j=1, 2, \ldots, 12)$ respectively. If there exists at least one eigenvalue $\beta_k\ (k\in\{1, 2, \ldots, 12\})$ such that

$\beta_k>0,$ or $Re(\beta_k)>\alpha_k,$ where $\alpha_k=\min\limits_{1\le j\le 6}|-a_j|$. Then system (6) generates a periodic oscillatory solution.

Proof Obviously, we only need to consider the instability of the trivial solution of system (7). Suppose that the eigenvalues of matrix A are α_j then $\alpha_1=-a_1+ib_1$, $\alpha_2=-a_1-ib_1,\ \alpha_3=-a_2+ib_2, \ldots, \alpha_{11}=-a_6+ib_6, \alpha_{12}=-a_6-ib_6$. Therefore, the characteristic equation corresponding to system (8) is the following

$$\prod_{j=1}^{12}\left(\lambda-\alpha_j-\beta_je^{-\lambda\tau}\right)=0 \tag{11}$$

Noting that $Re(\alpha_j)=-a_j<0,$ and there exists some $\beta_k>0$ or $Re(\beta_k)>\alpha_k$ thus system (11) has a positive real eigenvalue or an eigenvalue which has a positive real part. Therefore, the trivial solution of system (8) (or (7)) is unstable according to the basic result of delayed differential equation, implying that the trivial solution of system (6) is unstable. Since system (6) has a unique equilibrium point and all solutions are bounded, based on the extended Chafee's criterion [21, 22], this instability of the trivial solution will force system (6) to generate a limit cycle, namely, a periodic oscillatory solution.

Now set $\sigma=\max\limits_{1\le j\le 6}\{-a_j+|-b_j|\},\ b=\max\limits_{1\le j\le 12}\sum\limits_{i=1}^{12}|b_{ij}|.$ Then we have

Theorem 2 Assume that Lemma 1 and Lemma 2 hold for selecting parameter values of $a_j, b_j, m_{kj}, n_{kj}(k, j=1, 2, \ldots, 6)$. If

$$\sigma+b>0 \tag{12}$$

Then the unique equilibrium point of system (6) is unstable, implying that system (6) generates a periodic oscillatory solution.

Proof Similar to Theorem 1, we show that the trivial solution of system (7) is unstable, then the trivial solution of system (6) also is unstable. In system (7), let $v(t)=\sum\limits_{j=1}^{6}(|x_j(t)|+|y_j(t)|)$, then we have

$$\frac{dv(t)}{dt} \le \sigma v(t) + bv(t-\tau) \tag{13}$$

Corresponding to equation (13), we consider the following equation

$$\frac{dw(t)}{dt} = \sigma w(t) + bw(t-\tau) \tag{14}$$

The characteristic equation associated with equation (14) is

$$\lambda = \sigma + be^{-\lambda\tau} \tag{15}$$

We claim that there exists a positive root of (15). Let $f(\lambda) = \lambda - \sigma - be^{-\lambda\tau}$. Obviously, $f(\lambda)$ is a continuous function of λ. When $\lambda = 0$, we get $f(0) = -\sigma - b = -(\sigma + b) < 0$ since $\sigma + b > 0$. On the other hand, there exists a suitably large λ say $\lambda_1 > 0$ such that $f(\lambda_1) = \lambda_1 - \sigma - be^{-\lambda_1\tau} > 0$ since $\lim_{\lambda_1 \to \infty} e^{-\lambda_1\tau} = 0$. Based on the Intermediate Value Theorem, there exists a $\lambda_0 \in (0, \lambda_1)$ such that $f(\lambda_0) = \lambda_0 - \sigma - be^{-\lambda_0\tau} = 0$. In other words, λ_0 is a positive characteristic root of equation (15). Therefore, the trivial solution of equation (14) is unstable. Noting that $v(t) \le w(t)$. So the instability of the trivial solution of (14) implies that the trivial solution of system (7) (thus system (6)) is unstable. This instability of the trivial solution such that system (6) has a limit cycle, namely, a periodic oscillatory solution.

4. Simulation Result

This simulation is based on system (6). We first select the parameters as $a_1 = 0.45$, $a_2 = 0.65$, $a_3 = 0.48$, $a_4 = 0.35$, $a_5 = 0.25$, $a_6 = 0.18$, $b_1 = 0.24$, $b_2 = 0.56$, $b_3 = 0.24$, $b_4 = 0.32$, $b_5 = 0.45$, $b_6 = 0.32$; $m_{14} = 0.56$, $m_{15} = 0.42$, $n_{14} = -0.12$, $n_{15} = 0.32$, $m_{24} = -0.65$, $m_{25} = 0.36$, $m_{26} = 0.55$, $n_{24} = 0.32$, $n_{25} = 0.48$, $n_{26} = 0.25$ $m_{35} = -0.65$, $m_{36} = 0.45$, $n_{35} = 0.36$, $n_{36} = 0.36$, $m_{41} = 0.35$, $m_{42} = 0.58$, $n_{41} = 0.35$, $n_{42} = -0.65$, $m_{51} = -0.68$, $m_{52} = 0.56$, $m_{53} = 0.32$, $n_{51} = 0.45$, $n_{52} = -0.25$, $n_{53} = 0.25$, $m_{62} = 0.48$, $m_{63} = 0.32$, $n_{62} = 0.12$, $n_{63} = -0.18$. The activation functions $f_{kj}(x_j, y_j) = (\tanh(x_j) + \tanh(y_j)) + i(\tanh(x_j) + \tanh(y_j))$, *thus* $f_{kj}^R(x_j, y_j) = f_{kj}^I(x_j, y_j) = \tanh(x_j) + \tanh(y_j)$, $\frac{\partial f_{kj}^R(0,0)}{\partial x_j} = \frac{\partial f_{kj}^R(0,0)}{\partial y_j} = 1$, and $\frac{\partial f_{kj}^I(0,0)}{\partial x_j} = \frac{\partial f_{kj}^I(0,0)}{\partial y_j} = 1$ ($k, j = 1,2,...,6$), time delay is 0.5. We see that the eigenvalues of matrix B are 0.8903, -0.8903, 0.7645±0.6458 i, -07645±0.6558 i, 0, 0, 0, 0, 0, 0. Noting that there exists a positive eigenvalue $0.8903 > a_j$. The conditions of Theorem 1 are satisfied. Based on Theorem 1, there exists a periodic oscillatory solution (see Figure 1). In order to see the effect of the time delay, we change time delay as 1.5, the other parameters are the same as in Figure 1, we see that the oscillatory frequency and oscillatory amplitude both are changed (see Figure 2). Then we change the activation function as $f_{kj}(x_j, y_j) = (\arctan(x_j) + \arctan(y_j)) + i(\arctan(x_j) + \arctan(y_j))$, thus we still have $f_{kj}^R(x_j, y_j) = f_{kj}^I(x_j, y_j) = \arctan(x_j) + \arctan(y_j)$ $\frac{\partial f_{kj}^R(0,0)}{\partial x_j} = \frac{\partial f_{kj}^R(0,0)}{\partial y_j} = 1$ and $\frac{\partial f_{kj}^I(0,0)}{\partial x_j} = \frac{\partial f_{kj}^I(0,0)}{\partial y_j} = 1$ ($k, j = 1,2,...,6$), the parameters are the same as in Figure 2, we see that the oscillatory frequency and oscillatory amplitude both are changed slightly (see Figure 3). This means that the activation functions effect the oscillatory behavior not too much. Now we select another set of parameters as $a_1 = 0.45$, $a_2 = 1.15$, $a_3 = 1.28$, $a_4 = 0.42$, $a_5 = 0.76$, $a_6 = 1.35$, $b_1 = 1.68$, $b_2 = 0.65$, $b_3 = 0.92$, $b_4 = 0.58$, $b_5 = 0.75$, $b_6 = 0.85$, $m_{14} = 1.25$, $m_{15} = 0.76$, $n_{14} = -1.2$, $n_{15} = 0.45$, $m_{24} = -0.25$, $m_{25} = 0.56$, $m_{26} = 0.15$, $n_{24} = 0.38$, $n_{25} = 1.78$, $n_{26} = 0.25$, $m_{35} = -1.95$, $m_{36} = 0.45$, $n_{35} = 1.36$, $n_{36} = 0.24$, $m_{41} = 0.65$, $m_{42} = 0.98$, $n_{41} = 0.45$, $n_{42} = -0.65$, $m_{51} = -0.78$, $m_{52} = 0.65$, $m_{53} = 0.85$, $n_{51} = 0.45$, $n_{52} = -1.15$, $n_{53} = 0.36$, $m_{62} = 1.28$, $m_{63} = 0.32$, $n_{62} = 1.12$, $n_{63} = -0.18$. The activation function is as in Figure 3, time delay is 0.6. We see that $\sigma = -0.5$, $b = 7.44$. Therefore, $\sigma + b > 0$ holds. Based on Theorem 2, there exists a periodic oscillatory solution (see Figure 4).

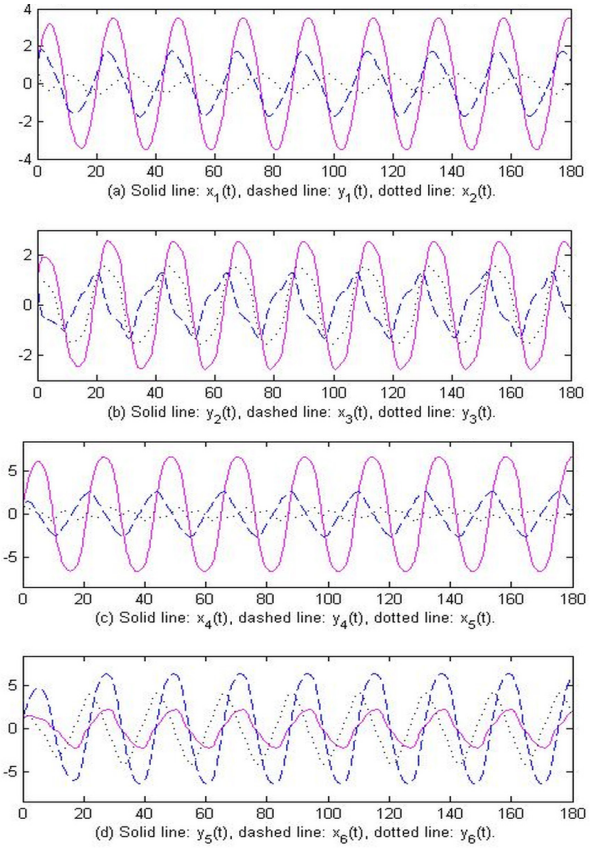

Figure 1. Oscillation of the solutions, activation function: tanh (z), time delay: 0.5.

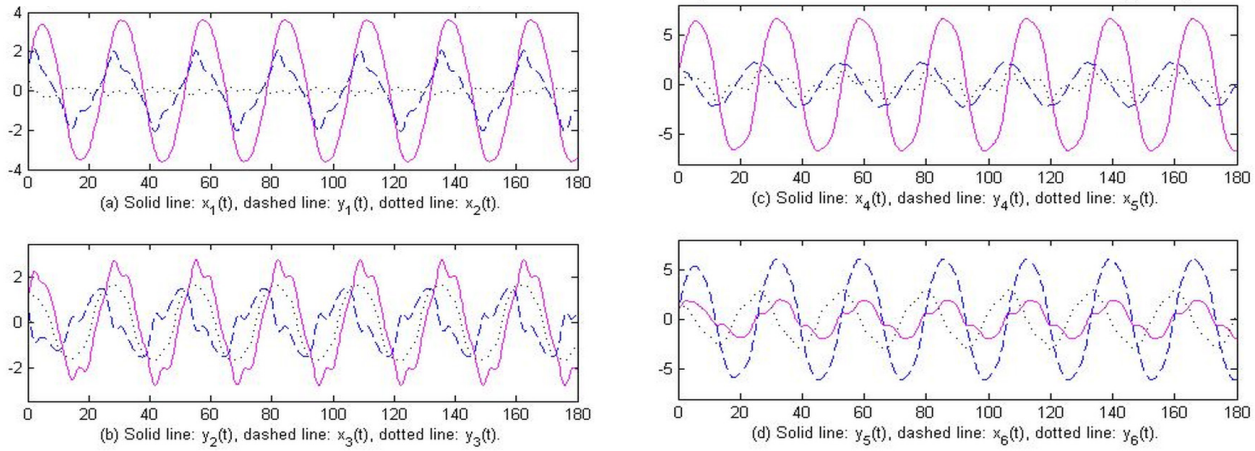

Figure 2. Oscillation of the solutions, activation function: tanh (z), time delay: 1.5.

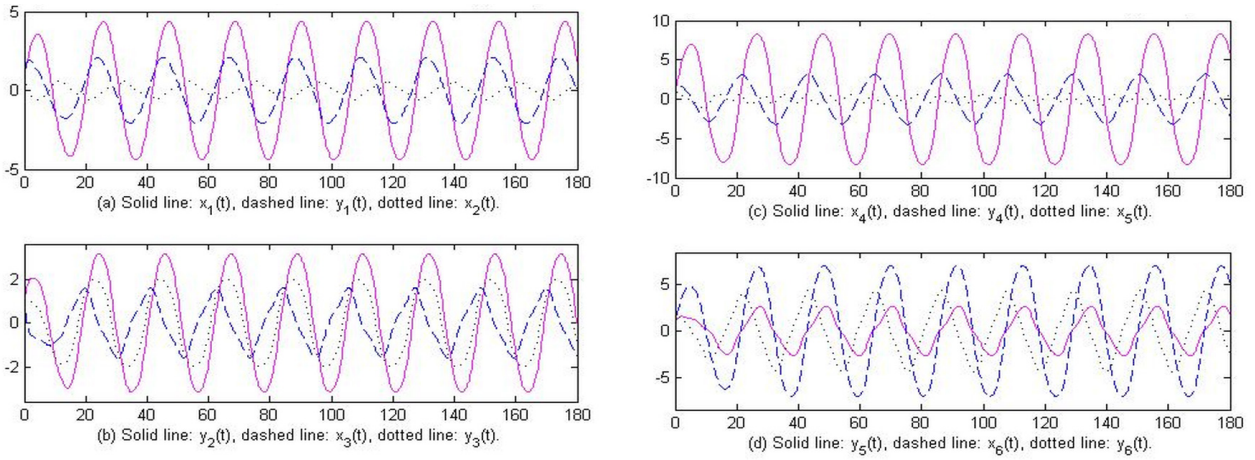

Figure 3. Oscillation of the solutions, activation function: arctan (z), time delay: 0.5.

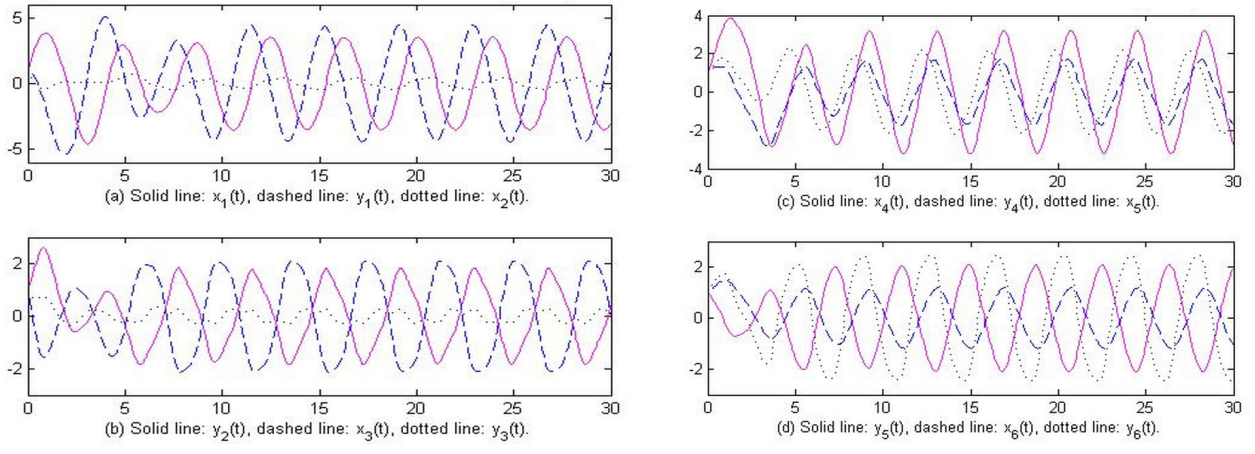

Figure 4. Oscillation of the solutions, activation function: arctan (z), time delay: 0.6.

5. Conclusions

The paper has discussed the oscillatory behavior of the solutions for a complex-valued neural network model with discrete delay. By means of the mathematical analysis method, two criteria to guarantee the existence of periodic oscillatory solution are provided which are easy to be checked. In this network, we decomposed the activation functions and connection weights into their real and imaginary parts, so as to discuss an equivalent real-valued system. The activation

functions affect the oscillatory behavior slightly.

Conflict of Interest

The author declares no conflict of interest.

References

[1] Ji, C.H., Qiao, Y.H., Miao, J., Duan, L.J., 2018. Stability and Hopf bifurcation analysis of a complex-valued Wilson-Cowan neural network with time delay. Chaos, Solitons and Fractals. 115, 45-61.

[2] Huang, C.D., Cao, J.D., Xiao, M., Alsaedi, A., Hayat, T., 2017. Bifurcation in a delayed fractional complex-valued neural network. Applied Mathematics and Computation. 292, 210-227.

[3] Li, L., Wang, Z., Li, Y.X., Shen, H., Lu, J.W., 2018. Hopf bifurcation analysis of a complex-valued neural network model with discrete and distributed delays. Applied Mathematics and Computation. 330, 152-169.

[4] Zhang, C.R., Sui, Z.Z., Li, H.P., 2017. Equivariant bifurcation in a complex-valued neural network rings. Chaos, Solitons and Fractals. 98, 22-30.

[5] Wang, T.S., Cheng, Z.S., Bu, R., Ma, R.S., 2019. Stability and Hopf bifurcation analysis of a simplified sex-neuron tridiagonal two-layer neural network model with delays, Nerocomputing. 332, 203-314.

[6] Dai, J.H., Lia, Y.W., Xiao, Jia, L., Liao, Q., Li, J.C., 2021. Comprehensive study on complex-valued ZNN models activated by novel nonlinear functions for dynamic complex linear equations. Information Sciences. 561, 101-104.

[7] Han, M., Cheng, P.Z., Ma, S.D., 2021. PPM-In VIDS: Privacy protection model for in-vehicle intrusion detection system based on complex-valued neural network. Vehicular Communications. 31, 100374.

[8] Yan, W.J., Yang, L., Yang, X., Ren, W.X., 2019. Statistical modeling for fast Fourier transform coefficients of operational vibration measurements with non-Gaussianity using complex-valued t distribution. Mechanical Systems and Signal Processing. 132, 293-314.

[9] Feng, L., Hu, C., Yu, J., Jiang, H.J., Wen, S.L., 2021. Fixed-time synchronization of coupled memristive complex-valued neural networks. Chaos, Solitons and Fractals. 148, 110993.

[10] Samidurai, R., Sriraman, R., Zhu, S., 2019. Leakage delay-dependent stability analysis for complex-valued neural networks with discrete and distributed time-varying delays, Nerocomputing. 338, 262-273.

[11] Sriraman, R., Cao, Y., Samidurai, R., 2020. Global asymptotic stability of stochastic complex-valued neural networks with probabilistic time varying delays. Mathematics and Computer in Simulation. 171, 103-118.

[12] Wang, P.F., Wang, X.L., Su, H., 2019. Stability analysis for complex-valued stochastic delayed networks with Markovian switching and impulsive effects. Commun. Nonlinear Sci. Numer. Simul. 731, 35-51.

[13] Guo, R., Zhang, Z., Liu, X., Lin, C., 2017. Existence, uniqueness, and exponential stability analysis for complex-valued memristor-based BAM neural networks with time delays. Applied Mathematics and Computation. 311, 100-117.

[14] Popa, C.A., 2020. Global -stability of neutral-type impulsive complex-valued BAM neural networks with leakage delay and unbounded time-varying delays. Nerocomputing. 376, 73-94.

[15] Wang, P.F., Zou, W.Q., Su, H., Feng, J.Q., 2019. Exponential synchronization of complex-valued delayed coupled systems on networks with aperiodically on-off coupling. Nerocomputing. 369, 155-165.

[16] Kan, Y., Lu, J.Q., Qiu, J.L., Kurths, J., 2019. Exponential synchronization of time-varying delayed complex-valued neural networks under hybrid impulsive controllers. Neural Networks. 114, 157-163.

[17] Li, L., Shi, X.H., Liang, J.L., 2019. Synchronization of impulsive coupled complex-valued neural networks with delay: The matrix measure method, Neural Networks. 117, 285-294.

[18] Hu, C., He, H.B., Jiang, H.J., 2020. Synchronization of complex-valued dynamic networks with intermittently adaptive coupling: A direct error method. Automatica. 112, 108675.

[19] Yu, J., Hu, C., Jiang, H.J., Wang, L.M., 2020. Exponential and adaptive synchronization of inertial complex-valued neural networks: A non-reduced order and non-separation approach, Neural Networks. 124, 50-59.

[20] Xu, W., Zhu, S., Fang, X.Y., Wang, W., 2019. Adaptive anti-synchronization of memristor-based complex-valued neural networks with time delays. Physica A. 535, 122427.

[21] Chafee, N., 1971. A bifurcation problem for a functional differential equation of finitely retarded type. Journal of Mathematical Analysis and Applications. 35, 312-348.

[22] Feng, C.H., Plamondon, R., 2012. An oscillatory criterion for a time delayed neural ring network model. Neural Networks. 29, 70-79.

BILINGUAL PUBLISHING CO.
Pioneer of Global Academics Since 1984

Journal of Computer Science Research
https://ojs.bilpublishing.com/index.php/jcsr

ARTICLE

A Study on Automatic Latent Fingerprint Identification System

Uttam U Deshpande[1*] V. S. Malemath[2]

1. KLS Gogte Institute of Technology, Udyambag, Belagavi, Karnataka, India
2. KLE Dr. M.S. Sheshgiri College of Engineering and Technology,Udyambag, Belagavi,India

ARTICLE INFO

Article history
Received: 22 January 2022
Accepted: 23 February 2022
Published Online: 28 February 2022

Keywords:
Fingerprint identification system
NIST
Latent fingerprints
Forensics fingerprint database

ABSTRACT

Latent fingerprints are the unintentional impressions found at the crime scenes and are considered crucial evidence in criminal identification. Law enforcement and forensic agencies have been using latent fingerprints as testimony in courts. However, since the latent fingerprints are accidentally leftover on different surfaces, the lifted prints look inferior. Therefore, a tremendous amount of research is being carried out in automatic latent fingerprint identification to improve the overall fingerprint recognition performance. As a result, there is an ever-growing demand to develop reliable and robust systems. In this regard, we present a comprehensive literature review of the existing methods utilized in latent fingerprint acquisition, segmentation, quality assessment, enhancement, feature extraction, and matching steps. Later, we provide insight into different benchmark latent datasets available to perform research in this area. Our study highlights various research challenges and gaps by performing detailed analysis on the existing state-of-the-art segmentation, enhancement, extraction, and matching approaches to strengthen the research.

1. Introduction

Data handling capacity has increased as a result of technological improvements, allowing for more reliable personal authentication systems. In the various civil, legal system, and forensics, fingerprint matching technology is widely used. Rolled or slap fingerprints are used in in-person authentication. This method was recently used in popular civil applications like India's Aadhaar (UIDAI) project. Other law enforcement and criminal investigation include access-control systems, finance monitoring systems, border security systems, and forensic applications. Human activities can be identified by his behavior and physical attributes. Among physiological (DNA, iris, face, fingerprints) and behavioral (typing pattern, gait, voice) biometrics [1], the fingerprint is the most widely used in person recognition. This is due to their reliability, accessibility, uniqueness, low cost, and sensor and algorithm maturity. In crime investigation, forensic professionals consider fingerprint matching to be a more reliable and extensively employed technique. In most cases, a person's fingerprints do not change over time. Only if a person is exposed to cuts and wounds on the finger, whether intentionally or accidentally, can change occur. Apart from fin-

*Corresponding Author:
Uttam U Deshpande,
KLS Gogte Institute of Technology, Udyambag, Belagavi, Karnataka, India;
Email: uttamudeshpande@gmail.com

DOI: https://doi.org/10.30564/jcsr.v4i1.4388

gerprint matching, palm-print, hand geometry, face, iris, and signature are also successfully deployed and used in personal identification. This is due to their individuality, universality, and invariability [2] properties.

In fingerprint applications, precision in fingerprint identification is critical. Fingerprint identification, validation, feature extraction, and classification are indeed stages of the fingerprint recognition system. A feature extraction stage is used to identify fingerprints, which is then followed by feature matching. The feature extraction approach used for identification is used to match extracted features. Fingerprint patterns are formed on the finger skin surface. Some of the features detected on fingerprints include ridge orientation-map, frequency-map, pores, dots, solitary points, and incipient. Aside from this, they contain various patterns such as Arch, Loop, and Whorl structures. These loops are then divided into nine different types of classifications [3], namely right, left, double, the right pocket, left pocket, whorl, and mixed figure are examples. These traits are characterized as Level-1, Level-2, and Level-3 [4]. Singular points, ridgeline flow, and ridge orientation form level-1 features. Level- 2 features comprise minutiae. These are the details obtained from ridge bifurcations and endings. The minutiae make up the second level of features. The details gathered from ridge bifurcations and termination are as follows. Low-level information is included in Level-3 features. Level-3 elements include sweat pore locations and ridge forms [5]. Figure 1 depicts these characteristics. Ridge orientation map refers to the direction of ridge and valley structure. Classification, augmentation, and filtering are all done with these features. The ridge frequency map is used to filter fingerprint data and is reciprocal to the ridge distance in the direction perpendicular to the ridge orientation. Singular points are discontinuities in the orientation field. After fingerprint registration, these are employed in classification. Core points and Delta points are two types of singular points. The core point is the uppermost component of a curved ridge, while the delta point is the place where three ridge flows meet. Local discontinuities of the ridge structures are used to generate minutiae points. This is useful for verifying and authenticating people. During enrolment, a person's fingerprint is captured using ink or live scan methods [6].

Latent fingerprints are accidentally left fingerprint impressions on objects, and the pressure of fingertip contact on objects varies. As a result, the data received from fingerprints are of poor quality and are directly not visible to human eyes. Overall, latent fingerprints pose different challenges compared to conventional fingerprint matching techniques. The results obtained may deviate from ideal to worst depending on the quality of the latent fingerprint. The fundamental reason for these outcomes is that minor details in latent patterns may be overlooked or corrupted by noise. Other obstacles include low image quality, poor texture, nonlinear distortion, inefficient matching techniques, and a readily available latent fingerprint database. The most basic prerequisite of latent fingerprint image enhancement is to develop a new image that contains more image information than the original image for assessment. This aids in the identification, verification, and matching process. In most cases, latent fingerprint pictures are of poor quality and polluted by noise. The success of latent fingerprint matching depends on the results obtained from the feature extraction stage. Choosing the right method of feature extraction is thus a difficult and complex problem. Capturing, pre-processing, fingerprint feature extraction, and matching are all phases in a typical latent fingerprint

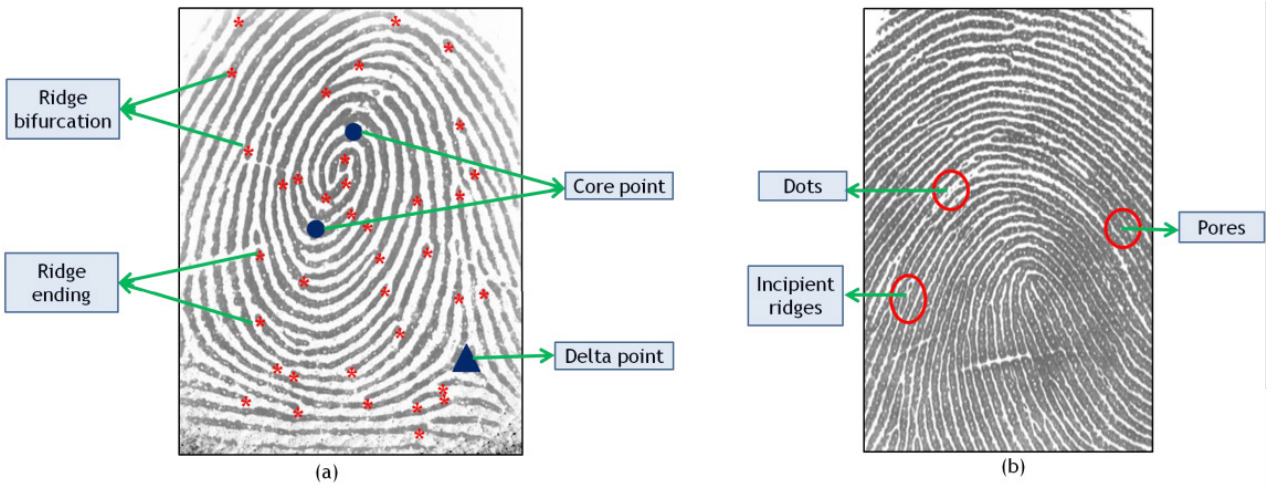

Figure 1. Fingerprint features highlighting: (a) Level-1 and Level-2 features and (b) Level-3 features.

matching system.

Figure 2 depicts an example of latent fingerprint scans from the ELFT-EFS (Evaluation of Latent Fingerprint Technologies - Extended Feature Set) database [7]. In pre-processing step quality of the image is enhanced. Hence, ridge quality enhancement is done followed by segmentation to remove background noise from the ridge-like patterns. The feature extraction step involves the extraction of Level-1, Level-2, Level-3, and extended fingerprint features from the latent image. Either specific or combination of these features is used for uniquely identifying latent fingerprints. In the matching step, the query fingerprint template is matched with the database to identify a person. Latent fingerprint identification systems can be semi-automated or fully automated. These techniques pose various challenges.

A. ACE-V Procedure

An automated fingerprint system can be created by following a set of standard methods for identifying latent fingerprint features and then having an expert examine the fingerprints manually to identify a person. The ACE-V (Analysis, Comparison, Evaluation, and Verification) technique is followed to examine the latent fingerprint manually [8]. The ACE-V approach is a consistent and structured method for comparing ridge impressions. ACE-V methodology is formed from four sequential phases. Namely Analysis, Comparison, Evaluation, and Verification. Knowledge gained after inspection of every step is applied in subsequent stages.

Manual observation of latent fingerprints is prone to inconsistency due to human participation [9]. This causes ACE-V procedure errors. This is a time-consuming, difficult process that can result in a biased outcome. These drawbacks can be overcome by automating the entire procedure. In circumstances where a large number of latent fingerprint needs to be matched automated latent fingerprint matching system can assist the experts. An Automatic Fingerprint Identification System (AFIS) is in its initial stages. ''Lights-out'' matching system [10] is in its development stage. For developing automated systems, researchers have to overcome several research challenges. Some of these research challenges are classified as resource-based and algorithmic-based. Efforts are being made to completely automate the process. But developing a system that has the efficiency of a human eye, knowledge, and decision-making ability is not an easy task.

The main objective of this review study is to introduce the existing latent fingerprint matching algorithms, and highlight their advantages, limitations against the available state-of-art algorithms. First, we analyze the existing state-of-the-art latent fingerprint segmentation, enhancement, feature extraction, and matching methods. Next, we bring out important observations by emphasizing their salient features and research gaps in the methods proposed by various researchers. Later, we discuss the publicly available benchmark latent datasets helpful in carrying out research. Finally, the study concludes by highlighting future research opportunities available at different latent fingerprint identification system stages. Section 2 further talks over about the steps involved in an automatic latent fingerprint matching system in detail. Section 3 discusses the techniques for segmenting the latent image and specifies the various preprocessing steps involved in latent image processing. The quality assessment and enhancement methods available for latent image feature extraction are highlighted in section 4. Section 5 explains different feature extraction techniques practised. Latent fingerprint matching methods are introduced in section 6. Section 7 lists publicly available latent fingerprint databases. Section 8 outlines the concerns and challenges in latent fingerprint matching, while Section 9 wraps up the study findings and offers some suggestions for future research.

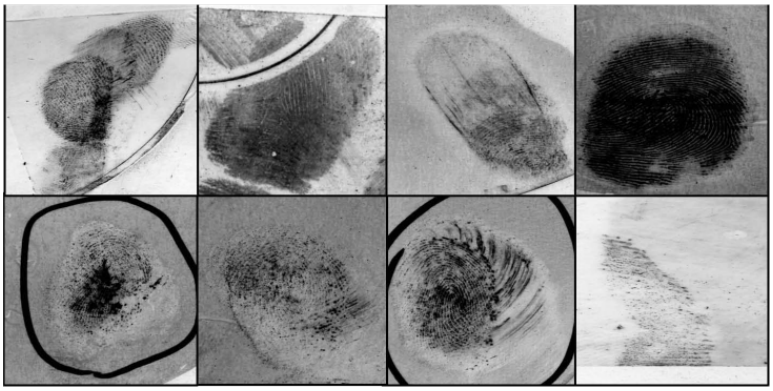

Figure 2. Different latent fingerprint images.

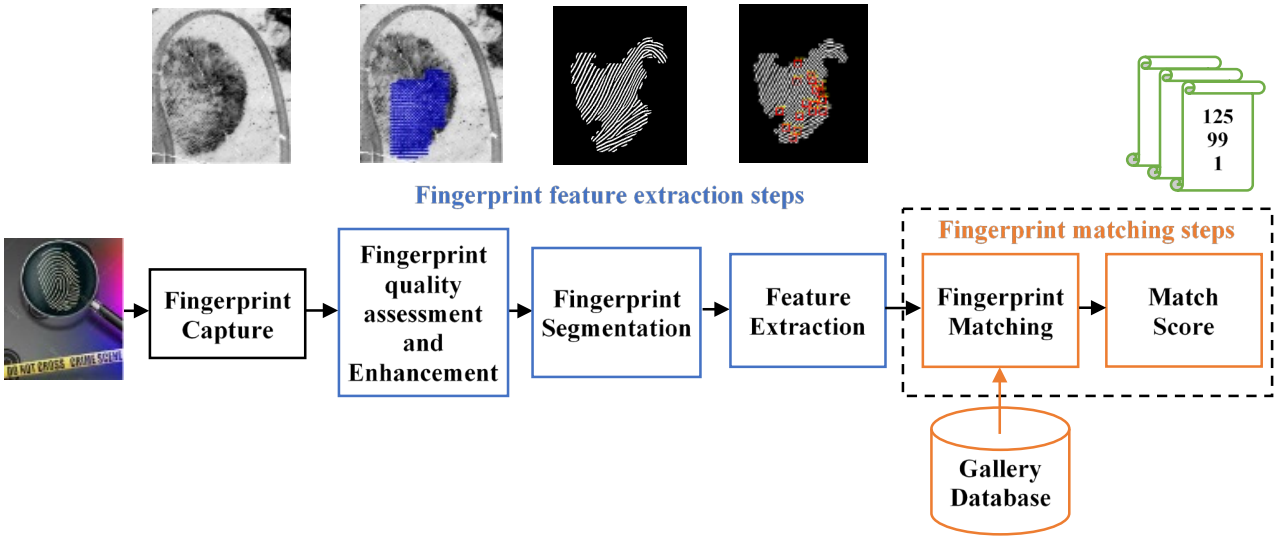

Figure 3. Automated latent fingerprint recognition system.

2. Automatic Latent Fingerprint Identification System

The fundamental goal of an automatic latent fingerprint recognition system, as previously said, is to reduce human participation. An automated matching system should be designed to make it deterministic and to overcome the problem of subjective inconsistency. It should also be designed to reduce the matching time. The Integrated Automatic Fingerprint Identification System (IAFIS) is capable of holding 70 million criminal fingerprint subjects from different regions of the world, including 31 million civilian fingerprint subjects, 73,000 known and suspected terrorist fingerprints collected by the US law enforcement agencies [11]. The average response time for 73K criminal fingerprints is about 27 minutes. In comparison, the response time reported in 2010 for 61 million civil ten-print submissions takes about an hour and 12 minutes. In comparison to manual matching, an automated latent fingerprint matching system should be able to give better, faster, and more deterministic results. The overall process of an automatic latent fingerprint matching system is depicted in Figure 3. Pre-processing, quality assessment as well as enhancement, feature extraction, and matching steps are all included. To identify and compare latent fingerprints, feature extraction is critical. An automatic latent fingerprint matching system typically receives a digitally scanned or camera-acquired latent print as input [11]. With the advancement in high-performance GPUs, it is now possible to develop Deep Learning-based Convolution Neural Networks (DCNN) in several medical diagnostics applications [12] including latent fingerprints. With hardware optimization, these DCNN algorithms can produce better results in lesser time. Digitized fingerprint data can help to transmit the data over remote systems for further processing and to perform recognition tasks. This poses serious concerns about a person's privacy information [13]. Face recognition system based on digitized data has proved that a person's identity can be achieved securely [14].

3. Pre-processing and Segmentation

Preprocessing is done on a digital image to enhance the features of the fingerprint by suppressing unwanted noise and image features. The following 5 major techniques are widely used in pre-processing.

- The process of transforming a grayscale image to a binary image is known as "binarization".
- To lessen the darkness of ridgelines, image thinning is utilized [15].
- Unraveling foreground fingerprint features from its background noise is called "Segmentation".
- The histogram equalization technique is used to improve contrast by boosting image intensities. Using this technology, low-quality latent fingerprint scans are upgraded to an acceptable level.
- Smoothing techniques are used to decrease noise in an image or to prepare it for subsequent processing.

Poor discrimination of information features and low-quality boundary foreground make the segmentation step a challenging one. Latent fingerprint segmentation is a process of marking the outline boundary, and is shown in Figure 4 (b)-(c) shows smudges and noises marked inside the boundary along with the outer boundary of latent fingerprint 4(a).

Because segmentation is such an important stage, the major goal should be to reliably mark all foreground re-

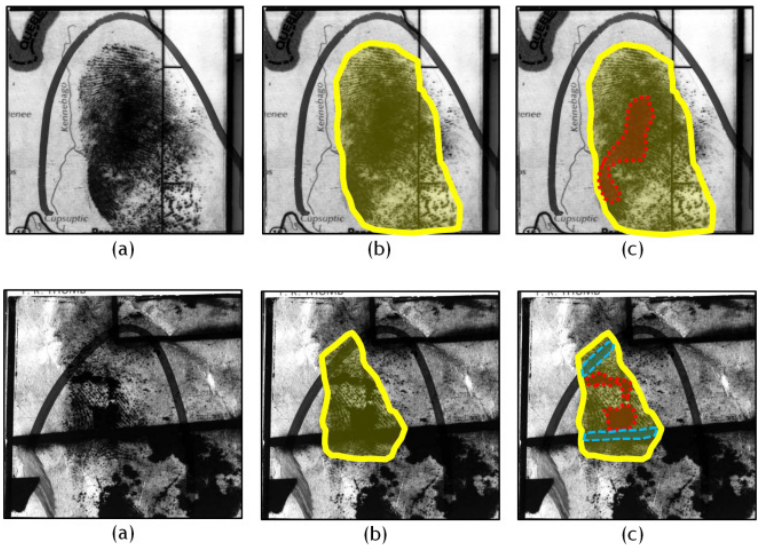

Figure 4. Segmented latent fingerprint images. (a) Original image, (b) segmentation done on the outside boundary, and (c) segmenting the outline of latent fingerprint (yellow lines) with simultaneous marking of structured noise (blue lines) and smudgy region.

gions while decreasing background noise as much as feasible. Research contributions made by several researchers can be classified as Non-convolution network (non-ConvNet) patch-based and convolution network (ConvNet) patch-based approaches.

A. Non-ConvNet patch-based approaches

Choi et al. [16] constructed orientation and frequency maps to use as reference points in evaluating latent patches in 2012. This dictionary lookup map was used to classify each patch into two classes. The classified patches-based dictionary technique was carried out in 2014 by Cao et al. [17]. In 2015, Ruangsakul et al. [18] proposed a Fourier sub-band method of segmentation. It further needs to be post-processed to fill gaps and eliminate islands. Segmented output quality depends on dictionary quality and needs post-processing to make the masks smooth. Texture information was utilized by Liu et al. [19] in 2016 to develop linear density on a set of line segments. But this requires further post-processing. Features used in most of the methods are "handcrafted" and rely on post-processing techniques. Latent fingerprint cropping using deep neural networks has also been implemented.

B. ConvNet patch-based approaches

Zhu et al. [20] used classification of patches using neural network framework in 2017. Ezeobiejesi et al. [21] used a stack of restricted Boltzmann machines in the year 2017. Apart from pre-processing techniques suggested to obtain thinned ridge patterns, various post-processing methodologies are listed to eliminate unwanted or noisy ridge patterns present after ridge thinning. It is very important to eliminate such unwanted ridge patterns as their presence contributes to false minutiae. In 2018, Dinh-Luan Nguyen et al. [22] proposed a fully automated convolution neural network segmentation method SegFinNet. This combines a fully convolutional neural network and a detection-based approach to process the entire input latent image in one shot instead of using latent patches.

Recently in 2019, Asif Iqbal Khan et al. [23] proposed a CNN approach for classifying fingerprint patches. They trained fingerprint patches with false patch elimination using the Stochastic Gradient Descent (SGD) technique. False match remover learns "most of the neighbors" to delete faulty or wrongly classified patches to construct the Region of Interest (ROI). An experiment conducted on the IIIT-D database achieves 5.2% MDR and 13.8% FDR respectively. They observed that the proposed patch-based segmentation system consumed more processing time. Some state-of-art segmentation algorithms are listed in Table 1. On the NIST Special Database-27 [24] and West Virginia University (WVU) latent databases [25], "SegFinNet," an automated segmentation method presented by Dinh-Luan Nguyen et al. [22], surpasses human latent markup and state-of-the-art latent segmentation algorithms [16,17,22,23]. Table 1 summarises the significant contributions made by several scholars to fingerprint pre-processing and segmentation.

4. Quality Assessment and Enhancement

Before performing extraction, ridge flow enhancement of a latent fingerprint is an extremely important and necessary procedure. To increase the quality of a latent fingerprint, the quality of the latent image is analyzed in this step, and enhancement is performed based on the assessment. Assessed data are used to determine whether the bare minimum of data is present to make a valid confidence match. FTE (Failure-To-Enroll) or FTR (Failure-To-Register) latent fingerprints that do not meet the criterion will be discarded [6]. These have no bearing on the precision of the matching system's performance. Overall, the quality enhancement procedure reduces noise from a latent fingerprint image and improves its quality. This will aid the feature extraction procedure in completing its duty. Hicklin et al. [26] conducted the first investigation on the quality of fingerprint features in 2007. In 2008, Karimi and Kuo [27] presented a Gabor filter-based approach for latent fingerprint picture segmentation and enhancement. Yoon et al. [28] introduced a technique for manually indicating singular points and Regions of Interest (ROI) for latent fingerprint enhancement in 2012. Experiments carried out on NIST SD27 datasets influenced the orientation estimation and match accuracy. To boost fingerprint enhancement performance, they developed a more robust and improved ridge orientation estimation algorithm. They went on to build "lights-out" mode devices to assess the quality of a latent fingerprint. Based on the quality of the input latent image, this system may anticipate whether or not complete automatic identification is possible. To determine the latent quality, the authors looked into ridge quality, high-quality minutia patches, and a reference point. Feng et al. [29] presented a relaxation labeling technique in 2013 to overcome the problem of matched latent fingerprint orientation. The unique fingerprint orientation field estimation algorithm was developed using prior information of fingerprint structure. Set of genuine patches that aid in the acquisition of prior knowledge about fingerprints. In 2014, Cao et al. [17] developed a method for improving fingerprints using a dictionary of high-quality ridges in 2014. To recreate the poor latent, the dictionary's same ridge patterns (orientation and frequency) were used. Ezhilmaran and Adhiyaman [30] explored contrast enhancement using an intuitionistic Type-2 fuzzy set later in 2016. They also devised an intuitive Type-2 fuzzy entropy algorithm for latent fingerprint edge detection. In 2018, Jian Li et al. [31] introduced "FingerNet", a CNN-based network. In FingerNet, they created an encoding convolutional component and two decoding deconvolutional components. These blocks serve as augmentation and orientation branches. In 2019, I. Joshi et al. [32] proposed the use of a trained enhancer and discriminator in a Generative Adversarial Network (GAN) for ridge structure amplification. The main research contribution made by various researchers in quality assessment and enhancement is tabulated in Table 1. State-of-art algorithm [17,29,31] provides better enhancement results compared to the research contributions discussed above.

5. Latent Fingerprint Feature Extraction

Fingerprint characteristics are the most exact representation of any data in a fingerprint matching system. To maintain the uniqueness of fingerprint matching systems, particularly robust feature representation methods are required. In latent fingerprint matching, the feature extraction technique is the most important stage. Due to the low quality of latent pictures, it is critical to capture all aspects of the latent fingerprints to match them efficiently. Extraction of latent fingerprint features is a complex technique. Sankaran et al. [33] suggested an automated technique for extracting latent fingerprint minutiae. Using an unsupervised feature learning technique, the minutiae and non-minutiae patches are discriminated from high-quality images. Later, they did a comprehensive study in which he described the advantages of the automated hierarchical fusion approach and the simultaneous latent fingerprint database. Paulino [34] offered manually marked minutiae with mechanically retrieved minutiae for latent to full fingerprint matching to improve the accuracy of the NIST SD27 database. These characteristics are integrated to perform Scale Invariant Feature Transformation (SIFT) on a large portion of the foundation database while retaining latent matching accuracy via indexing. The following fingerprint traits [6] are the most often employed in fingerprint recognition because of their limited data content and low quality of ridge information:

- Minutiae points - ridge termination and bifurcation.
- The singularities - Arch type (no singularity), Loop and Tented arch (one core and one delta), whorl and loop (two cores and two deltas).
- Region Of Interest (ROI) - It is a closed area that is limited at the external most trim of the latent.
- Ridge Orientation field - Represent the global structure of fingerprints.

The fingerprint feature can be classified into three levels: Level 1, Level 2, and Level 3. In comparison to Level 2 or Level 3 features, the Level 1 feature is the most extensively employed in latent fingerprint identification systems. For core point extraction of latent fingerprints, Su and Srihari [35] utilized a Gaussian process. Prior joint Gaussian distribution and regression methods were used

to derive the singular points and location, respectively.

Yao Tang and fellow researchers proposed the fully convolutional neural network (CNN) approach [36]. In this case, tiny points are fed into a CNN, which reclassifies them and calculates their orientations. Later, they created "FingerNet" a deep convolutional network that incorporates domain knowledge with deep learning representation. Traditional latent fingerprint feature extraction approaches that were tested on rolling and slap fingerprints were modified and combined into a basic unified network in a completely convolutional manner. On various minutiae orientation and distance settings, they got Precision, Recall, and F1 scores. Darlow et al. [37] proposed the "Minutiae Extraction Network (MENet)" Deep-Convolutional Neural Network in 2017 to learn a data-driven representation of minutia points. MENet is trained on a huge library to reduce manual data labeling and boost robustness. "MinutiaeNet", an automated, robust minutiae extractor, was presented by Nguyen et al. [22] in 2018. MinutiaeNet is a domain knowledge-based deep network representation. Nguyen et al. created "CoarseNet", a residual learning-based model, and "FineNet", an inception-residual network, using domain knowledge. Without a specified threshold, CoarseNet provides an automatic position and orientation of minutiae. FineNet is a patch-focused classifier that helps CoarseNet find and generate final findings. In 2021, U. U. Deshpande et al. [38] introduced a CNN-based automatic minutiae extractor using a dynamic thresholding filtration algorithm to suppress false minutiae points. Researchers' contributions are summarized in Table 1. In comparison to the other algorithms, the state-of-the-art [22,34,36,38] algorithms perform better.

6. Latent Fingerprint Matching

The primary goal of a latent fingerprint matching procedure is to determine the degree of resemblance between the fingerprint under inquiry and the gallery fingerprint. The matching algorithm should try and increase the matching accuracy while decreasing dissimilarities.

Latent fingerprint matching can be classified into three families based on fingerprint features:

- **Correlation-based matching:** The similarity of two fingerprint images is computed by determining the correlation between corresponding pixels at different alignments.
- **Minutiae-based matching:** This is the most well-known and widely used feature. The minutiae are extracted from the two fingerprints and placed on a two-dimensional plane. Minutia-based matching entails determining the relationship between the minutiae format and the information entered into pairs.
- **Non-Minutiae feature-based matching:** Minutiae extraction is difficult in low-quality fingerprint photos. Different traits, such as ridge shape, may be isolated from more reliable minutiae. However, their distinctiveness and consistency are generally lesser.

Jain et al. [10] presented minutiae points, unique points, ridge quality map, ridge flow map, ridge wavelength map, and skeleton characteristics for latent fingerprint matching. Sankaran et al. [33] created fusion and context switching frameworks for latent-to-latent fingerprint matching. Paulino et al. [34] demonstrated how to align two sets of minutiae, create correspondences, and generate a similarity score using a descriptor-based Hough transform. Liu et al. [39] presented feedback-based latent fingerprint matching from exemplar print. This is used in candidate list recovery from the database and score level-based matching.

Miguel Angel Medina-Pérez et al. [40] presented a clustering technique based on minutiae descriptors to improve MCC, M triplets, and nearby minutiae-based descriptors. The "Latent Minutiae Similarity" (LMS), "Clustered Latent Minutiae Pattern" (CLMP), and "Ratio of Minutiae Triangles" (RMT) algorithms, developed by U. U. Deshpande et al. [41], are alignment-free and rotation/scale-invariant. They clustered minutiae structures around a reference minutia and generated minutiae invariant feature vectors to develop discriminative feature vectors needed for fingerprint matching.

In 2018, Cao et al. [42] achieved automated latent fingerprint detection using the CNN (ConvNets) model. To estimate ridge flow, extract minutiae points, and build two minutiae templates as well as a texture template, ConvNets was employed. Furthermore, they proposed an improved algorithm that creates Virtual minutiae to account for missing minutiae and compensate for good minutiae points. Different texture templates are provided by minutiae descriptors created for virtual minutiae. The technique enhanced the distinctness of simulated minutiae descriptors by classifying the patches from the original fingerprints. To build numerous texture templates, they used hierarchical graph matching, which increased the matching accuracy. Ezeobiejesi et al. [43] employed deep networks to build a patch-based latent fingerprint representation and matching in 2018. To learn the finest minutiae representations from picture patches, deep networks were used. Ezeobiejesi et al. calculated the similarity scores between latent and reference fingerprint patches using a distance method. Combining minutiae patch and similarity scores yielded the final matching score.

Nguyen et al. [44] created an end-to-end automated latent AFIS using ridge pores in 2019. Using a manual graph matching approach, the system determines the relationship between pore and minutiae features.

Recently in 2020, U. U. Deshpande et al. [45] proposed

Table 1. Published works at different stages of latent fingerprint matching.

STEP	STUDY	METHOD	DATABASE	RESULTS
SEGMENTATION	Choi et al. [16], 2012.	The frequency of ridges and the orientation of the patches. Relies on the quality of the supplied image and the orientation estimation. **Drawbacks:** Fingerprint quality and orientation field estimates determine the performance.	32K NIST SD27 and WVU Background fingerprints	Matching: With a Commercial of The Shelf (COTS) ten-print matcher, 16.28 % on NIST SD27 and 35.1 % on WVU were achieved.
	Cao et al. [17], 2014.	Patch classification based on ridge flow enhancement of learned dictionary and smoothened mask using convex hull. **Drawbacks:** A fully automatic segmentation system that does not require manual markup. The method depends on the learned dictionary and convex hull.	NIST SD27 and WVU. Background: 32K images	Matching: 61.24% on NIST SD27 and 70.16% with COTS matcher
	Dinh-Luan Nguyen et al. [22], 2018.	Automatic segmentation (SegFinNet) based on Full CNN (FCN) and detection-based fusion. Uses Non-patch, Non-warp ROI, Visual attention, and Voting masks techniques. **Drawbacks:** A non-patch-based neural network operation on the complete image.	NIST SD27, WVU, Forensic database. Background: 100K images	Matching: With a COTS matcher, 70.8 % on NIST SD27 and 71.3 % on WVU; Matching: 12.6% on NIST SD27 and 28.9% on WVU with Verifinger SDK 6.3 on 27K images
	Asif Iqbal Khan et al. [23], 2019.	Patch foreground and background classifier based on convolutional neural networks (CNN). **Drawbacks:** Patch-based processing consumes a lot of time.	IIIT-D latent Fingerprints.	$MDR^{(+)}$: 5.2%, $FDR^{(-)}$: 13.8%. Match accuracy was not reported.
QUALITY ASSESSMENT AND ENHANCEMENT	Yoon et al. [29], 2012.	Short-Time Fourier Transforms (STFT) + RANSAC (randomized RANdom SAmple Consensus) on manually marked ROI **Drawbacks:** A human expert or AFIS does the quality assessment.	NIST SD27 and WVU DB	Rejection of 50% on poor quality latent information and improved rank-100 identification accuracy from 69 to 86 %.
	Cao et al. [17], 2014.	Ridge flow improvement approach based on a dictionary. The reconstructed fingerprint is computed, and the orientation and frequency elements are utilized to modify Gabor filters for fingerprint enhancement. **Drawbacks:** Fully automated segmentation with no manual marking is required.	NIST SD27, WVU	Rank-1 identification accuracy of 61% (NIST SD27) and 70% (WVU)
	Jian Li et al. [31], 2018.	To extract fingerprint characteristics, use a convolution layer. For improvement (removing structured noise) and orientation operations, two distinct deconvolution layers are used (multi-task learning). **Drawbacks:** When background noise is present, performance suffers.	NIST SD27	55% Rank-20 accuracy
FEATURE EXTRACTION	Paulino et al. [34], 2013.	Minutiae extraction and MCC descriptor-based indexing of minutiae triplets using Ridge improvement **Drawbacks:** An automated extractor was used to extract minutiae characteristics. Manually annotated minutiae (Level 2) characteristics to aid with fingerprint matching and alignment.	NIST SD27	Identification accuracy of 33% for the Rank-10 order.

(Continues)

Table 1 (Continued)

STEP	STUDY	METHOD	DATABASE	RESULTS
FEATURE EXTRACTION	Tang et al. [36], 2017.	To distinguish between minutiae and non-minutia patches, a CNN algorithm learns the fingerprint pixels. The minutia position is extracted using location regression. **Drawbacks:** Reliable minutiae (level 2 characteristics) that have not been segmented or enhanced. Candidate patches with minor details are excluded by the hard threshold, and candidate patches are generated and classified by the same network.	NIST SD27	Precision - 63%, Recall - 63.2%, F1 score - 0.631
	Dinh-Luan Nguyen et al. [22], 2018.	Domain knowledge and deep network representation combined (MinutiaeNet). CoarseNet is built using domain knowledge and residual learning, while FineNet is built using an inception-residual network. **Drawbacks:** Extraction of minutiae is done automatically. Genuine minutiae candidate areas are deleted by adaptive threshold filtration with a static threshold value.	NIST SD27	Precision - 71.2%, Recall - 75.7%, F1 score-0.734
	U. U. Deshpande et al. [38], 2021.	A residual learning framework to automatically segment, enhance, and extract minutiae features. A dynamic thresholding filtration algorithm to eliminate false minutiae points. **Drawbacks:** The suggested model struggled to detect actual minutiae near the fingerprint boundary or failed to identify fake minutiae.	NIST SD27	Precision-86.67%, Recall -92.85%, F1 score-0.896.
MATCHING	M. A. M. Perez et al. [40], 2016.	Clustering algorithm to improve Cylinder-Codes, m-triplets, neighboring minutiae-based descriptor. **Drawbacks:** The minutiae descriptors have no impact on the minutiae cluster.	NISTSD27	Rank-1 identification of Cylinder-Codes was 68.6%, m-triplets was 68.2%, and nearby minutiae-based descriptor was 64%.
	U. U. Deshpande et al. [41], 2021.	Alignment-free and rotation/scale-invariant LMS, CLMP, and RMT algorithms. **Drawbacks:** The fingerprint quality threshold has to be manually set. It requires a minimum of 8 minutiae neighbors.	NISTSD27	Rank-1 identification of LMS - 88.8%, CLMP - 93.80%, and RMT - 86.82%.
	K. Cao et al. [42], 2018.	For latent representation, ConvNets use two minutiae templates and one texture template. Virtual minutiae creation has been included to compensate for missing minutiae. **Drawbacks:** Using virtual minutiae, ConvNets were used to improve minutiae and extract minutiae descriptors.	NISTSD27	Rank-1 identification accuracy of 68.2%.
	U. U. Deshpande et al. [45], 2020.	CNN based End-to-End matching model (CNNAI) developed by integrating it with Minu-ExtractNet [38] model. **Drawbacks:** Matching accuracy highly depends on the trained model.	NISTSD27	Rank-1 identification accuracy of 84.5%.

$MDR^{(+)}$: Missed Detection Rate, $FDR^{(-)}$: False Detection Rate.

"Combination of the Nearest Neighbor Arrangement Indexing (CNNAI)", an end-to-end Convolution Neural Network (CNN) matching model. To detect fingerprints, this approach uses a local minutiae representation. They integrated the CNNAI matching model with the previously established Minu-ExtractNet [38] to demonstrate its potential to provide effective match results without human involvement in an end-to-end framework. Table 1 highlights the important features of proposed latent fingerprint matching algorithms. It can be observed that the state-of-art matching algorithm [40-42,45] performs better than other listed algorithms. Table 2 provides the details of the publicly available fingerprint databases.

7. Latent Fingerprint Databases

The lack of a publicly accessible public latent fingerprint database is a stumbling block to further study in this field.

- Card ink print, live scan fingerprint, multi-resolution fingerprint, multi-sensor fingerprint, and full fingerprint techniques are used to construct databases that are then made available to the public, among other issues. Print, live scan fingerprint, multi-resolution fingerprint, multi-sensor fingerprint, and full fingerprint techniques are used to create databases that are then made available to the public.
- Capturing or collecting latent fingerprints is done by professionals. The unavailability of professionals makes this process time-consuming and expensive.
- Very few cost-effective techniques are available for lifting latent fingerprints.
- Simulating latent fingerprints in real-world settings is a difficult task. This is because latent fingerprints acquired at crime scenes will have a wide range of qualities. Creating databases with enough diversity by combining numerous sensors, diverse backdrops, and multiple sessions is a time-consuming procedure.

Table 2 lists the public databases that can be used for research purposes. The WVU multimodal [25] database is a multi-session live scan fingerprint database. Tsinghua OLF [46], NIST SD-27A [24], IIIT-D SLF [47], IIIT-D latent fingerprint database [47], and IIIT-D MOLF (Multisensory Optical and Latent Fingerprint) Database [47] are some of the databases available. Databases are latent databases that have been collected several times with various backgrounds and have distinct properties.

8. Summary

There are many issues and challenges faced in latent fingerprint matching systems. These challenges are categorized as resource-based and algorithmic-based.

Resource-based: As discussed in the previous section, the lack of available professional experts and publicly available databases form a major issue in latent fingerprint matching. Although very fewer numbers of trained experts are available; error-free matching is a challenging task. Similarly, creating a special database with sufficient variability in latent fingerprints poses many questions.

Algorithmic based: Generally, latent fingerprint images are of poor quality. This is due to uneven pressure on the object, loss of information while lifting the fingerprint, or overlapped fingerprints. If proper procedures are not followed it may lead to spoiling of the complete matching system. Hence, appropriate pre-processing techniques are needed to obtain clear fingerprint features which intern improve the overall quality of the image.

Another major challenge in the fingerprint matching method is to tackle the large latent fingerprint database within a reasonable time. A detailed study on recent research contributions is highlighted after studying each stage. From the observations, it can be seen that the re-

Table 2. Fingerprint databases are available in public.

Capture type	Database	Classes	Images	Characteristics
Live-scan	WVU multimodal [25]	272	7219	**Capturing method:** CrossMatch, Precise Biometrics, SecuGen sensors at 500 dpi.
Latent	NIST SD-27A [24]	258	258	Manually annotated latent to exemplar fingerprint matching at 500 PPI and 1000 PPI respectively.
	Tsinghua OLF [46]	12	100	Overlapped latent fingerprints.
	IIIT-D SLF [47]	180	420	Manually annotated simultaneous slap latent fingerprints captured at 500 PPI.
	IIIT-D Latent Fingerprint [47]	150	1241	Latent to latent slap fingerprints with 500 PPI captured using a high-resolution camera.
	IIIT-D MOLF [47]	1000	19200	Manually annotated dap, slap, latent, and simultaneous latent fingerprints.

search is in its early phase of every stage and there is a large scope for research contribution in the respective fields. From the results, it can be seen that the manually annotated semi-automatic technique can achieve a maximum matching accuracy of 74% on the NIST SD-27 database. Whereas, End-to-End automatic fingerprint matching system produced the highest 84.5% Rank-1 identification accuracy. Hence, a fully automatic latent fingerprint matching system can significantly contribute to civil, law enforcement, and forensic applications.

9. Conclusions and Future Work

This survey provides detailed information on available latent fingerprint recognition methods. It also describes the issue and challenges of latent fingerprints. Both manual matching and the automated system based on latent fingerprint matching are discussed. Their merits and demerits are pointed out to develop an improved automated matching system. Studies reveal that automatic latent fingerprint identification technology is still in its nascent stage and there is a vast scope for research contribution in different fields of latent fingerprint matching. Moreover, issues with available resources and algorithms have led to open challenges for future researchers. The primary objective of this paper is to introduce the existing latent fingerprint matching algorithms, highlight their advantages and limitations against the available state-of-art algorithms. Finally, the paper concludes by highlighting future research opportunities available at different stages of the latent fingerprint identification system.

Conflict of Interest

The authors declare no conflict of interest.

References

[1] Integrated pattern recognition and biometrics lab, West Virginia University. http://www.csee.wvu.edu/ross/i-probe/.

[2] Hawthorne, M.R., 2009. Fingerprints analysis and understanding. CRC Press, Taylor and Francis Group, Boca Raton, London, New York.

[3] Jain, A.K., Flynn, P., Ross, A.A., 2007. Handbook of biometrics. Springer Science and Business Media, New York.

[4] Kawagoe, M., Tojo, A., 1984. Fingerprint pattern classification. Pattern Recognition. 17(3), 295-303.

[5] Sankaran, A., Vatsa, M., Singh, R., 1984. Latent fingerprint matching: A survey. IEEE Access. 2(2014), 982-1004.

[6] Maltoni, D., Maio, D., Jain, A.K., et al., 2009. Handbook of Fingerprint Recognition. 2nd ed. New York, NY, USA: Springer-Verlag.

[7] Evaluation of Latent Fingerprint Technologies. [Online] Available: http://www.nist.gov/itl/iad/ig/latent.cfm. (Accessed Oct. 24, 2013).

[8] Ashbaugh, D., 1999. Quantitative-Qualitative Friction Ridge Analysis: An Introduction to Basic and Advanced Ridgeology. Boca Raton, FL, USA: CRC Press. pp. 134-135.

[9] Ulery, B.T., Hicklin, R.A., Buscaglia, J., et al., 2011. Accuracy and reliability of forensic latent fingerprint decisions. Proc. Nat. Acad. Sci. USA. 108(19), 7733-7738.

[10] Jain, A.K., Feng, J., Jan. 2011. Latent fingerprint matching. IEEE Trans. Pattern Anal. Mach. Intell. 33(1), 88-100.

[11] Fact Sheet, 2013. Integrated Automated Fingerprint Identification System. [Online] Available: http://www.fbi.gov/about-us/cjis/fingerprints_ biometrics/iafis/iafis_facts. (Accessed Dec. 5, 2013).

[12] Shrestha, H., Dhasarathan, C., Kumar M., et al., 2022. A Deep Learning Based Convolution Neural Network-DCNN Approach to Detect Brain Tumor. In: Gupta G., Wang L., Yadav A., Rana P., Wang Z. (eds) Proceedings of Academia-Industry Consortium for Data Science. Advances in Intelligent Systems and Computing, vol 1411. Springer, Singapore. DOI: https://doi.org/10.1007/978-981-16-6887-6_11.

[13] Bhardwaj, A., Mohamed, A., Kumar, M., 2021. Real-time Privacy-Preserving Framework for COVID-19 Contact Tracing. Computers, Materials and Continua. 70. DOI: https://doi.org/10.32604/cmc.2022.018736.

[14] Singh, S., Chintalacheruvu, S.C.K., Garg, S., et al., 2021. Efficient Face Identification and Authentication Tool for Biometric Attendance System. 2021 8th International Conference on Signal Processing and Integrated Networks (SPIN). pp. 379-383. DOI: https://doi.org/10.1109/SPIN52536.2021.9565990.

[15] Diefenderfer, G.T., 2006. Fingerprint Recognition. DTIC Document, Naval Post Graduate School, Monterey, California.

[16] Choi, H., Boaventura, M., Boaventura, I.A., et al., 2012. Automatic segmentation of latent fingerprints. In IEEE International Conference on Biometrics: Theory, Applications and Systems. pp. 303-310.

[17] Cao, K., Liu, E., Jain, A.K., 2014. Segmentation and enhancement of latent fingerprints: A coarse to fine ridge structure dictionary. in IEEE Transactions on Pattern Analysis and Machine Intelligence. 36(9), 1847-1859.

[18] Ruangsakul, P., Areekul, V., Phromsuthirak, K., et al., 2015. Latent fingerprints segmentation based on rearranged fourier subbands. in IEEE International Conference on Biometrics. pp. 371-378.

[19] Liu, S., Liu, M., Yang, Z., 2016. Latent fingerprint segmentation based on linear density. In IEEE International Conference on Biometrics. pp. 1-6.

[20] Zhu, Y., Yin, X., Jia, X., et al., 2017. Latent fingerprint segmentation based on convolutional neural networks," in IEEE Workshop on Information Forensics and Security. pp. 1-6.

[21] Ezeobiejesi, J., Bhanu., B., 2017. Latent fingerprint image segmentation using deep neural network. in Deep Learning for Biometrics. Springer. pp. 83-107.

[22] Nguyen, D.L., Cao, K., Jain., A.K., 2018. Robust minutiae extractor: Integrating deep networks and fingerprint domain knowledge. in IEEE International Conference on Biometrics.

[23] Khan, A.I., Wani, M.A., 2019. Patch-based Segmentation of Latent Fingerprint Images Using Convolutional Neural Network. in Appl. Artif. Intell. 33(1), 87-100.
DOI: https://doi.org/10.1080/08839514.2018.1526704.

[24] Fingerprint Minutiae from Latent and Matching Tenprint Images - NIST special database 27 (a). http://www.nist.gov/srd/nistsd27.htm, 2010.

[25] Hornak, L., Ross, A., Crihalmeanu, S.G., et al., 2007. A protocol for multibiometric data acquisition storage and dissemination. tech. rep., West Virginia University, https://eidr. wvu. edu/esra/documentdata. eSRA.

[26] Hicklin, A., 2007. Latent quality survey, Noblis .Org, Falls Church, VA, USA.

[27] Karimi, A.S., Kuo, C.C.J., 2008. A robust technique for latent finger- print image segmentation and enhancement. in Proceedings of the 15th IEEE International Conference on Image Processing. pp. 1492-1495.

[28] Ezhilmaran, D., Adhiyaman, M., 2016. Edge Detection Method for Latent Fingerprint Images Using Intuitionistic Type-2 Fuzzy Entropy. Cyber- netics and Information Technologies. 16(3), 205-218.

[29] Yoon, S., Liu, E., Jain, A.K., 2012. On latent fingerprint image quality. In Proceedings of the International Workshop on Computational Forensics.

[30] Feng, J., Zhou, J., Jain, A.K., 2013. Orientation field estimation for latent fingerprint enhancement. IEEE Transactions on Pattern Analysis and Machine Intelligence. 35(4), 925-940.

[31] Li, J., Feng, J., Kuo, C.C.J., 2018. Deep-Convolutional Neural Network for latent fingerprint enhancement. Signal Process. Image Commun. 60, 52-63.

[32] Joshi, I., Anand, A., Vatsa, M., et al., 2019. Latent Fingerprint Enhancement Using Generative Adversarial Networks. in {IEEE} Winter Conference on Applications of Computer Vision, {WACV}, Waikoloa Village, HI, USA. pp. 895-903.
DOI: https://doi.org/10.1109/WACV.2019.00100.

[33] Sankaran, A., Pandey, P., Vatsa, M., 2014. On latent fingerprint minutiae extraction using stacked denoising sparse autoencoders. In Proceedings of the International Joint Conference on Biometrics. pp. 1-7.

[34] Paulino, A., Liu, E., Cao, K., et al., 2013. Latent fingerprint indexing: Fusion of Level- 1 and Level- 2 features. In Proceedings of the IEEE Sixth International Conference on Biometrics: Theory, Applications and Systems. pp. 1-8.

[35] Su, C., Srihari, S., 2010. Latent fingerprint core point prediction based on Gaussian processes. In Proceedings of the 20th International Confer- ence on Pattern Recognition. pp. 1634-1637.

[36] Tang, Y., Gao, F., Feng, J., et al., 2017. FingerNet: An unified deep network for fingerprint minutiae extraction. in IEEE International Joint Conference on Biometrics (IJCB), Denver, CO, USA. pp. 108-116.
DOI: https://doi.org/10.1109/BTAS.2017.8272688.

[37] Darlow, L.N., Rosman, B., 2017. Fingerprint minutiae extraction using deep learning. in IEEE International Joint Conference on Biometrics, (IJCB), Denver, CO, USA. pp. 22-30.
DOI: https://doi.org/10.1109/BTAS.2017.8272678.

[38] Deshpande, U.U., Malemath, V.S., 2021. MINU-EXTRACTNET: Automatic Latent Fingerprint Feature Extraction System Using Deep Convolutional Neural Network. In Recent Trends in Image Processing and Pattern Recognition. RTIP2R 2020. Communications in Computer and Information Science, vol 1380. Springer, Singapore. pp. 44-56.
DOI: https://doi.org/10.1007/978-981-16-0507-9_5.

[39] Liu, E., Arora, S.S., Cao, K., et al., 2013. A feedback paradigm for latent fingerprint matching. In Proceeding of the IEEE International Conference on Biometrics. pp. 1-8.

[40] Miguel Angel Medina-Pérez, Aythami Morales Moren,, Miguel Ángel Ferrer Ballester, et al., 2016. Latent fingerprint identification using deformable minutiae clustering. Elsevier, Neurocomputing. 175, 851-865.

[41] Deshpande, U.U., Malemath, V.S., Patil, S.M., et al., 2021. Latent fingerprint identification system based on local combination of minutiae feature points. Journal of SN Computer Science (SNCS), Springer,

Article number - 206.
DOI: https://doi.org/10.1007/s42979-021-00615-7.

[42] Cao, K., Jain, A.K., 2018. Latent Fingerprint Recognition: Role of Texture Template. in 9th IEEE International Conference on Biometrics Theory, Applications and Systems, (BTAS), Redondo Beach, CA, USA. pp. 1-9.
DOI: https://doi.org/10.1109/BTAS.2018.8698555.

[43] Ezeobiejesi, J., Bhanu, B., 2018. Patch Based Latent Fingerprint Matching Using Deep Learning. 25th IEEE International Conference on Image Processing (ICIP), Athens. pp. 2017-2021.
DOI: https://doi.org/10.1109/ICIP.2018.8451567.

[44] Nguyen, D.L., Jain, A.K., 2019. End-to-End Pore Extraction and Matching in Latent Fingerprints: Going BeyondMinutiae. CoRR, vol. abs/1905.11472. [Online] Available: http://arxiv.org/abs/1905.11472.

[45] Deshpande, U.U., Malemath, V.S., Patil, S.M., et al., 2020. CNNAI: A Convolution Neural NetworkBased Latent Fingerprint Matching Using the Combination of Nearest Neighbor Arrangement Indexing. Front. Robot. AI, vol. 7.
DOI: https://doi.org/10.3389/frobt.2020.00113.

[46] Feng, J., Shi, Y., Zhou, J., 2012. Robust and efficient algorithms for separating latent overlapped fingerprints. IEEE Transactions on Information Forensics and Security. 7(5), 1498-1510.

[47] Sankaran, A., Vatsa, M., Singh, R., 2015. Multisensor Optical and Latent Fingerprint Database. in IEEE Access. 3, 653-665.

BILINGUAL PUBLISHING CO.
Pioneer of Global Academics Since 1984

Journal of Computer Science Research
https://ojs.bilpublishing.com/index.php/jcsr

EDITORIAL

Recent Advancement in the Healthcare Domain Using Various Methods

Manoj Kumar*

School of Computer Science, University of Petroleum and Energy Studies, Dehradun, India

ARTICLE INFO

Article history
Received: 22 January 2022
Accepted: 24 February 2022
Published Online: 25 February 2022

1. Introduction

In cities, the world's population is rising at an exponential rate, and the more people there are, the greater the strain on resources. Even though cities have medical resources and facilities, which are growing by the day, the level of adequacy has not yet been reached, putting an undue strain on government resources. Cities' healthcare systems have evolved, bringing with them the necessary solutions to lightning-related issues. Because a huge number of sensors are being used to produce a new multidimensional monitoring approach for the activity of a wide range of diseases, the new research represents a significant stride in e-health [1]. The real-world medical industry [2] is a major impediment to IoT integration. Lorem's students' lives have several safety implications, and by lowering medical costs, it achieves that aim while also enhancing the accuracy of sickness prediction in general. When applying IOT in the real world of healthcare, this piece presents a technical tune model, as well as lucrative worries used for uncomplaining reassuring and open space challenges [3].

The Learning (ML) / Deep Learning (DL) system has benefitted a variety of industries, including manufacturing, transportation, and government. In terms of population, DL has just exceeded the state. Computer visualisation, text analysis, and word processing are just a handful of the disciplines where art is flourishing. In addition, the ML/DL calculation approach is having a growing posi-

*Corresponding Author:
Manoj Kumar,
School of Computer Science, University of Petroleum and Energy Studies, Dehradun, India;
Email: Wss.manojkumar@gmail.com

DOI: https://doi.org/10.30564/jcsr.v4i1.4471

tive impact on health-care delivery. Treatment of diseases has long been hampered by large-scale technology [4]. Body organ identification in medical imaging, long-range pneumonia categorization, lung cancer diagnosis, image reconstruction treatment, and brain tumour sections are just a few of the areas where machine learning and deep learning have made significant progress.

Clinician-assisted analysis has moved to the top of the list of potential application areas for ML/DL models, and several models have already been created to meet this demand. In domains including clinical pathology, radiation therapy, eye diseases, and skin difficulties, human doctors are being phased out and replaced by DL models. Many studies have been published on DL models, which, according to the findings, outperform human physicians in various areas [5,6]. Furthermore, technology and machine learning/deep learning may aid in the evaluation of results and the creation of intellectual solutions based on human intelligence. Peripheral medical services play a critical role in the modernisation of health-care technology in rural and low-income areas, and they make a substantial contribution [7,8].

2. Possible Method

This device can monitor a patient's electrocardiogram (ECG), temperature, electromyography, and muscle activity in breathing, sweating, and blood sugar, as well as infections like arrhythmias, passion nerve diseases, muscular disorders, blood stress, and diabetes. Sensors can now be easily placed to the skin, and many sections of the body have seen considerable improvements, so proceed with caution. Sensors implanted in the bodies of patients acquire a variety of physiological data, including numerous physiological indices. The data are then delivered via a small handheld device running pre-purchased data and communications software. Sensors should be compact and light in weight to avoid getting in the way of the patient's motions. Small, low-energy batteries are recommended for powering these sensors. This means that the sensors can be used indefinitely without needing to be sent or recharged. With the correct transmission components, transmitting patient data from the health center's accurate and secure location should be doable. Bluetooth can be used to carry out the transmission. It is possible to activate the system's connected devices via the hub, which can be done using a Smartphone. Figure 1 shows a possible data transmission solution.

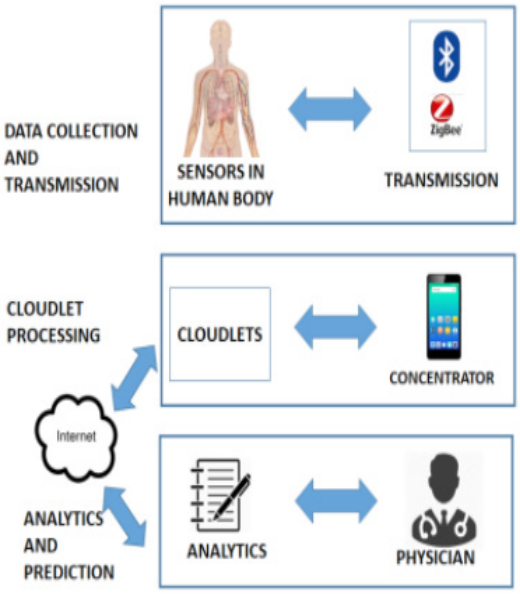

Figure 1. Data Transmission Approach

3. Conclusions

The proposed solution aims to give patients with better-connected economic health services, allowing experts and doctors to build on this knowledge and reach more rapid and favourable conclusions for their patients, using IOT, machine learning, and a cloud-based information system. At any one time, the final model comprises all of the features that a doctor is looking for in a patient. As a result of the connected economic support to unwell nations, the suitable expert would take action against the healthcare victim in the clinic, resulting in shortened hospital lines and direct consultation with physicians, minimising contextual dependence, and allowing full use of the website. The proposed method's main purpose is to provide patients with a high-quality financial existence that is linked to their services.

Doctors may be able to use this information to deliver a rapid and cost-effective solution to their patients. Several features of the finished product allow the doctor to test the patient at any time and from any location. This would result in a financial benefit for sick persons who desire to go to the hospital and have doctor consultations in order to lower their family's health-care costs.

Conflict of Interest

The authors declare no conflict of interest.

References

[1] Sullivan, H.T., Sahasrabudhe, S., 2017. Envisioning inclusive futures: technology-based assistive sensory and action substitution. Futur. J. 87, 140-148.

[2] Yin, Y., Zeng, Y., Chen, X., et al., 2016. The Internet of Things in healthcare: an overview. J. Ind. Inf. Integr. 1, 3-13.

[3] Saha, H.N., Supratim Auddy, S.P., 2017. Health Monitoring using Internet of Things (IoT). IEEE Journal. pp. 69-73.

[4] Khan, S.F., 2017. Health Care Monitoring System in Internet of Things (loT) by Using RFID. IEEE International Conference on Industrial Technology and Management. pp. 198-204.

[5] Moeen Hassanalieragh, Alex Page, TolgaSoyata, et al., 2015. Health Monitoring and Management Using Internet-of-Things (IoT)Sensing with Cloud-Based Processing: Opportunities and Challenges.

[6] Gupta, M.S.D., Patchava, V., Menezes, V., Oct 2015. Healthcare based on iot using raspberry pi. In 2015 International Conference on Green Computing and Internet of Things (ICGCIoT). pp. 796-799.

[7] Gupta, P., Agrawal, D., Chhabra, J., March 2016. Iot based smart healthcare kit. In 2016 International Con- ference on Computational Techniques in Information and Communication Technologies (ICCTICT). pp. 237- 242.

[8] Lopes, N.V., Pinto, F., Furtado, P., et al., Oct 2014. Iot architecture proposal for disabled people. In 2014 IEEE 10th International Conference on Wireless and Mobile Computing. Networking and Communications (WiMob). pp. 152-158.

BILINGUAL
PUBLISHING CO.
Pioneer of Global Academics Since 1984

Tel:+65 65881289
E-mail: contact@bilpublishing.com
Website:ojs.bilpublishing.com

2630-5151
01
9 772630 515223